Diploma Thesis WS 05/06
Institute of Energy Technology, ETHZ Zürich

Direct Feed Flow Controlled Solar Combisystem with Non-pressurized Storage: a Simulation Case

Martino Poretti

Prof. Aldo Steinfeld
Supervisor: P. Vogelsanger

Zürich, 17. February 2006

Martino Poretti
Diplomsemester D-MAVT
00-911-206

Via Bonzaglio 14
CH-6997 Sessa
Email: martino.poretti@ticino.com
Tel: +41 78 824 13 53

Table of Contents

List of Tables

List of Figures

1. *Abstract*

The key design challenge for a solar combisystem is how to integrate the different requirements of the heating source and the heating loads into a single, cost-effective, durable and reliable heating system while achieving the most benefit from each installed square meter of collector.

The assignment of this diploma project was to simulate a new concept of solar combisystem using the program TRNYS 16. This system is characterized by a non-pressurized storage tank and drain back collectors. All the load and unload process performed on the storage tank is done directly, without use of any heat exchanger. In addition, the space heating loop control is uncommon, the heat power is controlled by the space heating pump mass flow rate, and not, as in a traditional system, by varying the space heating supply temperature.

The results of this concentrated simulation effort show that a Direct Feed Flow Controlled combisystem has a good potential of efficiency improvement compared to a standard solar combisystem. Through this special space heating controller the return temperature to the storage can by significantly lowered, thus increasing the solar gain and the boiler efficiency.

The results also show that a storage tank directly fed allows a much higher overall system efficiency if compared to a combisystem storage with integrated heat exchangers.

2. *Introduction*

2.1. Actual Situation

Throughout the world, hundreds of thousands of domestic solar hot water systems are demonstrating the possibilities of this renewable energy source. Due to the success of these hot water systems, more builders are turning to solar energy for space heating. The heating requirements of a single- or multi-family house can be met at acceptable costs by combining solar heating systems with short-term heat storage and well-insulated buildings.

The further development of this solar thermal system is characterized by two key factors that are of major interest for the future development of solar heating systems for household use. These factors are:

- Drain-back system
- Non-pressurized storage tank

The SPF (Solartechnik Prüfung Forschung) institute of Rapperswill is a member of the international program IEA SHC (International Energy Agency for Solar Heating and Cooling) and is responsible for the optimization of hot water storage concepts. Its attention is most of all focused on the load and unload loop of different solar systems in combination of non-pressurized storage tanks. The goal is first of all to achieve a significant cost reduction of the solar combisystem while maintaining maximum system efficiency.

In a combisystem there are at least two energy sources used to supply heat to the two heat consumers (domestic hot water and space heating). The solar collectors deliver heat as long as solar energy is available, and the auxiliary energy source (oil, gas, wood, electricity, etc.) supplements the missing heat required. The key challenge in creating a combisystem is to combine the different requirements of heat suppliers and heat consumers into one single, cost-effective, durable and reliable heating system, achieving the most benefit from each installed square meter of collectors.

Figure 2-1: Standard combisystem example

2.2. Technology Description

2.2.1. Drain-back technology

Drain-back technology provides an interesting alternative for protection against overheating of the fluid in the solar collector loop and also prevents the heat transfer fluid from freezing. The use of a drain-back system allows the operation of the circulation using natural water without antifreeze additives.

The system concept is based on draining the water from the tilted collector and out of the collector pipes using gravitational force, while replacing the liquid with air from the top. Without water in collector and pipes ice cannot form and damage is therefore avoided. The water also drains back if the heat store is fully charged, avoiding boiling of water and high pressure inside pressurized systems.

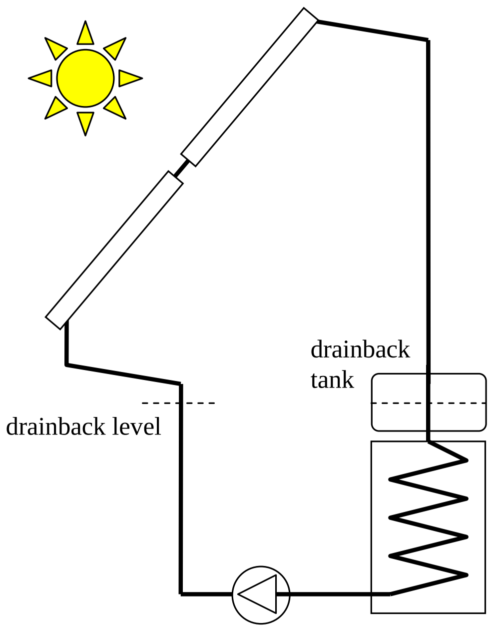

Figure 2-2: Example of the drain-back technology

In comparison with the use of heat transfer fluids (antifreeze) drain-back technology using water features shows both advantages and disadvantages.

+ Heat transfer properties of water (thermal capacity and viscosity) are better than those of other heat transfer fluids.

+ Water is much cheaper than all other collector fluids and easily available

+ The collector loop generally does not face high overpressure

+ Level of maintenance for drain-back systems is lower

- Less flexibility in the choice of the solar collector

- Collector loop design and installation need particular attention

The potential of drain-back technology is high due to excellent thermal properties, inherent safety, low cost and easy maintenance. The major barrier far drain-back technology is a lack of skilled workers needed for proper installation.

2.2.2. Non-pressurized storage tank

In a traditional combisystem the storage tank is under pressure; this implies a much more expensive storage system because good mechanical properties of the materials are required.

A non-pressurized storage tank can instead be made of plastic materials or low quality steels, achieving a reduction in material and manufacturing cost that can be significant. One problem with a polymer made storage tank is the maximal temperature allowed, which could be lower than that of a traditional storage tank under pressure.

3. *Goals*

The goal of this diploma thesis is to check the performance of a Direct Feed Flow Controlled solar combisystem that includes the two technologies described in chapter 2.2 and to compare it to a standard reference combisystem.

Direct Feed Flow Controlled means that the heating power for the space heating is not varied as in a traditional system by changing the supply temperature. Instead, the modulation of the heating power is performed by modulating the flow rate of the water supply entering the space heating loop. This feature yields, in an optimum case, a much lower return temperature to the storage tank, which results in theoretical benefits such as higher solar efficiency and better water condensation in a gas boiler. This supposition should be confirmed by the simulation.

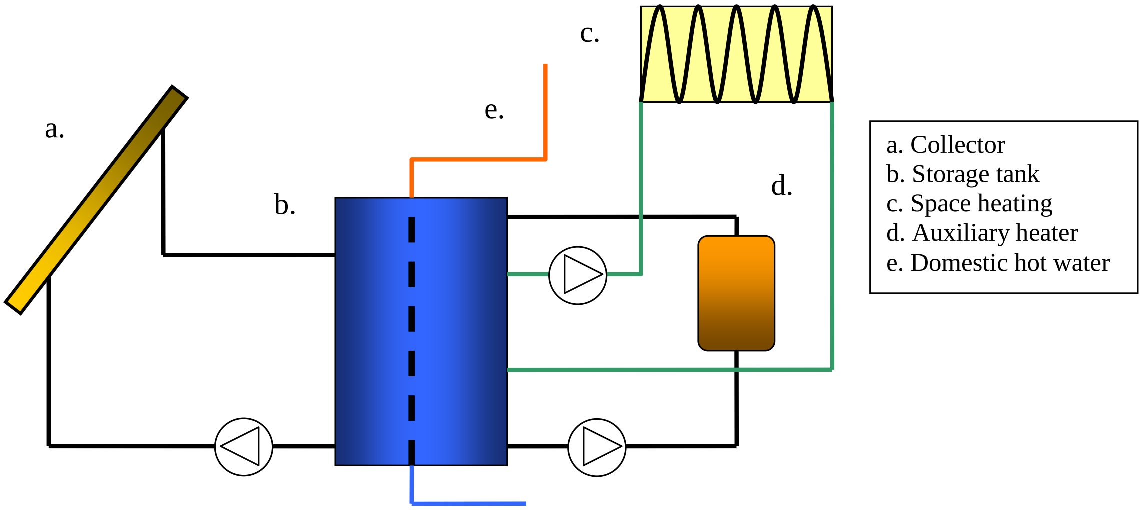

Figure 3-1: Direct feed flow controlled combisystem

The system is schematically represented in Figure 3-1. The drain-back collector-loop (a.) is directly connected to a non-pressurized storage tank (without the use of any heat exchanger) and the auxiliary heater (d.) is directly coupled to the storage tank. Compared to common solar systems this is uncommon. The auxiliary heater runs at a constant temperature to keep a determined temperature at the top of the tank, the zone reserved for domestic hot water. The power adjustment for space heating (c.) is obtained by variation of the mass flow of the space heating pump; this is also uncommon.

A reference model, characterized by a traditional space heating controller must also be modeled.

The systems are simulated using the program TRNSYS 16; the model should be written in a clear manner and documented so as to provide the basis for further developments.

The task to achieve can be summarized in the following points:

- Research of existing simulation models and methods to simulate the auxiliary heater: possibly a gas heater with condensing technology.
- Definition of the Direct Feed Controlled System concept to be investigated and a reference model to allow direct comparisons between the two systems.
- Parameter studies for the two different concepts and optimization of both.
- Comparison of the simulation results relative to the overall system efficiency.

4. *TRNSYS 16*

To simulate the to different variants of the solar combisystem is used the simulation program TRNSYS version 16.

TRNSYS 16 is a transient systems simulation program with a modular structure. TRNSYS library includes many of the components commonly found in thermal and electrical energy systems, as well as component routines to handle input of weather data or other time-dependent forcing functions and output of simulation results.

The modular nature of TRNSYS gives the program tremendous flexibility, and facilitates the addition to the program of mathematical models not included in the standard TRNSYS library. TRNSYS is well suited to detailed analyses of any system whose behavior is dependent on the passage of time. Main applications include: solar systems (solar thermal and photovoltaic systems), low energy buildings and HVAC systems, renewable energy systems, cogeneration, fuel cells.

5. *Direct Feed Flow Controlled System*

5.1. Introduction

In this chapter is presented the TRNSYS model, with its components and the control strategies used to simulate the Direct Feed Flow Controlled solar combisystem.

5.2. TRNSYS Model

Some parts of the TRNSYS model are directly taken from the Solar Reference System v.17 developed by Richard Heimrath within the framework of the IEA Solar Heating and Cooling international program. These components are: the weather processor and weather data, the solar collector module and the domestic hot water heat exchanger. From Heimrath's Solar Reference System are also generated the load file for the space heating using the weather data of Zürich, since in the this simulation is not present any building model. Unfortunately there isn't any written documentation concerning the v.17 of the reference system model used in the IEA task.

The choice to eliminate the building model type 56 is made because of two reasons, first to have a very fast simulation so to make possible a wide parameter study and optimization. The second reason is to have exactly the same amount of heat energy delivered by the space heating in each simulation so to make possible a fair comparison between all the results.

The Direct Feed Flow Controlled system represent a drain-back solar combisystem with a non-pressurized storage tank. What makes this concept uncommon is the space heating control philosophy. In this concept the heating power is varied by changing the flow rate of the water supply and not the supply temperature as in traditional systems.

Figure 5-1 shows an overall view of the system model, each component is described in greater detail in the next section.

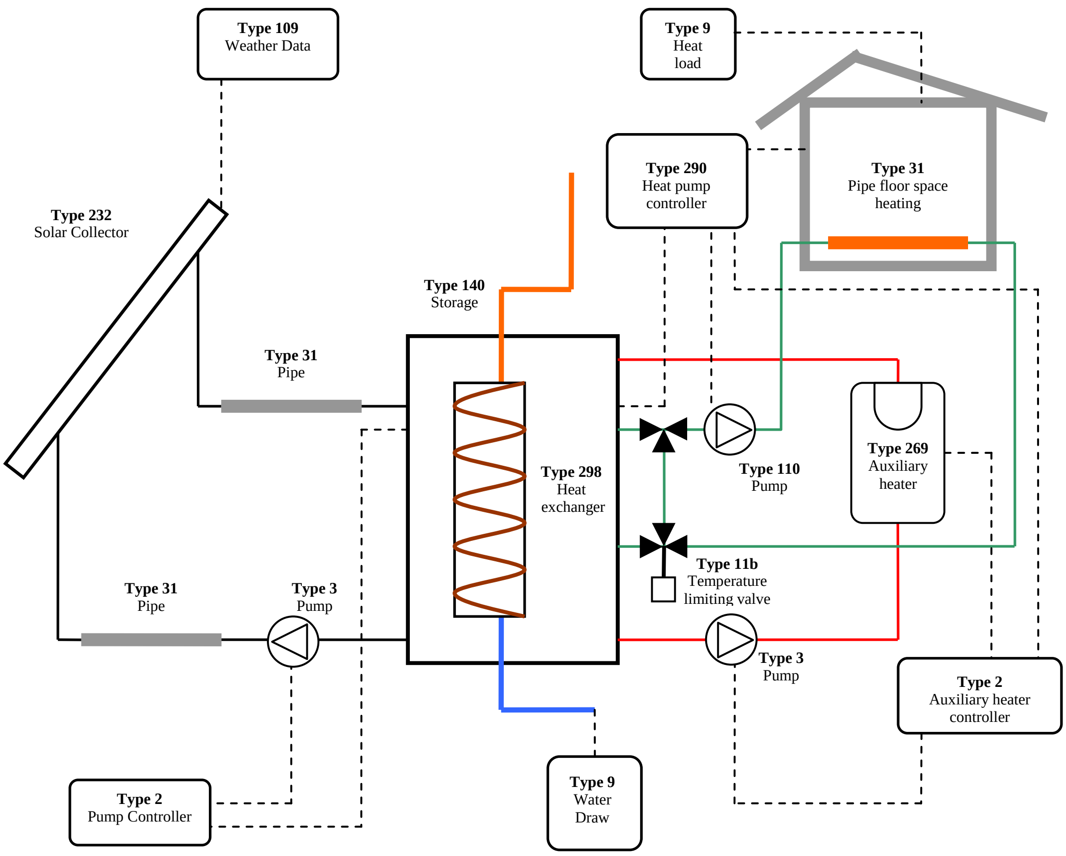

Figure 5-1: Direct Feed Flow Controlled system diagram

5.3. Definition of the components included in the system

In following subsections are described the components and their parameters chosen as „base case“ for the Direct Feed Flow Controlled simulation model.

5.3.1. Collector

The collector is modeled with the non-standard TRNSYS Type 232. The parameter are chosen to match a standard flat plate collector and are described in Table 5-1. The collector pipe are directly connected to the storage tank (without use of any heat exchanger).

The collector loop is a low flow system with a specific mass flow rate through the collectors of 12 l/(m^2.h). The overall collector area is 12 m^2. The drain-back system is not simulated because it has no influence on the solar gain and on the simulation results, but has to be considered during practical planning and assembly of the solar loop.

Table 5-1: Collector loop data

Collector	a_0	0.8
	a_1	3.5 W/m^2.K
	a_2	0.015 W/m^2.K
	Area	12 m^2
	Tilt angle	45 °
	Specific mass flow	12 Kg/m^2.h
	Inc. Angle Modifier	0.9 [-]
	Effective heat capacity	7000 [J/m^{2}K]
	Heat transfer media	Water

5.3.2. Pipes between collector and storage

The pipes in the collector loop are modeled with a standard TRNSYS Type 31. The geometry and the insulation thickness of the pipes connecting the collectors and the storage tank are given in Table 5-2. For the heat loss calculations, a surrounding temperature of 15°C is given.

The pipes are made of copper (28x1.5) with a 25 mm insulation. A standard length of 15 meters have been chosen for both pipes.

In Equation 5-1 and Equation 5-2 is showed how the pipe U-coefficient is calculated. The resulting U-value is 10.65 W/m^2.K

$$C = \frac{D_i}{2\lambda_{pipe}} \cdot \ln\left(\frac{D_a}{D_i}\right) + \frac{D_i}{2\lambda_{iso}} \cdot \ln\left(\frac{D_a + 2 \cdot d_{iso}}{D_i}\right) + \frac{D_i}{\alpha_a \cdot \left(D_a + 2 \cdot d_{iso}\right)}$$ ***Equation 5-1***

$$U_{pipe} = \frac{\alpha_i}{\left(1 + \alpha_i \cdot C\right)} \cdot 3.6 = 10.65 \text{ [W/m}^2\text{.K]}$$ ***Equation 5-2***

Table 5-2: Collector pipe data

Collector pipes	Length, tank to collector (cold side)	15 m
	Length, tank to collector (hot side)	15 m
	Inner diameter (D_i)	0.025 m
	Outer diameter (D_a)	0.028 m
	Insulation thickness (d_{iso})	0.025 m
	Insulation thermal conductivity (λ_{iso})	0.042 W/m.K
	Pipe thermal conductivity (λ_{pipe})	372.0 W/m.K
	Lambda internal (α_i)	1000 W/m^2.K
	Lambda external (α_a)	10 W/m^2.K
	U-value pipe (U_{pipe})	10.65 W/m^2.K
	Heat transfer media	Water

5.3.3. Storage

The storage tank is modeled with a non-standard TRNSYS Type 140 (version 1.99). This multiport store model is chosen because of the need of an high number of inlet and outlet ports, this possibility wasn't offered by the standard storage models contained in the TRNSYS libraries.

The storage tank has a volume of 800 liters. As basis values for the thermal heat losses are chosen these of the IEA Reference System, but modified to match a storage volume of 800 liters. The overall heat loss coefficient is 18.08 kJ/h.

The height of the storage is 1.965 m and the diameter is 0.72 m. The insulation thickness is set to 0.15 m for all the storage. At the top of the storage a volume of 240 liters is reserved to the domestic hot water.

The storage tank includes four inlet and four outlet ports, these are reserved for the collector loop, the space heating loop, the auxiliary heater loop and for the domestic hot water heat exchanger loop. Only the solar inlet and the space heating inlet port are stratified-charged, all the others have a fix inlet and outlet height.

The main parameters of the storage tank are summarized in Table 5-3. Figure 5-2 shows the storage system in detail.

Table 5-3: Storage tank data. [1)]Relative height: Storage bottom = 0, Storage top = 1 (HE = heat exchanger)

Storage tank	Total volume	0.8 m^3
	Height	1.965 m
	Diameter	0.72 m
	Heat loss coefficient	18.08 kJ/h
	Thermal conductivity of insulation material	0.032 W/m.K
	Insulation material thickness	0.15 m
	Vertical thermal conductivity	2.0 W/m.K
	Solar inlet (stratified-charged) [1)]	0.0 - 0.8
	Solar outlet [1)]	0.0
	Auxiliary heater inlet [1)]	1.0
	Auxiliary heater outlet [1)]	0.4
	Space heating outlet [1)]	0.6
	Space heating inlet (stratified-charged) [1)]	0.0 – 0.6
	Domestic hot water outlet to HE [1)]	1.0
	Cold water inlet form HE [1)]	0.0
	Position of sensor 1: DHW storage temperature [1)]	0.7
	Position of sensor 2: SH storage temperature [1)]	0.55
	Position of sensor 3: Collector control temp. [1)]	0.0
	Position of sensor 4: Storage max temp. protection [1)]	1.0

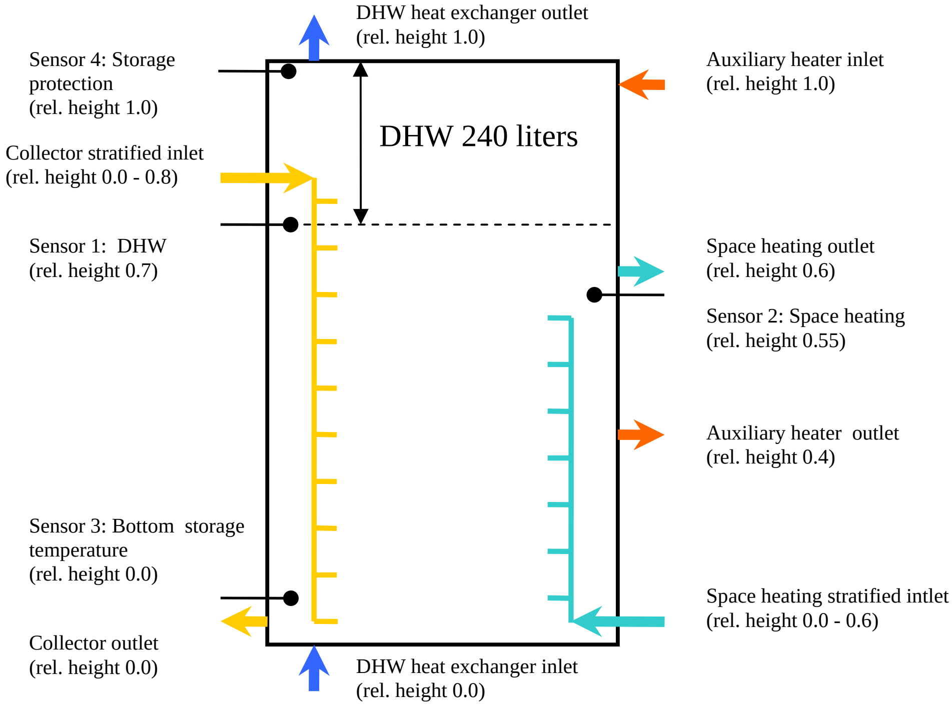

Figure 5-2: Storage tank detail

5.3.4. Boiler

The choice of the boiler model was the most difficult to take. It was first tried to implement in the simulation the TRNSYS non-standard Type 170 [6] but because of the lack in good documentation and the impossibility to understand exactly how this model worked under certain conditions it was decided to use the new non-standard Type 269 (version 1.13) [7] recently developed by Michel Haller of the SPF institute. This new TRNSYS module is not yet used in any simulation so it is tested alone to understand how it behaves in different conditions (analysis performed in section 9.2)

TRNSYS non-standard Type 269 is a carbon-based fuels auxiliary heater with condensing technology that allows power modulation. In this case the fuel used is gas. The boiler has a nominal power of 12 kW and modulates in the range of 30%-100%. The chosen parameters are them of the Hoval TopGas® 12 [9] matched to fit the experimental measured values.

When the boiler operates to heat up domestic hot water in the storage tank or to heat the space heating water reserve, the set supply temperature is fixed at 65°C. Hot water enters always at the fixed relative height of 1.0 (the top of the storage tank).

The water mass flow rate of the auxiliary gas heater is instead variable: when the boiler is charging the DHW it's value is fixed at 200 kg/h but when it charges the storage tank space heating zone the mass flow varies depending on the space heating pump flow rate (for a detailed description see 5.4.2: Control of the auxiliary heater).

For the heat loss calculations a surrounding temperature of 15°C is used. The combustion air temperature is also set to 15°C. The auxiliary heater data are summarized in Table 5-4. Figure 5-3 shows the auxiliary loop in detail.

Table 5-4: Boiler data.

Boiler	Nominal Power	12 kW
	Minimal Power (30%)	3.5 kW
	Set supply temperature (DHW and SH)	65 °C
	Hysteresis for Tset	5 °C
	Fuel type	Natural gas
	Ambient temperature in the boiler house	15 °C
	Air surplus number (λ)	1.2
	Modulation range	30%-100%
	Thermal mass of empty boiler	17.6 kJ/K
	Volume of water in the boiler	1.5 dm^3
	Boiler-environment heat transfer coeff.	4.3 kJ/h.K
	Gas-water heat transfer	110 kJ/h.K
	Water supply mass flow rate (DHW)	200 kg/h
	Water supply mass flow rate (SH)	variable
	Air temperature	15°C
	Relative humidity	0.5
	Pressure	1.01325 bar

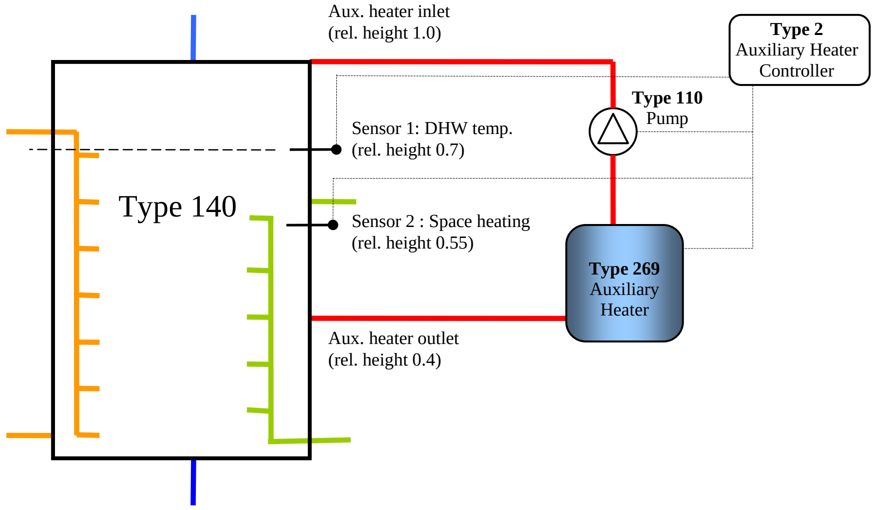

Figure 5-3: Boiler loop in detail

5.3.5. Domestic hot water

The domestic hot water preparation is simulated using the non-standard heat exchanger TRNSYS Type 298. This module acts like a external DHW heat exchanger but without taking into account the heat losses to the environment.

The heat exchanger primary side (hot side) is connected to a double port of the TRNSYS Type 140. The storage tank inlet for the water coming from the heat exchanger is located at a relative height of 0.0 and the outlet at 1.0 as Figure 5-4 illustrates.

The secondary side of the heat exchanger (cold side) is the draw profile of the domestic hot water. This profile was created using the tool for the generation of domestic hot water profiles programmed by Ulrike Jordan [12].

The text file generated contains a list of flow rate values for each time step. The total mean draw-off volume was set to 200 l/day, which represent the daily hot water need of a single family house.

Table 5-5: Domestic hot water heat exchanger data

DHW Heat Exchanger	HX heat transfer capacity	10800 [kJ/h.K]
	Maximum flux primary side	1065 [kg/h]

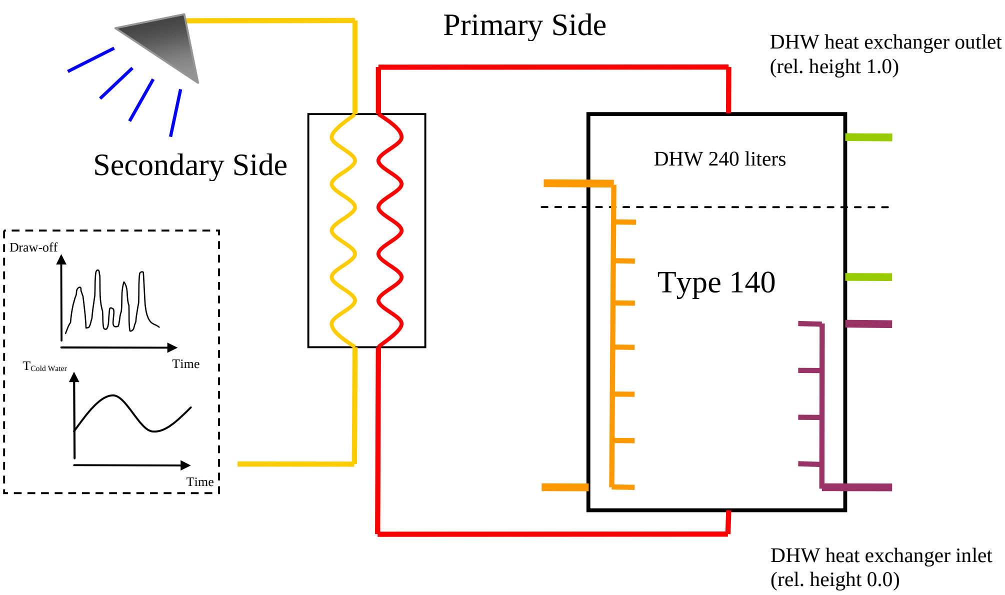

Figure 5-4: Domestic hot water heat exchanger in detail

The mass flow rate of the primary side is varied so to have the set temperature of 45°C on the secondary side heat exchanger outlet. This mass flow can vary from 0 to a maximum of 1065 kg/h. The heat transfer capacity of the heat exchanger as a fix value of 10800 kJ/h.K.

The temperature at the secondary side inlet (cold water temperature) is determined by a sinus function that takes into account the temperature oscillations during the year as Figure 5-5 shows. The curve is plotted from the function described by Equation 5-4.

$$T_{ColdWater} = T_{Average} + T_{Shift} \cdot \sin\left(360 \cdot \frac{\left(t + \left(273.75 - D_{Shift}\right) \cdot 24\right)}{8760}\right)$$ ***Equation 5-3***

$T_{Average}$ = 9.7 °C

T_{Shift} = 6.3 °C

D_{Shift} = 60 days

$$T_{ColdWater} = 9.7 + 6.3 \cdot \sin\left(360 \cdot \left(t + 5130\right) / 8760\right)$$ ***Equation 5-4***

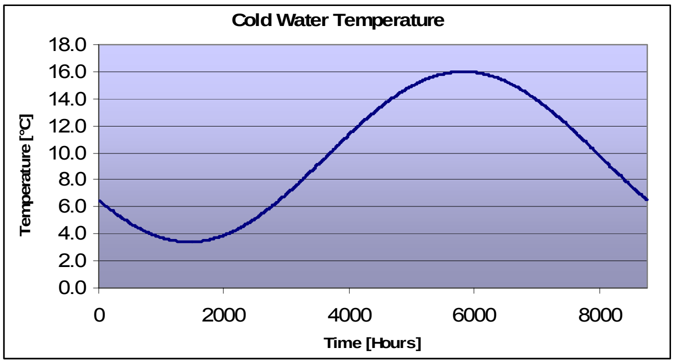

Figure 5-5: Cold water temperature profile over an year

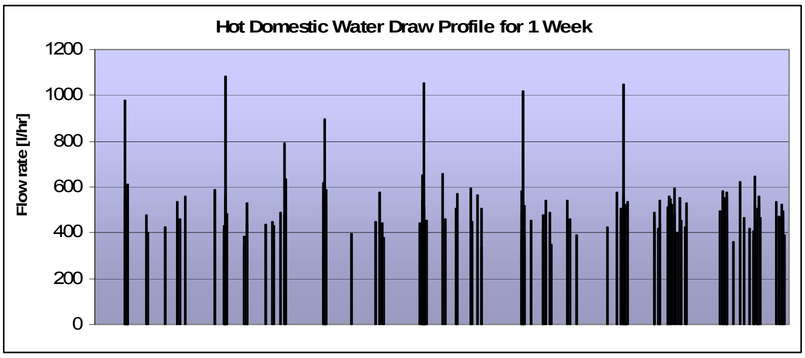

Figure 5-6: Example of draw profile over one week

5.3.6. Building

The building is not simulated directly into the system. The heat load demand of the building is contained in an external file. This file was generated from the Solar Reference System v. 17 made by R. Heimrat. In the file is contained the temperature inside the building and the heat power needed for each time step to maintain a constant temperature inside the building (this temperature is practically constant during all the heating season at about 20 °C).

The basis case heat load file was generated from an house model with a specific yearly space heat demand for Zürich climate amounting to 60 $kWh/m^2.a$. The building model parameters used in the Solar Reference System developed by R. Heimrat are described in Table 5-6.

Table 5-6: Building data

Building	Specific space heating demand for Zürich climate	60 kWh/m^2 per year
	Area	70 m^2
	Total window area	23 m^2
	Window U-value	1.4
	Window g-value	0.622
	External walls, U-value	0.283 $W/m^2.K$
	Roof, U-value	0.283 $W/m^2.K$
	Ground floor, U-value	0.283 $W/m^2.K$
	Mean power (during heat season)	1.5 kW
	Maximum power	4.3 kW
	Total space heat needed per year	8379 kWh

Figure 5-7 shows the heat power contained into the heat load file plotted over a year.

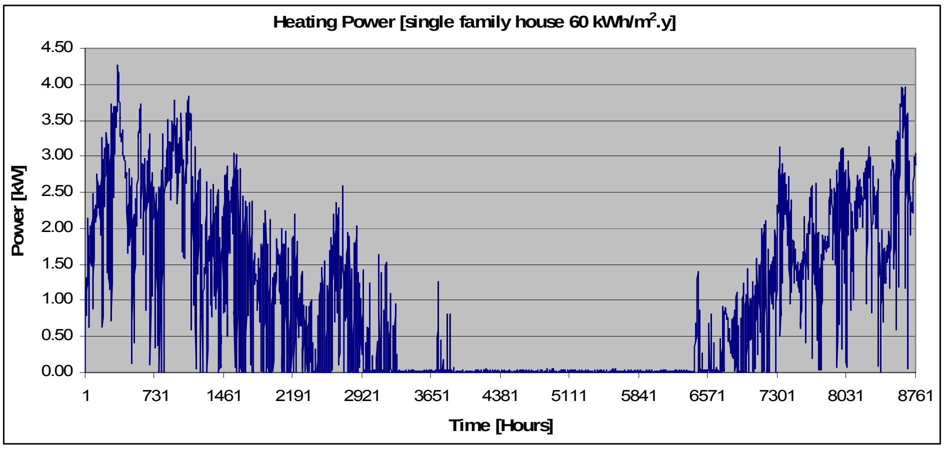

Figure 5-7: Heat power demand over one year in kW

5.3.7. Heat distribution

The heat distribution of the space heating loop is represented by a pipe (TRNSYS standard Type 31), simulating a floor space heating system. The temperature of the environment in which the pipe is located (the room temperature) is given by the building load file but it is practically constant during the heating season (about 20 °C). The water used for the space heating loop is directly taken from the storage tank without the use of any heat exchanger.

Table 5-7: Floor heating pipe data

Space Heating Pipe	Pipe length	100 m
	Pipe diameter	0.025 m
	Loses coefficient	25 W/m^2.K
	Maximum flow rate	400 kg/h

A Tee-piece and a temperature limiting valve are installed to limit the temperature that goes into the heating pipe to a set value of 55 °C. Below this value the water is directly taken out of the storage and goes into the space heating loop. If the temperature in the storage goes upper the set temperature of 55 °C, the temperature limiting valve mixes the water returning to the storage form the space heating loop with that coming out of the storage to mach the set maximum temperature of 55 °C. The maximum flow rate of the space heating pump is set to 400 kg/h. Figure 5-8 illustrates the space heating loop in detail.

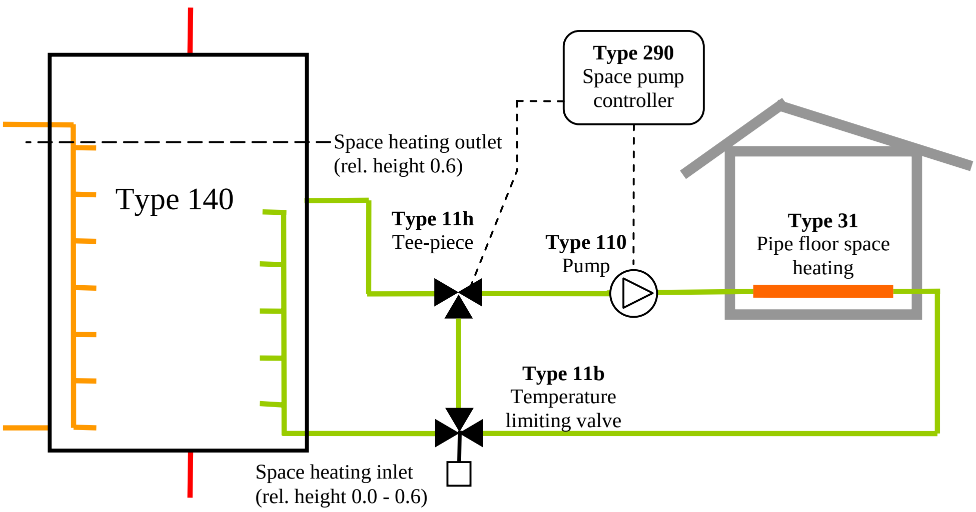

Figure 5-8: Space heating loop in detail

5.4. Control strategy

There are three main controllers that control the system. One controls the collector loop pump. Another controls the auxiliary heater and the last one controls the space heating pump.

The collector loop pump and the auxiliary heater controllers are modeled with TRNSYS standard Type 2 controllers. For the space heating a special non-standard TRNSYS Type 290 has been written.

5.4.1. Control of the collector loop

The control strategy of the collector loop has three main functions, in brief:

1. If the water from the collector T_{coll} (sensor 5) is at least 11°C warmer than that of the bottom of the storage $T_{store,b}$ (sensor 3) the pump is activated. The pump stops working when this temperature difference is lower than 2 °C
2. If the water supply of the collector is above 100°C ($T_{coll,max}$) the pump shuts down.
3. If the store reaches 95°C $T_{store,max}$ (sensor 4) the flow of the collector loop pump is stopped.

The control is managed by comparing the following 4 temperatures:

T_{coll} : Collector supply temperature (sensor 5) [°C]

$T_{coll,max}$: Maximum supply collector temperature [°C]

$T_{store,b}$: Temperature at the bottom of the storage (sensor 3) [°C]

$T_{store,t}$: Temperature at the top of the storage (sensor 4) [°C]

$T_{store,max}$: Maximum temperature of storage tank [°C]

Figure 5-9 shows how the collector loop is controlled.

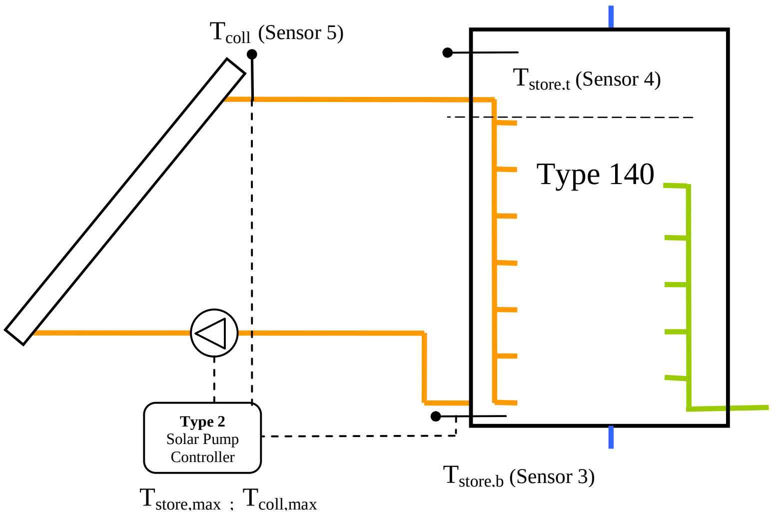

Figure 5-9: Collector loop control system in detail

5.4.2. Control of the auxiliary heater

The auxiliary heater always supplies hot water at the set temperature of 65°C (T_{setAUX}). The auxiliary heater is controlled after the following principles:

1. When the temperature of the DHW; $T_{store\ DHW}$ (measured by the sensor 1 Figure 5-10) gets below the set temperature of 54°C ($T_{store,set}$) auxiliary heat will be supplied to the storage at a flow rate of 200 kg/h ($\dot{m}_{AUX}$) until the water reaches the set temperature of 60°C.

2. If the water temperature below the storage tank outlet that goes to the space heating (sensor 2 Figure 5-10) gets below the minimum temperature needed to match the heat demand of the building plus a reserve factor of 2°C ($T_{heat,min}$+ 2°C) the auxiliary heater is started. In this case the flow rate for the auxiliary heater ($\dot{m}_{AUX}$) depends on the supply mass flow rate of the space heating loop ($\dot{m}_{SH}$) and follows this simple relation:

$$\dot{m}_{AUX} = \dot{m}_{SH} + 30 \text{ kg/h}.$$

   The addition of 30 kg/h was necessary to avoid very low mass flow rate of the boiler, causing too many on-off cycles of the auxiliary heater. The auxiliary heater shuts down when the temperature $T_{storeSH}$ gets 5°C higher than the minimum temperature needed to match the heat demand of the house $T_{heat,min}$.

Following temperature are used to control the auxiliary system:

T_{setAUX}: Set supply temperature of the auxiliary heater for both DHW and SH.

$T_{store\ DHW}$: Store temperature measured by sensor 1, Figure 5-10 [°C]

$T_{store\ SH}$: Store temperature measured by sensor 2, Figure 5-10 [°C]

$T_{store,set}$: Set temperature of store for the DHW [°C]

$T_{heat,min}$: Minimum temperature needed at the space heating tank outlet to match the needed heating power contained in the heat load file (measured by sensor 2, Figure 5-10) [°C]

$\dot{m}_{SH}$: Mass flow rate of the space heating loop [kg/h]

$\dot{m}_{AUX}$: Mass flow rate of the auxiliary heater [kg/h]

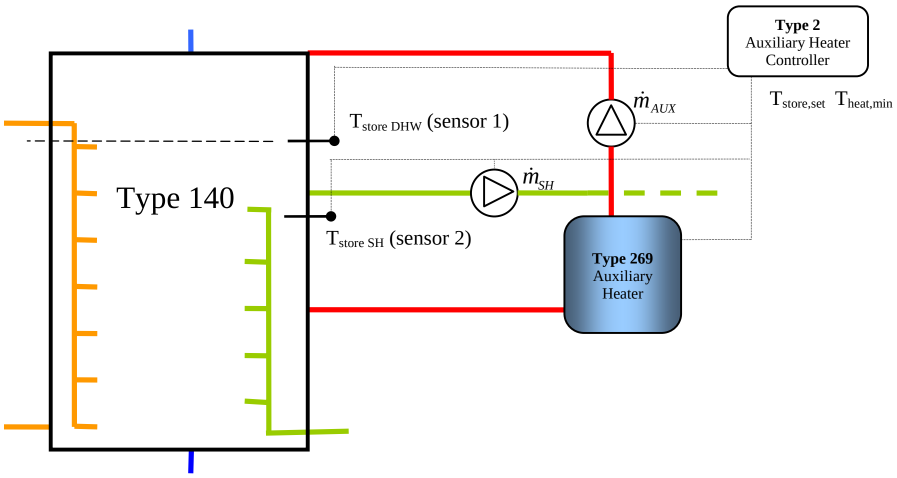

Figure 5-10: Boiler loop control system in detail

5.4.3. Control of the space heating

In the Direct Feed Flow Controlled system the heating power is not varied by changing the inlet temperature of the supply water as in traditional systems but changing the pump flow rate. A special controller, TRNSYS Non-standard Type 290, is written and compiled to control the pump and achieve this goal.

The power needed at each time step is contained in an external load file as described in section 5.3.6. The space heat controller 290; using as input the room temperature inside the building T_{room}, the heat power needed P_{needed} at each time step and the temperature entering the space heating pipe ($T_{pipe,SH}$); chooses the adequate flow rate of the space heating pump to match the needed heating power.

If the temperature at the storage tank outlet ($T_{tank,SH}$) is higher than 55°C the tempering valve mixes the storage tank water with the return temperature to have a space heating supply temperature ($T_{pipe,SH}$) of 55°C. Other parameter that the controller takes into account for calculation of the flow rate are the heating pipe's length l_{pipe} its diameter d_{pipe} and the pipe loss coefficient K_{pipe}.

A more detailed mathematical description of this special controller is presented in appendix A.

Following temperature are used to control the space heating system:

T_{room} : Room temperature inside the house [°C]

P_{needed} : Needed heating power at each timestep [°kW]

$T_{storage,SH}$: Storage temperature at the space heating outlet port [°C]

$T_{pipe,SH}$: Water temperature entering the space heating pipe [°C]

$T_{SH,max}$: Maximum temperature allowed to enter the space heating pipe [°C]

m_{SH} : Mass flow of the space heating pump [kg/h]

l_{pipe} : Length of the space heating pipe [m]

d_{pipe} : Diameter of the space heating pipe [m]

K_{pipe} : Space heating pipe loses coefficient [W/m^2.K]

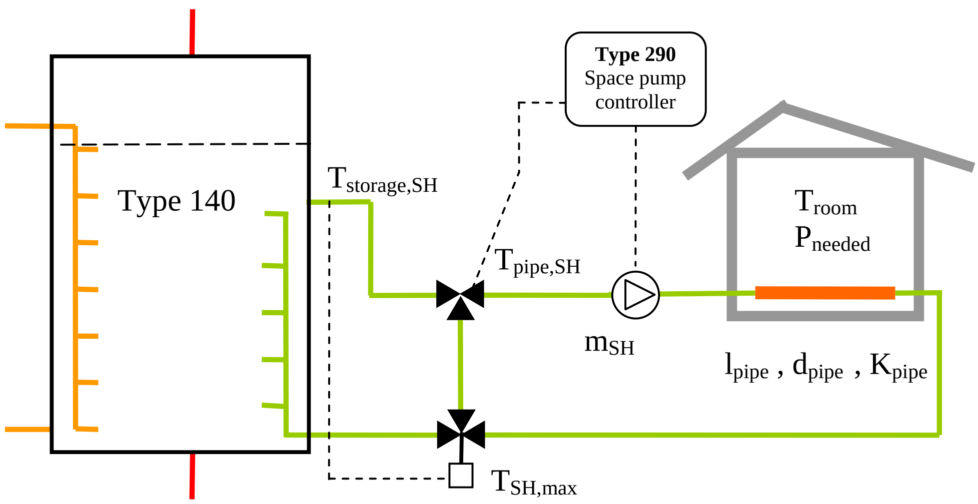

Figure 5-11: Space heating loop control system in detail

6. *The Reference System*

6.1. Introduction

A reference model is also modeled in TRNSYS to allow a comparison between the Direct Feed Flow Controlled solar combisystem concept described in chapter 5 and a solar combisystem with a standard space heating control management. In this chapter are described the TRNSYS model, the components used in the simulation and the control strategies of the “base case” of the reference system.

6.2. TRNSYS Model

This reference system model represents also a drain-back solar combisystem with direct feed, therefore also in this case there are no heat exchanger in the storage tank. The big difference between this model and the Direct Feed Flow Controlled concept is within the space heat management philosophy. In this case the power of the space heating system is controlled by changing the supply water temperature entering the heating pipes by means of a tempering valve and not varying the mass flow rate of the space heating pump. This control strategy characterize almost all the traditional heating systems.

To make a fair comparison the collector loop, the storage tank and the auxiliary heater parameters as all the load files and weather files are the same as for the Direct Feed Flow Controlled concept. The only changes introduced are in the space heating management and in the storage tank auxiliary heater charging concept that was also adapted to match a traditional charging strategy. Both modification are described in greater detail in the following sections.

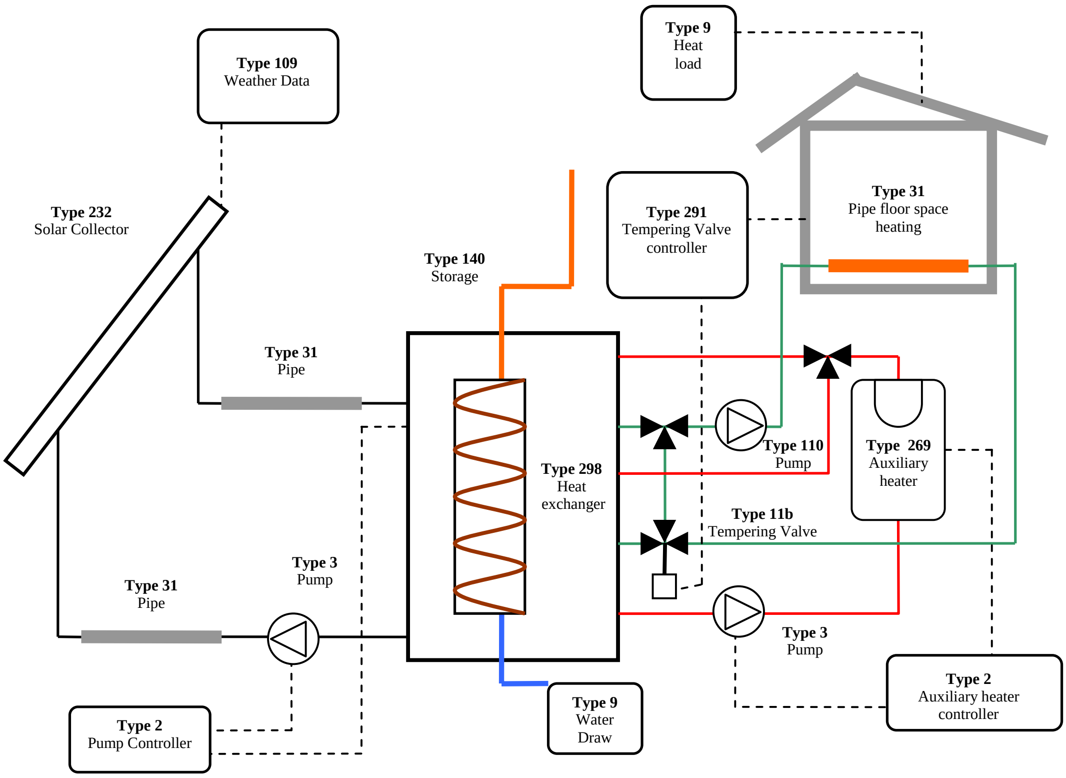

Figure 6-1: Reference system diagram

6.3. Definition of the components included in the system

In the following subsections are described the components and their parameters chosen as „base case" for the reference system.

6.3.1. Collector

The collector is exactly the same as that used for the Direct Feed Flow Controlled system described in section 5.3.1.

6.3.2. Pipes between Collector and Storage

The pipes are the same as them of the Direct Feed Flow Controlled system of section 5.3.2.

6.3.3. Storage

The main storage tank parameters are the same as them employed in the Direct Feed Flow Controlled system. In this case there are two separate storage inlet ports for the auxiliary heater supply. The first at the top of the tank (at a relative height of 1.0) used for the domestic hot water charging loop and a second one at a relative height of 0.55 for the space heating charging loop. It was decided to introduce this modification because almost all the conventional combisystem operate in a similar way.

The position of the temperature sensor for the space heating water (sensor 2 Figure 6-2) has been moved and it's now at a relative height of 0.6; the same height as the space heating outlet.

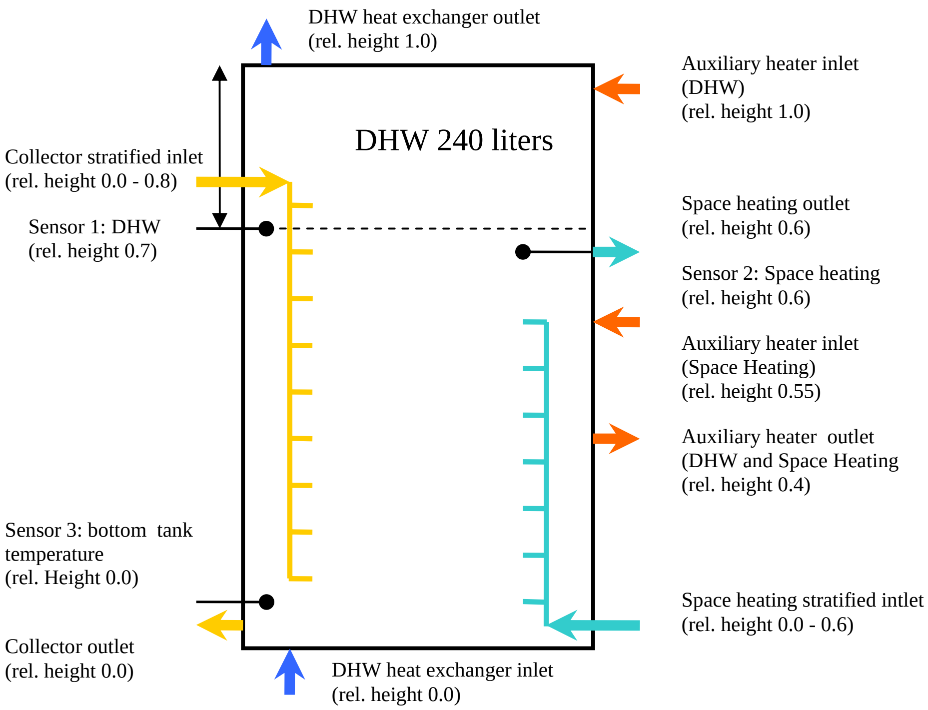

Figure 6-2: Storage tank detail

6.3.4. Boiler

The boiler model parameters are the same as them used for the Direct Feed Flow Controlled system. As said before in this case there are two different charging loops, the first for the domestic hot water and the second for the space heating. This is a very common characteristic of the standard combisystem configuration. A mixing valve switches to the fist or the second charging port depending on the signals coming from sensor 1 and sensor 2. Figure 6-3 illustrates schematically how the auxiliary heater operates.

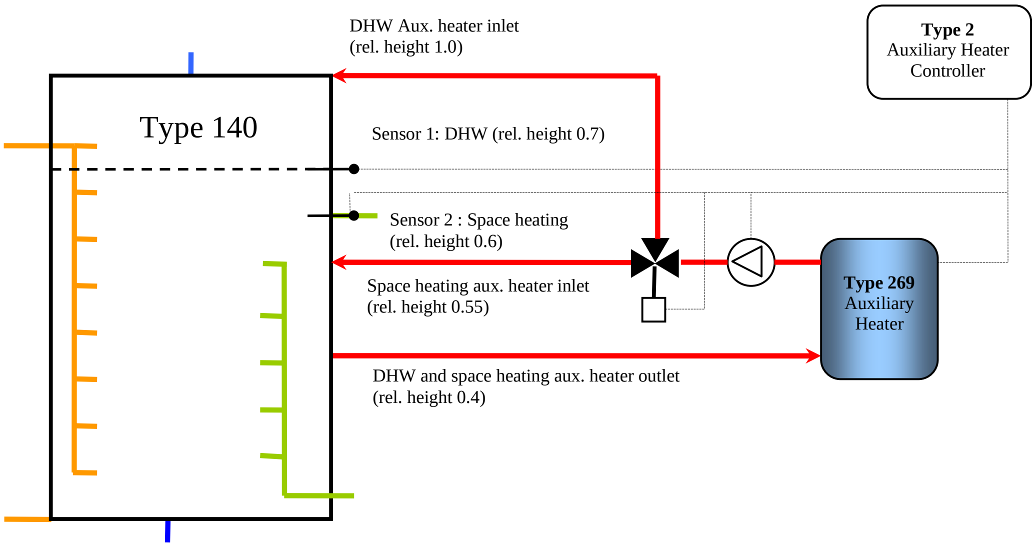

Figure 6-3: Boiler loop in detail

6.3.5. Domestic hot water

Same as that for the Direct Feed Flow Controlled system

6.3.6. Building

The building heat load demand file is the same as that for the Direct Feed Flow Controlled system.

6.3.7. Heat distribution

As for the system of chapter 5.3.7 the space heating element is modeled as a pipe (TRNSYS Type 31). The pipe simulates a floor space heating system. The parameters are maintained the same as them of the Direct Feed Flow Controlled concept. Also in the reference system the water used for the space heating loop is directly taken from the storage without use of any heat exchanger.

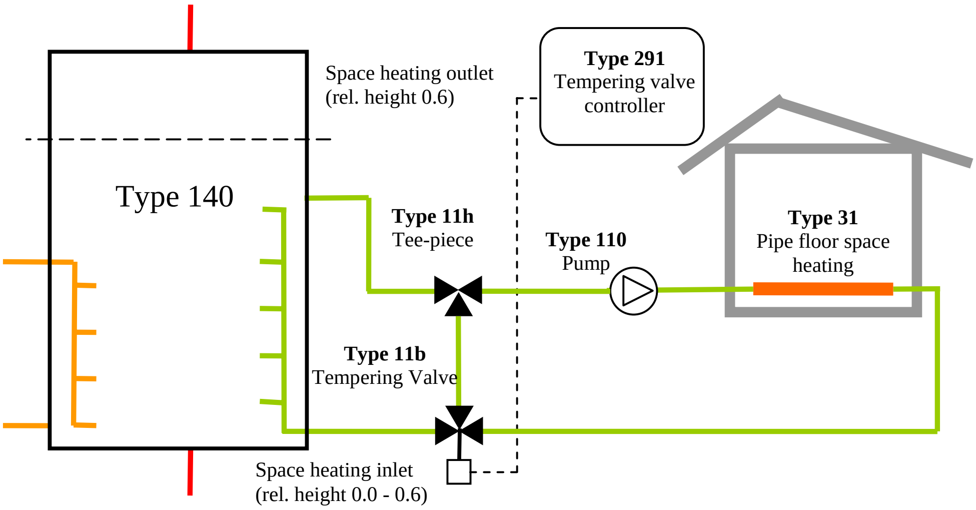

Figure 6-4: Space heating loop in detail

As Figure 6-4 illustrates a Tee-piece and a tempering valve are installed to make possible the choice of a set temperature of the water entering the heating pipes.

The space heating loop pump flow rate in the reference system is much higher than that of the Direct Feed Flow Controlled system, which is limited to 400 kg/h. Higher values are common for traditional systems. In the reference system for water supplies higher than 35°C the pump flow rate has a constant value of 1000 Kg/h, for a lower temperature water supply demand the pump flow rate is reduced linearly. This is done because of convergence problems within TRNSYS Type 11b (tempering valve), that occur when the set supply temperature is near to the room temperature.

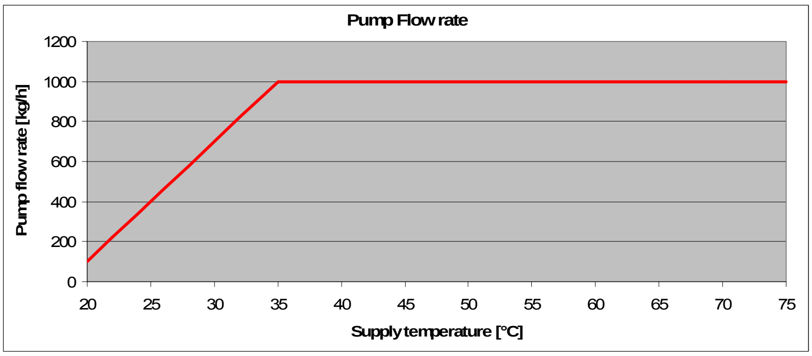

Figure 6-5: Space heating pump flow rate curve

6.4. Control strategy

As for the Direct Feed Flow Controlled model also in the reference system there are three main controllers that control the system. The collector loop pump controller is exactly the same as for the Direct Feed Flow Controlled system. The controller used for the auxiliary heater is modified to allow the charging strategy operated using two storage ports. The space heating controller is totally different from that of the Direct Feed Flow Controlled system. A detailed description of the controllers follows in the next sections.

6.4.1. Control of the collector loop

Same as for the Direct Feed Flow Controlled concept of section 5.4.1

6.4.2. Control of the auxiliary heater

The auxiliary heater is controlled after the following principles:

1. When the temperature of the DHW ($T_{store\ DHW}$) measured by the sensor 1 (Figure 6-6) gets below the set temperature of 54°C ($T_{store,set}$) auxiliary heat will be supplied to the top storage inlet (relative height of 1.0) at a flow rate of 200 kg/h ($\dot{m}_{AUX,DHW}$) until the water reaches the set temperature of 60°C. The auxiliary heater supply temperature has in this case a constant value of 65°C ($T_{setAUX,DHW}$)

2. If the temperature near the storage tank outlet to the space heating, measured by sensor 2 (Figure 6-6), gets below the minimum temperature needed to match the heat demand of the house plus a reserve factor of 2°C ($T_{heat,min}$+ 2°C); the auxiliary heater is started and hot water is supplied in the second storage tank inlet at a relative height 0.55. The auxiliary heater shuts down when the temperature of the sensor 2 is 7°C higher than $T_{heat,min}$. During the space heating charging loop the supply temperature of the auxiliary heater ($T_{setAUX,SH}$) is variable and depends on the set supply temperature of the space heating ($T_{supply,SH}$), which is controlled by the tempering valve. This correlation can be resumed by the following relation:

   $$T_{setAUX,SH} = T_{supply,SH} + 5°C.$$

   The auxiliary heater mass flow rate during the space heating charging loop ($\dot{m}_{AUX,SH}$) is instead constant and it's set to 400 kg/h.

Following temperature are used to control the auxiliary heating system:

$T_{setAUX,DHW}$: Auxiliary heater set temperature during the domestic hot water charging loop. [°C]

$T_{setAUX,SH}$: Auxiliary heater set temperature during the space heating charging loop. [°C]

$T_{store\ DHW}$: Store temperature (measured by sensor 1, Figure 6-6) [°C]

$T_{store\ SH}$: Store temperature (measured by sensor 2, Figure 6-6) [°C]

$T_{store,set}$: Store set temperature for the domestic hot water reserved volume [°C]

$T_{supply,SH}$: Supply temperature to the space heating loop [°C]

$T_{heat,min}$: Minimum temperature needed at the storage tank outlet to the space heating to match the needed heating power [°C]

$\dot{m}_{AUX,DHW}$: Auxiliary heater mass flow rate during the domestic hot water charging loop [kg/h]

$\dot{m}_{AUX,SH}$: Auxiliary heater mass flow rate during the space heating charging loop [kg/h]

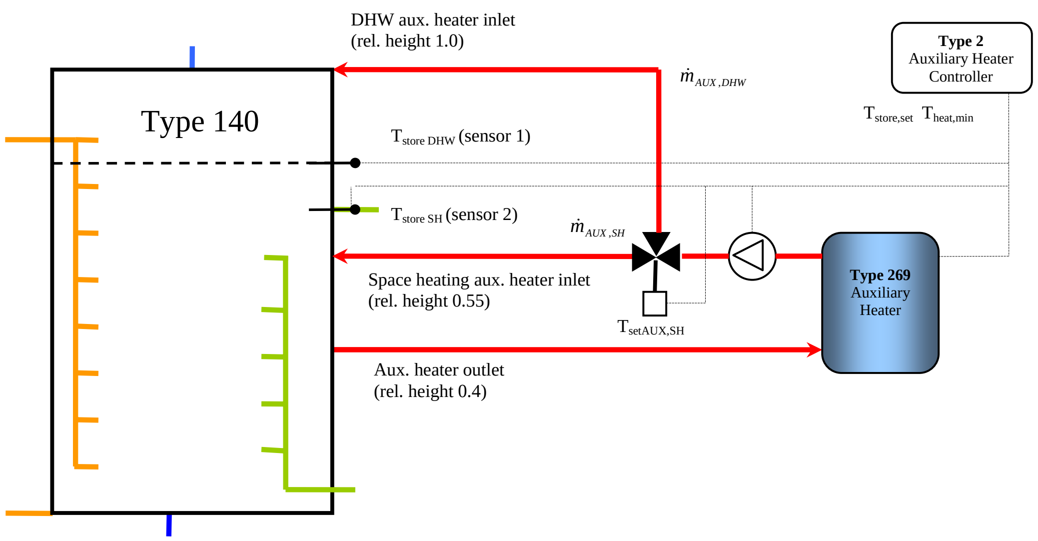

Figure 6-6: Boiler loop control system in detail

6.4.3. Control of the space heating

As the Figure 6-7 shows, in the reference model, like in traditional systems, the heating power is controlled varying the supply temperature that enters the heating pipe. A special controller, TRNSYS Non-standard Type 291, has been created to control the set temperature of the tempering valve and achieve this goal.

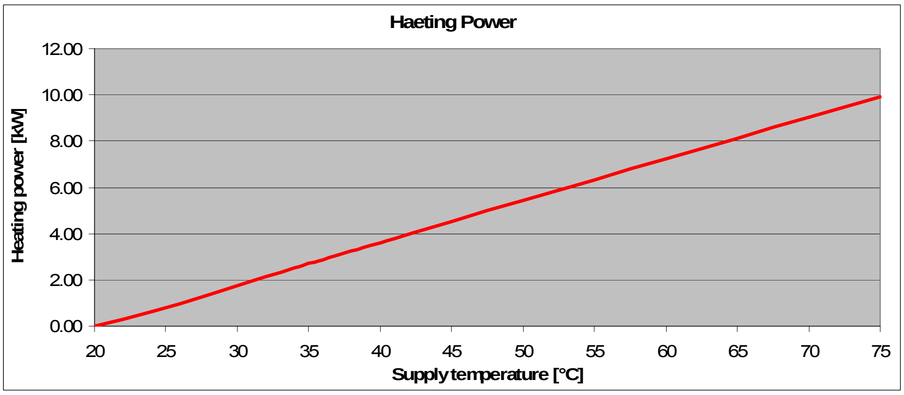

Figure 6-7: Heat power in function of the SH supply temperature

This controller has as input the needed heating power contained into the external load file and the space heating pump flow rate (see section 5.3.6). By means of these inputs the controller chooses the set temperature of the space heating water supply to match the requested heat power.

A more detailed mathematical description of this special controller is presented in appendix B.

7. *Definitions*

7.1. Nomenclature

As expression of the system performance during the optimization process and to make some comparison between the Direct Feed Flow Controlled system and the reference model the following indicators are used:

$Q_{SH,\text{target}}$ Space heating energy demand (based on load file) [kWh/a].

$Q_{SH,eff}$ Effective space heating energy delivered to the building [kWh/a].

$Q_{solar,\text{tank}}$ Usable solar energy that enter the storage tank [kWh/a].

$Q_{solar,loses}$ Solar loop pipe losses [kWh/a].

Q_{DHW} Energy delivered to the domestic hot water [kWh/a].

Q_{boiler} Energy supplied from gas boiler to heating media [kWh/a].

$Q_{cond,gain}$ Thermal energy gain from condensate gas flue exiting the boiler [kWh/a].

E_{boiler} Final energy consumption of auxiliary boiler (based on H_u) [kWh/a].

$E_{boiler,ref}$ Annual final auxiliary energy demand of the basis case or the reference system [kWh/a].

$Q_{\text{tank,loses}}$ Thermal loses of the storage tank [kWh/a].

n_{boiler} Number of boiler ON-OFF cycles during a year [1/a].

t_{boiler} Boiler run time in hours per year [h/a].

$V_{DHW\,40}$ Number of liter of domestic hot water under the comfort temperature of 40°C per year [l/a].

$\eta_{boiler} = \frac{Q_{boiler}}{E_{boiler}}$ Mean annual efficiency of auxiliary boiler [-].

$Q_{load} = Q_{SH,eff} + Q_{DHW} + Q_{\text{tank,loses}}$ Total heat load of the system [kWh/a].

$Solar_{\%} = \frac{Q_{load} - Q_{boiler}}{Q_{load}}$ Annual solar fraction [-].

7.2. Target Function

The target function used for the optimization process is based on fractional energy savings f_{sav} of the solar combisystem compared to the base case or to the reference system.

$f_{sav,ref} = 1 - \frac{E_{boiler}}{E_{boiler,ref}}$ Final energy saved referred to the base case

8. *Validation of the model*

8.1. Time step

For all the simulations a time step of 3 minutes is chosen. The models don't allow to change it because otherwise the space heating file is not read correctly. The timestep selected is be a good compromise between accuracy and simulation speed.

8.2. Convergence and integral tolerances

The TRNSYS models accuracy calculation is evaluated by varying the convergence and integral tolerance from 0.1 to 0.001. It is decided that the necessary accuracy is obtained when the differences in f_{sav} , Q_{SH} , Q_{Boiler}, E_{boiler} , E_{solar} between actual and previous run are below 0.2%. As Table 8-1 to Table 8-4 show, an integral and convergence accuracy value of 0.01 are chosen.

8.2.1. Direct Deed Flow Controlled

Table 8-1: Influence of the TRNSYS convergence and integral tolerances

Integration and Convergence tolerance	Q_{SH} [kWh]	Q_{Boiler} [kWh]	E_{boiler} [kWh]	E_{solar} [kWh]	$f_{sav,ref}$ [%]
0.05	-8324.76	8789.34	8385.89	4266.25	-0.698
0.04	-8345.68	8807.15	8400.06	4271.36	-0.869
0.03	-8325.78	8788.51	8360.13	4271.71	-0.389
0.02	-8355.87	8815.99	8344.20	4275.96	-0.198
0.01	-8358.02	8813.70	8327.73	4283.49	0.000
0.005	-8358.73	8808.50	8319.62	4289.52	0.097
0.001	-8359.64	8809.09	8321.62	4288.28	0.073
0.0005	-8362.03	8812.04	8324.92	4287.30	0.034
0.0001	-8363.13	8813.32	8326.06	4286.66	0.020

Table 8-2: Difference caused by the convergence and the integral tolerances variation

	Relative difference				
Integration and Convergence tolerance	Q_{SH} [kWh]	Q_{Boiler} [kWh]	E_{boiler} [kWh]	E_{solar} [kWh]	$f_{sav,ref}$ [%]
0.04	0.251%	0.202%	0.169%	0.120%	0.170%
0.03	-0.239%	-0.212%	-0.478%	0.008%	0.480%
0.02	0.360%	0.312%	-0.191%	0.099%	0.191%
0.01	0.026%	-0.026%	-0.198%	0.176%	0.198%
0.005	0.009%	-0.059%	-0.097%	0.141%	0.097%
0.001	0.011%	0.007%	0.024%	-0.029%	0.024%
0.0005	0.029%	0.033%	0.040%	-0.023%	0.040%
0.0001	0.013%	0.014%	0.014%	-0.015%	0.014%

8.2.2. Reference model

Table 8-3: Influence of the TRNSYS convergence and integral tolerances

Integration and Convergence tolerance	Q_{SH} [kWh]	Q_{Boiler} [kWh]	E_{boiler} [kWh]	E_{solar} [kWh]	$f_{sav,ref}$ [%]
0.05	-8332.86	8927.05	8556.25	4144.15	-2.74
0.04	-8334.17	8922.05	8542.11	4155.56	-2.57
0.03	-8338.20	8920.56	8531.66	4158.16	-2.45
0.02	-8338.33	8914.73	8524.53	4164.43	-2.36
0.01	-8345.23	8915.19	8522.71	4170.96	-2.34
0.005	-8347.51	8907.49	8512.83	4180.85	-2.22
0.001	-8331.85	8895.23	8497.71	4176.96	-2.04
0.0005	-8330.53	8894.38	8495.81	4176.49	-2.02
0.0001	-8328.38	8894.33	8492.70	4174.15	-1.98

Table 8-4: Difference caused by the convergence and the integral tolerances variation

	Relative difference				
Integration and Convergence tolerance	Q_{SH} [kWh]	Q_{Boiler} [kWh]	E_{boiler} [kWh]	E_{solar} [kWh]	$f_{sav,ref}$ [%]
0.04	0.016%	-0.056%	-0.165%	0.275%	0.170%
0.03	0.048%	-0.017%	-0.122%	0.063%	0.125%
0.02	0.002%	-0.065%	-0.084%	0.150%	0.086%
0.01	0.083%	0.005%	-0.021%	0.157%	0.022%
0.005	0.027%	-0.086%	-0.116%	0.236%	0.119%
0.001	-0.188%	-0.138%	-0.178%	-0.093%	0.181%
0.0005	-0.016%	-0.010%	-0.022%	-0.011%	0.023%
0.0001	-0.026%	-0.001%	-0.037%	-0.056%	0.037%

8.3. Energy balance

The energy balance of the calculation is checked at the chosen tolerance of 0.01 and with a time step of 3 minutes.

8.3.1. Direct Feed Flow Controlled

Table 8-5: Energy balance of the Direct Feed Flow Controlled System

Energy supplied from gas boiler to heating media (Q_{boiler})	8813.698	kWh
Energy supplied from collector loop to storage ($Q_{solar,usable}$)	4283.49	kWh
Energy in	**13097.19**	kWh

Energy supplied from tank to space heating loop ($Q_{SH,eff}$)	-8358.02	kWh
DHW consumption (Q_{DHW})	-3038.43	kWh
Energy loses storage tank ($Q_{tank,loses}$)	-1680.11	kWh
Energy out	**-13076.6**	kWh

Difference in-out	**20.632**	kWh
Relative difference	0.158	%

8.3.2. Reference model

Table 8-6: Energy balance of the Reference Model

Energy supplied from gas boiler to heating media (Q_{boiler})	8915.19	kWh
Energy supplied from collector loop to storage ($Q_{solar,usable}$)	4170.96	kWh
Energy in	**13086.15**	kWh

Energy supplied from tank to space heating loop ($Q_{SH,eff}$)	-8345.23	kWh
DHW consumption (Q_{DHW})	-3036.89	kWh
Energy loses storage tank ($Q_{tank,loses}$)	-1683.78	kWh
Energy out	**-13065.91**	kWh

Difference in-out	**20.247**	kWh
Relative difference	0.155	%

9. *Sensitivity analysis and optimization*

9.1. Introduction

In order to optimize the two concept systems described in the previous sections and to check how they behave under different conditions a sensitivity analysis is performed. The study is executed starting from the base case of the systems and varying a parameter or maximal two at the same time maintaining the other constant to check how the model reacts.

9.2. Boiler Type 269 analyses

The auxiliary boiler is probably the most sensitive part of the simulated systems. It follows that the results of a good optimization depend most of all on it. For this reason in this chapter the performances of this unit are analyzed in detail. The parameters of the boiler unit TRNSYS non-standard Type 269 are them described in section 5.3.4. The inputs used as basis case in this chapter are described in Table 9-1. During this tests the boiler model is simulated alone in a separated TRNSYS deck file without any other element.

Table 9-1: Basis case inputs of the boiler stand alone analysis

Boiler basis case inputs	Set supply temperature (DHW and SH)	65 °C
	Water supply mass flow rate	200 kg/h
	Cold water temperature	30°C
	Air surplus number (λ)	1.2
	Hysteresis for Tset	5 °C
	Air temperature	15°C
	Fuel type	Natural gas

9.2.1. Steady state

The first analysis is performed on the boiler running in steady state condition. The auxiliary heater is maintained always on but allowing power modulation between 30% and 100%. Figure 9-1 shows the boiler efficiency as function of the feed water temperature entering the boiler. As the curve illustrates the efficiency is strongly dependent on the feed water temperature flowing into the boiler. In Figure 9-2 is plotted the efficiency as function of the boiler mass flow rate. For a fix value of the feed water temperature entering the boiler the efficiency variation due to the change in the mass flow is not so relevant.

In Figure 9-3 and Figure 9-4 is shown the thermal energy percent gain due to the exiting gas flue condensation. The curves demonstrate a relevant dependence on the boiler feed water temperature. Other side for a set fix water temperature of 30 °C (basis case) the condensation gain isn't much dependent of the mass flow rate trough the boiler.

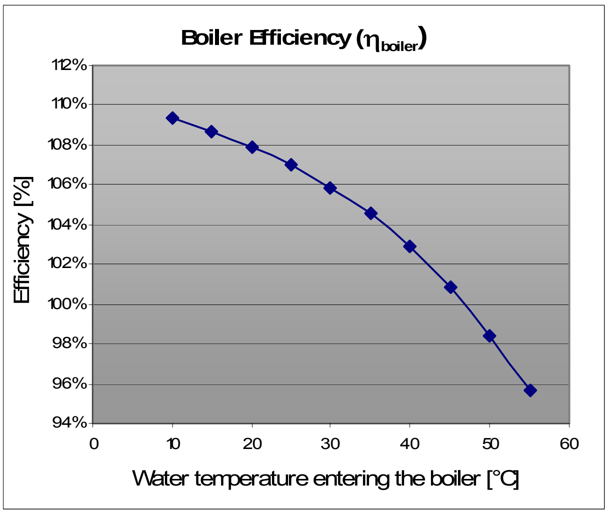

Figure 9-1: Boiler efficiency vs. feed water temperature

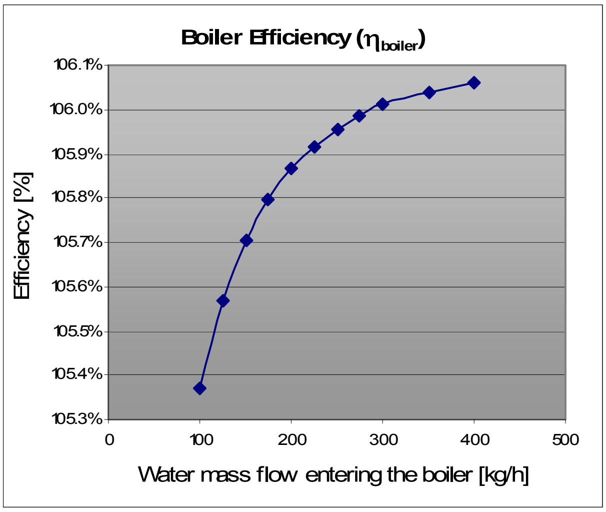

Figure 9-2: Boiler efficiency vs. water mass flow rate

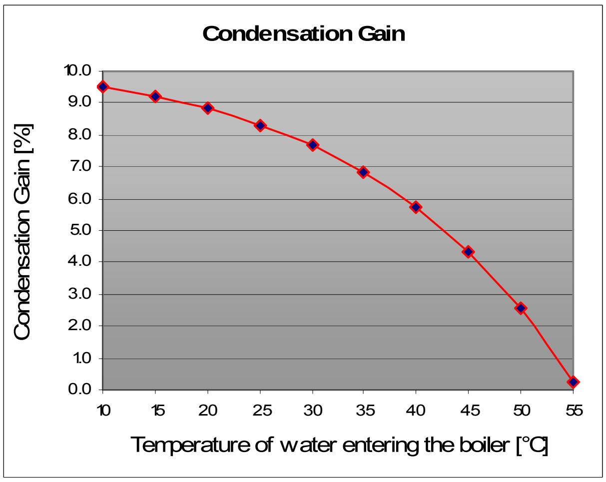

Figure 9-3: Condensation gain vs. feed water temperature

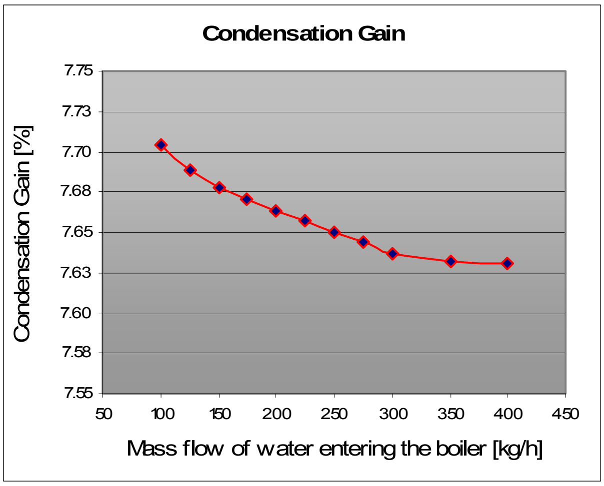

Figure 9-4: Condensation gain vs. water mass flow

As Figure 9-5 shows, for a different lambda value (varied from 1.0 to 1.3), a change in the boiler efficiency is only relevant for an high feed water temperature, condition that makes the boiler modulate the power at a very low level.

Figure 9-6 demonstrates hat the boiler efficiency is about 0.4-0.6% higher when the combustion air temperature is 10°C higher than the basis case value, this effect is a consequence of the less energy loosed to heat the air in the combustion chamber.

For a mass flow of 200 Kg/h the efficiency of the boiler is not dependant on the boiler water supply set temperature as Figure 9-7 shows.

Last test is performed to check which influence has the air humidity on the auxiliary heater efficiency. As the Figure 9-8 illustrates this parameter don't have any effect on the boiler performance.

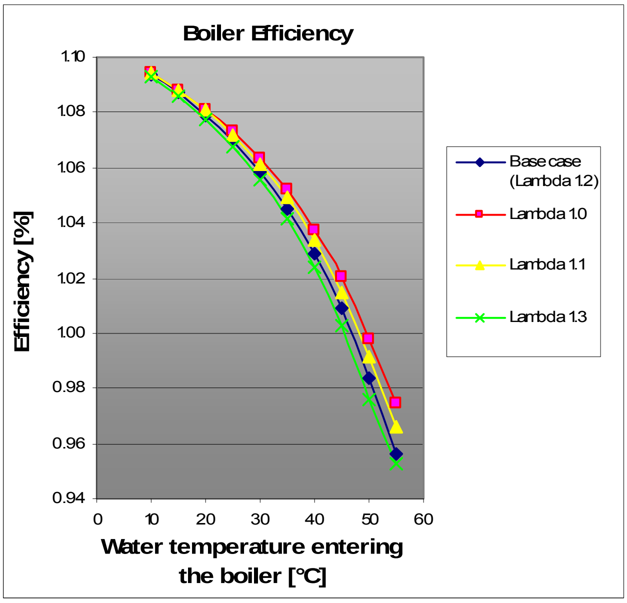

Figure 9-5: Boiler efficiency as function of the feed water temperature and the lambda value

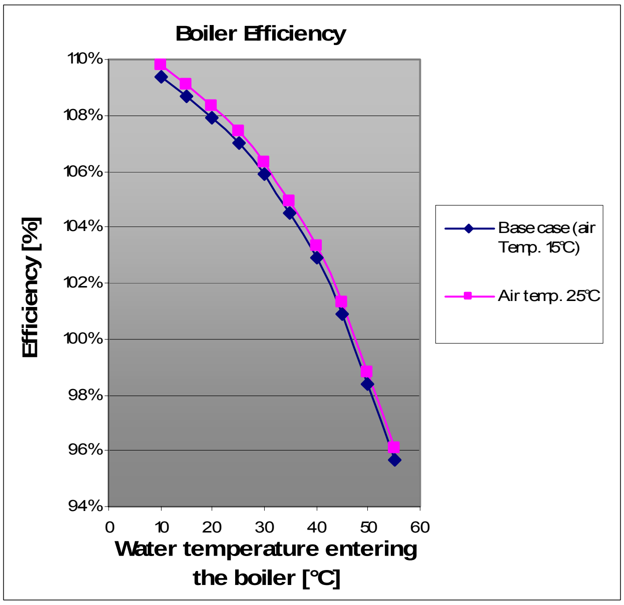

Figure 9-6: Boiler efficiency as function of the feed water temperature and the combustion air temperature

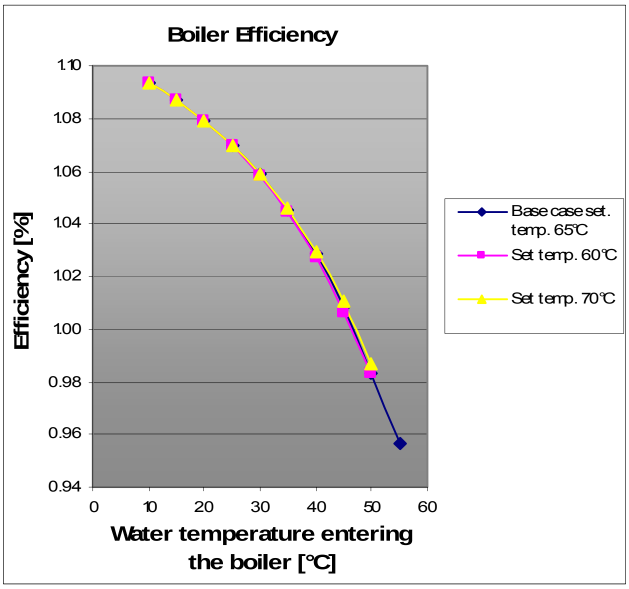

Figure 9-7: Boiler efficiency as function of the feed water temperature and the set supply temperature

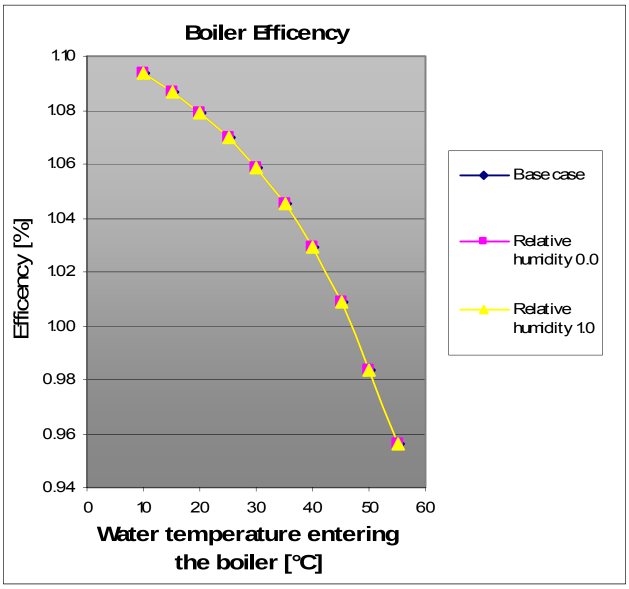

Figure 9-8: Boiler efficiency as function of the feed water temperature and the relative humidity of the air

9.2.2. Unsteady state

A second analysis is performed when the boiler is operating in an "unsteady state". As "Unsteady state" is described the condition when the boiler runs in a sequence of on-off cycles. This conditions might appear when the temperature of the water flowing into the boiler is very high and near its set supply temperature, or it could happen when the pump mass flow rate of the auxiliary heater is very low. Both of these conditions make the boiler run at the minimum of the allowed modulation power (in this case 30% of the maximum power: equivalent to 3.5 kW). In case that the minimum power is still too high, so to make the temperature at the boiler outlet rise more than 5°C higher than the set temperature, the gas firing is stopped until the supply temperature reaches the set value again.

Figure 9-9 shows the change between steady and unsteady state caused by the rise of the temperature of the water entering the boiler. As the curve demonstrates the efficiency continues approximately the same curve plotted for the steady state boiler run.

In Figure 9-10 is represented the boiler efficiency curve as function of the mass flow rate flowing through the auxiliary heater. In this case to maintain a set temperature of 65°C the boiler, because of the on-off cycles, shows a wavering curve with a maximum boiler efficiency variation in the order of 0.8%.

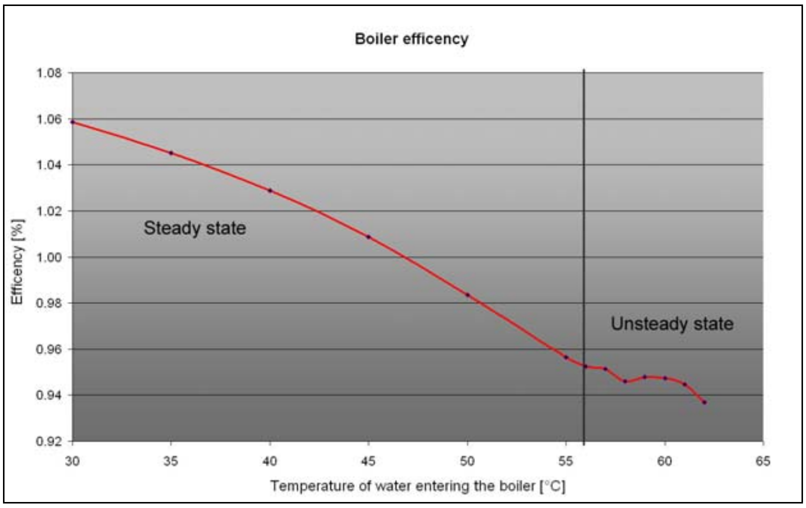

Figure 9-9: Boiler efficiency as function of the water feed temperature

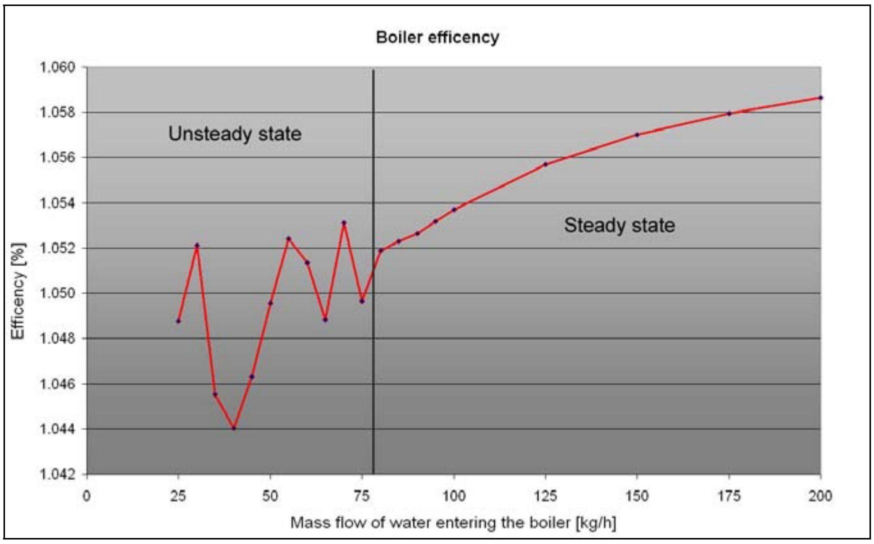

Figure 9-10: Boiler efficiency as function of the boiler mass flow rate

9.2.3. Conclusion

The results of the boiler operation analysis of section 9.2.1 and 9.2.2 show that the new boiler model (TRNSYS non-standard Type 269) created by Michel Haller satisfies all the operational condition and its outputs could be considered plausible in all the working conditions.

9.3. Direct Feed Flow Controlled system parameter analysis

9.3.1. Introduction

In this section is presented a complete parameter analysis of the Direct Feed Flow Controlled system described in chapter 5. The goal is to find possibility of optimization and to check the solidity of the simulation model. The study is subdivided into the main parts of the system: Auxiliary heater, storage tank, collector loop, space heating loop and domestic hot water.

The value of the saving function is always referred to the basis case of the Direct Feed Flow Controlled system. A positive value of the saving function means a better overall system efficiency than that of the basis case (see section 7.2)

9.3.2. Auxiliary heater

As said before the auxiliary heater is probably the most sensitive part of the entire system, only achieving to understand how the model behave in different situations can lead to a real possibility of system optimization. The followings parameter were analyzed:

Storage tank outlet to the auxiliary heater

The first parameter analysis has as goal to determine the optimum storage outlet position to the boiler, trying to find a good compromise between the solar and the boiler efficiency. Both the two heat sources have a better efficiency when they are fed with low temperature water, they are so in a kind of "competition".

Figure 9-12 shows the boiler efficiency (η_{boiler}) and the solar fraction ($solar_{\%}$). As was predictable the two curves have opposite course. For a lower position of the storage outlet to the boiler, therefore a lower temperature of the water entering the auxiliary heater, the boiler have an higher efficiency but "steals" some point to the solar part. For an higher outlet position the net solar gain is higher but the performance of the auxiliary heater drop down. So it's necessary to find a compromise between both heat sources efficiency.

The correlation between a lower outlet port position (lower water temperature) and a better boiler efficiency is due to a better energy gain from the condensation of the gas flue exiting the auxiliary heater as Figure 9-13 shows.

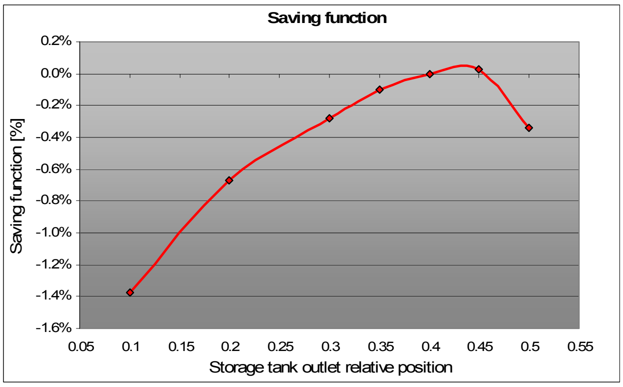

Figure 9-11: Saving function as function of the relative position of the storage outlet to the boiler

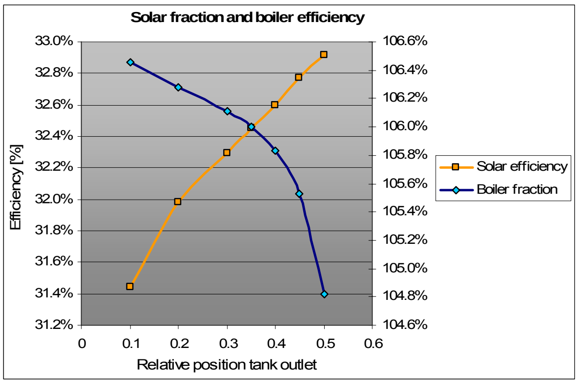

Figure 9-12: Solar fraction and boiler efficiency as function of the relative position of the storage outlet to the boiler

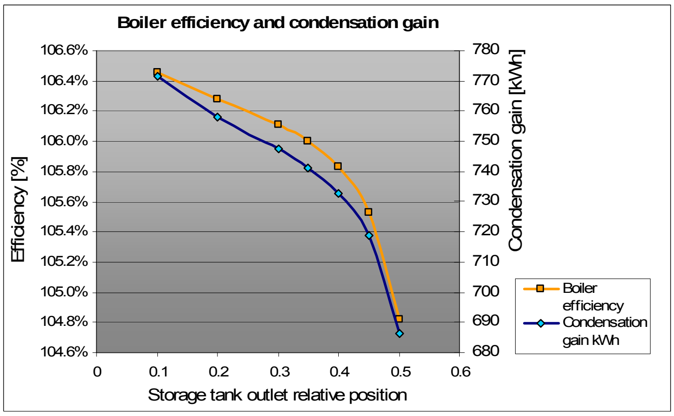

Figure 9-13: Boiler efficiency and condensation gain as function of the relative position of the storage outlet to the boiler

As Figure 9-11 illustrates the best compromise between the performances of the heat sources is given at a relative outlet height of 0.4-0.45. This value isn’t far from the base case value of 0.4, that can already be considered as optimized.

Table 9-2: Simulation results as function of the relative height of the storage outlet to the boiler

Relative height of the tank outlet to the auxiliary heater															
Parameter [-]	$Q_{SH,target}$ [kWh/a]	$Q_{SH,eff}$ [kWh/a]	$Q_{solar,tank}$ [kWh/a]	Qsolar,loses [kWh/a]	Q_{boiler} [kWh/a]	E_{boiler} [kWh/a]	Q_{DHW} [kWh/a]	V_{DHW40} [l/a]	Qtank,loses [kWh/a]	$Q_{cond,gain}$ [kWh/a]	n_{boiler} [1/a]	t_{boiler} [kWh/a]	$Solar_{\%}$ [%]	η_{boiler} [%]	f_{sav} [%]
0.10	-8379	-8359	4147	645	8987	8442	-3039	0	-1712	771	4286	1672	31.4%	106.5%	-1.37%
0.20	-8379	-8360	4213	639	8910	8383	-3039	0	-1700	758	4569	1701	32.0%	106.3%	-0.67%
0.30	-8379	-8359	4248	635	8861	8351	-3038	0	-1690	747	4802	1731	32.3%	106.1%	-0.28%
0.35	-8379	-8359	4267	632	8836	8336	-3038	0	-1684	741	4988	1752	32.5%	106.0%	-0.10%
0.40	-8379	-8358	4283	632	8814	8328	-3038	0	-1680	733	5242	1782	32.6%	105.8%	0.00%
0.45	-8379	-8356	4302	629	8786	8325	-3039	0	-1673	719	5879	1849	32.8%	105.5%	0.03%
0.50	-8379	-8349	4317	627	8759	8356	-3039	0	-1670	686	7906	2010	32.9%	104.8%	-0.34%

Auxiliary heater minimal modulation range

Allowing the auxiliary heater to run at very low power levels should reduce the number of boiler starts significantly. In this case, as Figure 9-15 shows, if the minimal boiler power is reduced under 30% of the maximal power, there are no further significant reduction in the number of boiler starts. This is due to the relative high boiler set temperature and boiler mass flow rate. These factors practically don't permit to the boiler to run at lower modulation range also when it would be possible. Another cause is the low feed water temperature entering the boiler which make the heat power needed increase.

If the minimal allowed power of the running boiler is raised above 30% of the maximal power, the number of boiler starts grow exponentially as we can see in Figure 9-15. There isn't any correlation between boiler starts and boiler efficiency in the simulation model, but in reality there should be a sink in efficiency for a very high number of boiler starts.

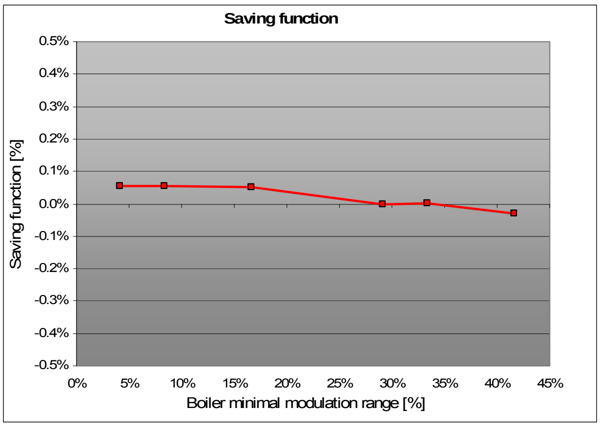

Figure 9-14: Saving function as function of the minimal modulation range of the gas boiler

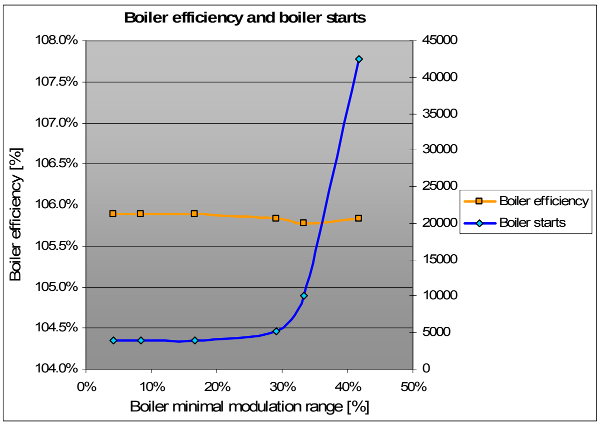

Figure 9-15: Boiler efficiency and number of boiler starts as function of the minimal modulation range of the gas boiler

Table 9-3: Simulation results as function of the minimal modulation range of the gas boiler

Minimal modulation range of the auxiliary heater															
Parameter [%]	$Q_{SH,target}$ [kWh/a]	$Q_{SH,eff}$ [kWh/a]	$Q_{solar,tank}$ [kWh/a]	$Q_{solar,loses}$ [kWh/a]	Q_{boiler} [kWh/a]	E_{boiler} [kWh/a]	Q_{DHW} [kWh/a]	V_{DHW40} [l/a]	$Q_{tank,loses}$ [kWh/a]	$Q_{cond,gain}$ [kWh/a]	n_{boiler} [1/a]	t_{boiler} [kWh/a]	$Solar_{\%}$ [%]	η_{boiler} [%]	f_{sav} [%]
4.2%	-8379	-8358	4283	631	8814	8323	-3039	0	-1679	732	3892	1782	32.6%	105.9%	0.05%
8.3%	-8379	-8358	4283	631	8814	8323	-3039	0	-1679	732	3892	1782	32.6%	105.9%	0.05%
16.7%	-8379	-8358	4283	631	8814	8323	-3039	0	-1679	732	3892	1782	32.6%	105.9%	0.05%
29.2%	-8379	-8358	4283	632	8814	8328	-3038	0	-1680	733	5242	1782	32.6%	105.8%	0.00%
33.3%	-8379	-8359	4290	631	8809	8328	-3038	0	-1682	733	10147	1776	32.6%	105.8%	0.00%
41.7%	-8379	-8359	4291	630	8816	8330	-3038	0	-1690	736	42546	1741	32.6%	105.8%	-0.03%

Boiler mass flow rate for the DHW charging loop

As shown in chapter 9.2.1 the boiler mass flow rate could bring an increase of the boiler efficiency if optimized. As described in section 5.4.2 the auxiliary heater has two differed charging cycles, one for the domestic hot water and another for the space heating charging loop. Figure 9-16 illustrates how the boiler behaves when the mass flow rate for the DHW charging loop is changed. As the plotted curve shows in this case any improvement in the boiler efficiency is noticeable for both lowering o increasing the mass flow rate.

During this analysis the auxiliary heater mass flow rate for the space heating charging loop remain the same as in the basis case.

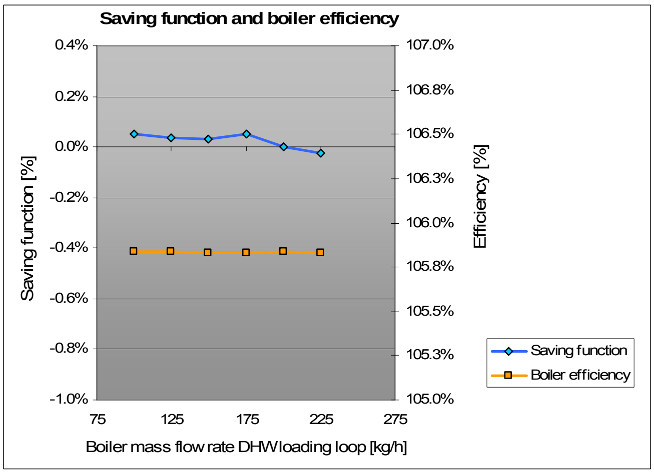

Figure 9-16: Saving function and boiler efficiency as function of the boiler mass flow rate for the DHW charging loop

Table 9-4: : Simulation results as function of the boiler mass flow rate for the DHW charging loop

Boiler mass flow rate for the DHW charging loop															
Parameter [kg/h]	$Q_{SH,target}$ [kWh/a]	$Q_{SH,eff}$ [kWh/a]	$Q_{solar,tank}$ [kWh/a]	$Q_{solar,loses}$ [kWh/a]	Q_{boiler} [kWh/a]	E_{boiler} [kWh/a]	Q_{DHW} [kWh/a]	V_{DHW40} [l/a]	$Q_{tank,loses}$ [kWh/a]	$Q_{cond,gain}$ [kWh/a]	n_{boiler} [1/a]	t_{boiler} [kWh/a]	$Solar_{\%}$ [%]	η_{boiler} [%]	f_{sav} [%]
100	-8379	-8354	4283	630	8809	8324	-3038	0	-1679	733	7343	1860	32.6%	105.8%	0.05%
125	-8379	-8356	4284	631	8811	8325	-3038	0	-1679	733	6076	1828	32.6%	105.8%	0.04%
150	-8379	-8357	4284	631	8811	8325	-3038	0	-1679	733	5525	1809	32.6%	105.8%	0.03%
175	-8379	-8358	4287	631	8809	8324	-3038	0	-1679	733	5214	1793	32.6%	105.8%	0.05%
200	-8379	-8358	4283	632	8814	8328	-3038	0	-1680	733	5242	1782	32.6%	105.8%	0.00%
225	-8379	-8359	4282	631	8816	8330	-3038	0	-1680	733	5424	1779	32.6%	105.8%	-0.02%

Boiler mass flow rate for the space heating charging loop

In the base case of the Direct Feed Flow Controlled system the mass flow rate of the boiler, when operating for the space heating charging loop, is a function of the space heating pump flow rate and it follows the relation given by Equation 9-1 (as described in section 5.4.2).

$$\dot{m}_{AUX,SH} = \dot{m}_{SH} + C \qquad \textit{Equation 9-1}$$

The "plus" factor given by the constant *C* for the base case is set to 30 kg/h. Figure 9-18 shows how the boiler efficiency and the solar fraction change if the value of *C* is varied. As is demonstrated by Figure 9-17 the optimum value of *C* is between 30-35 kg/h, it follows that the chosen basis case value of 30 kg/h can considered as already optimized.

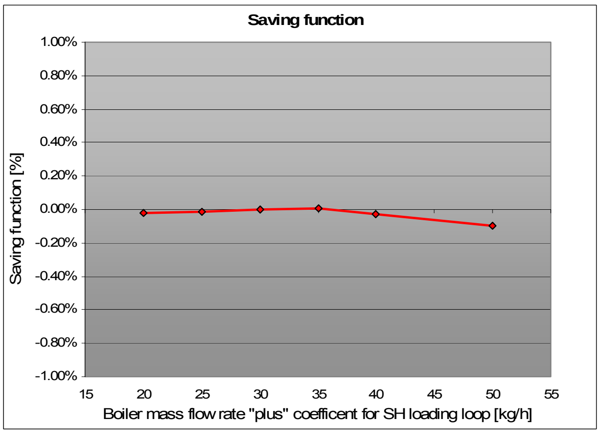

Figure 9-17: Saving function as function of the C constant

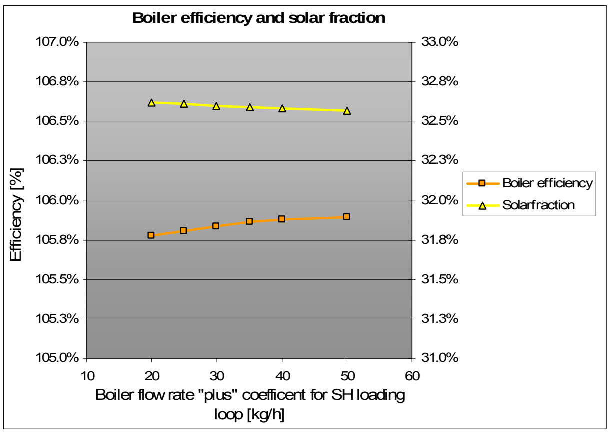

Figure 9-18: Boiler efficiency and solar fraction as function of the C constant

Table 9-5: Simulation results as function of the C constant

Constant boiler mass flow rate for the SH charging loop (C parameter)																
Parameter [kg/h]	$Q_{SH,target}$ [kWh/a]	$Q_{SH,eff}$ [kWh/a]	$Q_{solar,tank}$ [kWh/a]	$Q_{solar,loses}$ [kWh/a]	Q_{boiler} [kWh/a]	E_{boiler} [kWh/a]	Q_{DHW} [kWh/a]	V_{DHW40} [l/a]	$Q_{tank,loses}$ [kWh/a]	$Q_{cond,gain}$ [kWh/a]	n_{boiler} [1/a]	t_{boiler} [kWh/a]	$Solar_{\%}$ [%]	η_{boiler} [%]	f_{sav} [%]
75	-8379	-8092	4281	632	8555	8096	-3038	0	-1686	710	11484	2263	33.2%	105.7%	2.78%
80	-8379	-8162	4281	632	8619	8154	-3038	0	-1680	713	6002	2196	33.1%	105.7%	2.09%
85	-8379	-8216	4283	632	8668	8197	-3038	0	-1678	718	3140	2105	33.0%	105.7%	1.57%
90	-8379	-8242	4282	632	8696	8222	-3038	0	-1677	720	2916	2014	32.9%	105.8%	1.27%
95	-8379	-8270	4284	632	8721	8244	-3038	0	-1677	723	3157	1925	32.8%	105.8%	1.01%
100	-8379	-8292	4283	632	8746	8265	-3038	0	-1677	726	3411	1840	32.8%	105.8%	0.75%
125	-8379	-8360	4283	632	8814	8327	-3039	0	-1678	732	4454	1504	32.6%	105.8%	0.01%
150	-8379	-8383	4283	632	8837	8349	-3039	0	-1678	734	5192	1275	32.5%	105.8%	-0.26%
175	-8379	-8400	4285	631	8854	8365	-3039	0	-1678	735	5690	1110	32.5%	105.8%	-0.45%
200	-8379	-8415	4285	631	8868	8379	-3039	0	-1678	736	6239	985	32.5%	105.8%	-0.62%
225	-8379	-8429	4285	631	8882	8393	-3039	0	-1678	737	6430	888	32.4%	105.8%	-0.79%
250	-8379	-8438	4284	632	8893	8405	-3040	0	-1679	737	6274	811	32.4%	105.8%	-0.93%
300	-8379	-8446	4269	633	8898	8415	-3037	0	-1665	730	6187	770	32.3%	105.7%	-1.05%
350	-8379	-8448	4252	635	8905	8440	-3035	250	-1655	717	6172	819	32.2%	105.5%	-1.35%
400	-8379	-8434	4235	638	8918	8472	-3036	293	-1665	700	5565	912	32.1%	105.3%	-1.74%

Instead of a variable mass flow rate of the boiler when it operates controlled by the space heating sensor (sensor 2) it's now tried to maintain this flow constant as Equation 9-2 describes.

$$\dot{m}_{AUX,SH} = D \qquad \textit{Equation 9-2}$$

Figure 9-19 and Figure 9-20 show the saving function, the solar fraction and the boiler efficiency for different values of the constant *D*.

For a constant value of $\dot{m}_{AUX,SH}$ it seems that the overall system efficiency is higher but as Figure 9-21 demonstrates the energy delivered to the space heating is not constant and differs from the goal value of 8379 kWh is some cases for more than 3.5%. It is so impossible to make a fair comparison.

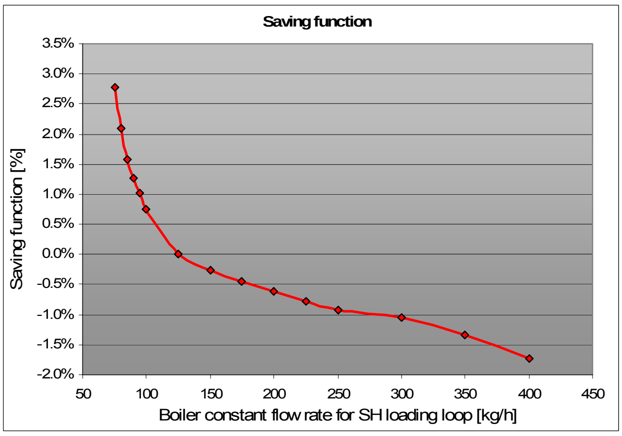

Figure 9-19: Saving function as function of the D constant

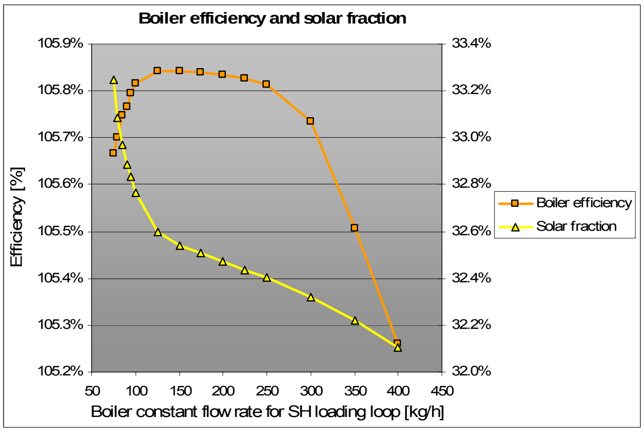

Figure 9-20: Boiler efficiency and solar fraction as function of the D constant

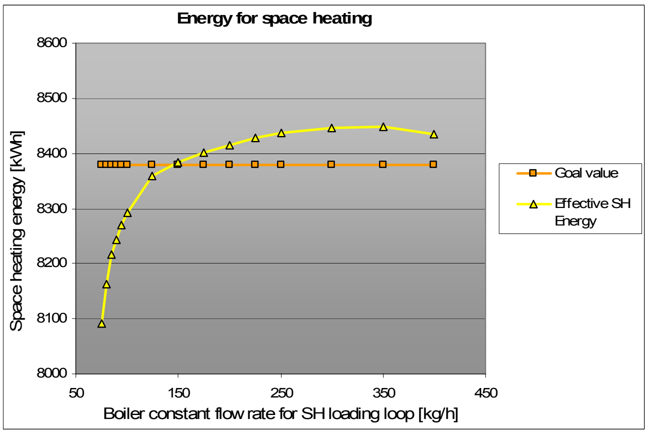

Figure 9-21: Heat energy delivered by the space heating as function of the D constant

Table 9-6: Simulation results as function of the D constant

Boiler mass flow rate D parameter for the SH charging loop															
Parameter [kg/h]	$Q_{SH,target}$ [kWh/a]	$Q_{SH,eff}$ [kWh/a]	$Q_{solar,tank}$ [kWh/a]	$Q_{solar,loses}$ [kWh/a]	Q_{boiler} [kWh/a]	E_{boiler} [kWh/a]	Q_{DHW} [kWh/a]	V_{DHW40} [l/a]	$Q_{tank,loses}$ [kWh/a]	$Q_{cond,gain}$ [kWh/a]	n_{boiler} [1/a]	t_{boiler} [kWh/a]	$Solar_{\%}$ [%]	η_{boiler} [%]	f_{sav} [%]
20	-8379	-8356	4287	631	8811	8329	-3038	0	-1682	734	10235	1964	32.6%	105.8%	-0.02%
25	-8379	-8357	4284	632	8812	8329	-3038	0	-1681	733	6981	1869	32.6%	105.8%	-0.01%
30	-8379	-8358	4283	632	8814	8328	-3038	0	-1680	733	5242	1782	32.6%	105.8%	0.00%
35	-8379	-8360	4283	632	8816	8327	-3039	0	-1679	732	4575	1704	32.6%	105.9%	0.00%
40	-8379	-8364	4283	632	8819	8330	-3039	0	-1679	733	4477	1633	32.6%	105.9%	-0.03%
50	-8379	-8372	4283	632	8827	8336	-3039	0	-1679	733	4701	1508	32.6%	105.9%	-0.10%

Boiler set temperature

Next analysis is performed on the set supply temperature of the auxiliary heater. As Figure 9-23 shows a slight increase of the boiler efficiency is noticeable rising the supply temperature. Figure 9-23 demonstrates that this boiler efficiency increase don't lead to any final energy saving improvement of the system. The cause is probably to be found in the increased heat loses of the storage tank, compensating so the higher boiler efficiency. A set supply temperature optimum value is found between 62 and 67 °C. It follows that the chosen set temperature of 65°C for the base case can already de considered as optimized.

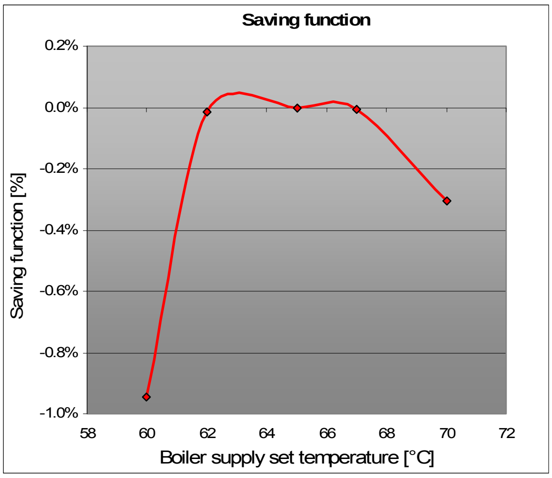

Figure 9-22: Saving function as function of the boiler set supply temperature

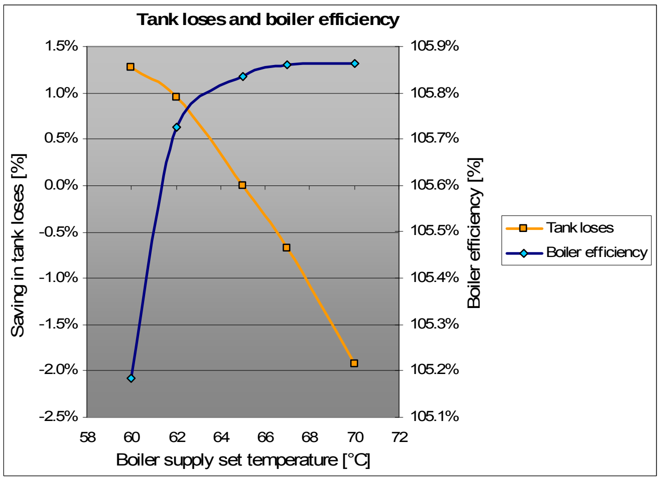

Figure 9-23: Storage loses and boiler efficiency as function of the boiler set supply temperature

Table 9-7: Simulation results as function of the boiler set supply temperature

Boiler set temperature for DHW and SH															
Parameter [°C]	$Q_{SH,target}$ [kWh/a]	$Q_{SH,eff}$ [kWh/a]	$Q_{solar,tank}$ [kWh/a]	$Q_{solar,loses}$ [kWh/a]	Q_{boiler} [kWh/a]	E_{boiler} [kWh/a]	Q_{DHW} [kWh/a]	V_{DHW40} [l/a]	$Q_{tank,loses}$ [kWh/a]	$Q_{cond,gain}$ [kWh/a]	n_{boiler} [1/a]	t_{boiler} [kWh/a]	$Solar_{\%}$ [%]	η_{boiler} [%]	f_{sav} [%]
60	-8379	-8361	4243	637	8842	8406	-3036	0	-1659	698	7814	1952	32.3%	105.2%	-0.95%
62	-8379	-8360	4275	632	8806	8329	-3037	0	-1664	724	5455	1854	32.6%	105.7%	-0.01%
65	-8379	-8358	4283	632	8814	8328	-3038	0	-1680	733	5242	1782	32.6%	105.8%	0.00%
67	-8379	-8359	4294	631	8816	8328	-3039	0	-1691	736	5368	1739	32.6%	105.9%	-0.01%
70	-8379	-8359	4289	630	8843	8353	-3039	0	-1712	741	5165	1660	32.6%	105.9%	-0.31%

9.3.3. Storage tank

Cut off temperature in storage tank

The maximum allowed temperature inside the storage tank and it's influence on the overall system efficiency is of major interest for the Direct Feed Flow Controlled system. Most of all to check if a cheap plastic-made storage with a limited maximal temperature have an negative repercussion on the overall solar gain.

During the operation the maximum temperature inside the tank is only reached when there's lot of sun and the solar collectors are working at full load, this means when it were possible to increase the solar gain.

Figure 9-24 and Figure 9-25 show the variation of the saving function and the solar fraction by changing the cut off temperature in the storage tank. As it's demonstrated limiting the maximum storage tank temperature by 70°C about 3.0% more final energy (gas) is needed and the overall solar fraction is about 3.5% lower.

These results are interesting because they show that also in the worst case, strongly limiting the temperature inside the storage, the drop in the saving function isn't so pronounced. The explanation is to be found in the fact that the system, also with a limited maximal allowed temperature, can practically cover the domestic hot water load during the sunny months. During the heating season instead the collectors don't have the capacity to heat the storage above 70°C it follows that the maximal storage tank temperature is never reached.

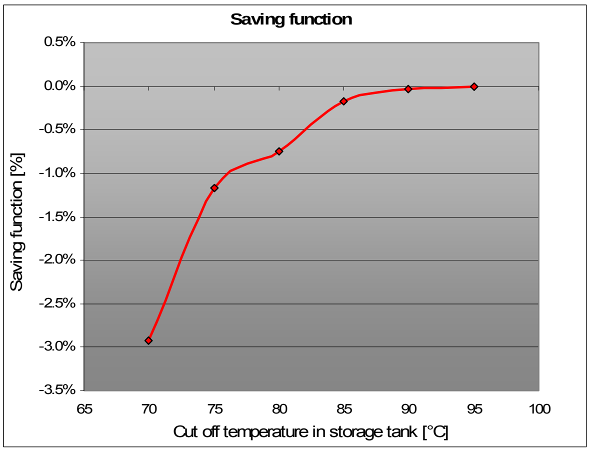

Figure 9-24: Saving function as function of the cut off temperature in the storage tank

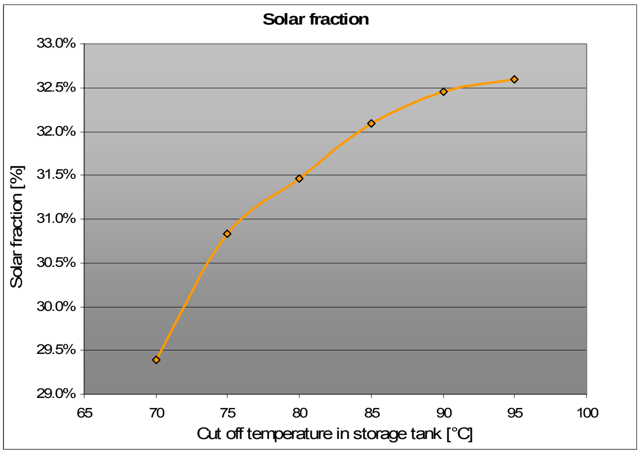

Figure 9-25: Solar fraction as function of the cut off temperature in the storage tank

In Figure 9-26 are plotted the storage tank and the collector pipes loses in function of the storage cut off temperature.

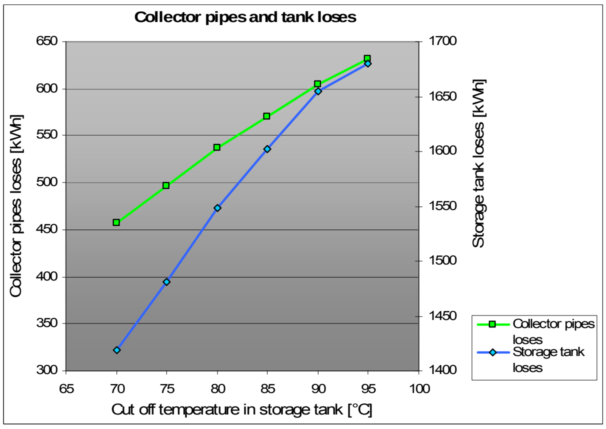

Figure 9-26: Collector pipes and storage tank loses as function of the cut off temperature in the storage

Table 9-8: Simulation results as function of the cut off temperature in the storage tank

Storage tank cut off temperature															
Parameter [°C]	$Q_{SH,target}$ [kWh/a]	$Q_{SH,eff}$ [kWh/a]	$Q_{solar,tank}$ [kWh/a]	$Q_{solar,loses}$ [kWh/a]	Q_{boiler} [kWh/a]	E_{boiler} [kWh/a]	Q_{DHW} [kWh/a]	V_{DHW40} [l/a]	$Q_{tank,loses}$ [kWh/a]	$Q_{cond,gain}$ [kWh/a]	n_{boiler} [1/a]	t_{boiler} [kWh/a]	$Solar_{\%}$ [%]	η_{boiler} [%]	f_{sav} [%]
65	-8379	-8363	1081	161	11489	10867	-3038	133	-1148	960	8736	2371	8.5%	105.7%	-30.50%
70	-8379	-8358	3787	457	9049	8571	-3038	0	-1419	745	5272	1840	29.4%	105.6%	-2.92%
75	-8379	-8358	3991	496	8907	8425	-3038	0	-1481	737	5323	1806	30.8%	105.7%	-1.17%
80	-8379	-8358	4094	537	8871	8390	-3038	63	-1549	735	5162	1795	31.5%	105.7%	-0.74%
85	-8379	-8358	4191	570	8827	8343	-3038	0	-1602	733	5231	1786	32.1%	105.8%	-0.18%
90	-8379	-8358	4256	604	8815	8330	-3038	0	-1655	733	5244	1783	32.5%	105.8%	-0.03%
95	-8379	-8358	4283	632	8814	8328	-3038	0	-1680	733	5242	1782	32.6%	105.8%	0.00%

Storage tank volume

The volume of the storage tank has a big influence on the cost of the solar combisystem. In this section the effect of the this parameter variation is analyzed referred to the overall energy efficiency of the system. Table 9-9 shows how the storage tank loss coefficient is recalculated in function of the usable volume. The DHW sensor (sensor 1), as all other parameters such as the inlet and outlet ports and sensors relative height are maintained unaltered. It follows that the volume reserved for the DHW varies in function of the overall storage tank volume (third colon of Table 9-9).

Table 9-9: Storage loses coefficient and DHW reserved volume as function of the total storage tank volume

Storage Volume [Liters]	**Loses coefficient** [kJ/h]	**DHW volume** [liters]
400	13.84	120
500	14.98	150
600	16.11	180
700	17.10	210
800	18.08	240
900	18.97	270
1000	19.86	300
1100	20.70	330
1200	21.53	360

As Figure 9-28 demonstrates, varying the storage volume from 400 to 1200 liter a solar fraction change from 29% to 36% is noticeable. The saving function don't vary much also for big difference in storage tank volume compared to the base case.

As Figure 9-27 shows the auxiliary final energy saved with a storage volume increased by 50% (from 800 to 1200 liters) is only about 0.7%. This fact is to conduct to the higher storage tank loses derived by a bigger volume that aren't balanced by a so high solar gain. This fact is illustrated by Figure 9-29.

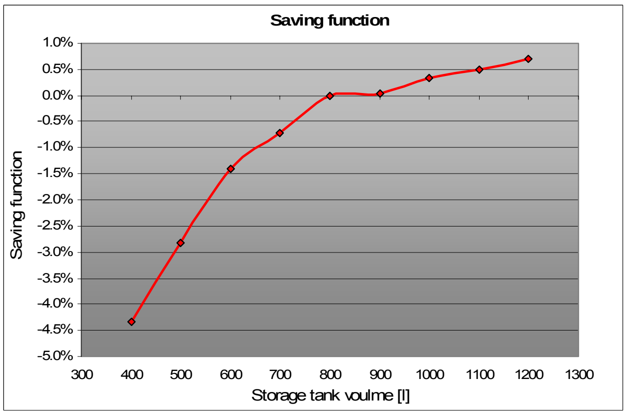

Figure 9-27: Saving function as function of the storage tank total volume

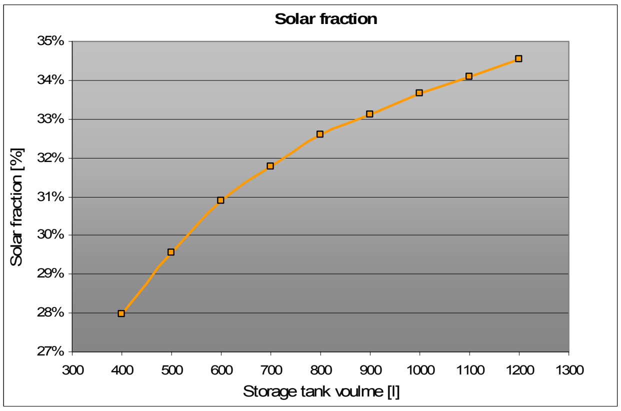

Figure 9-28: Solar fraction as function of the storage tank total volume

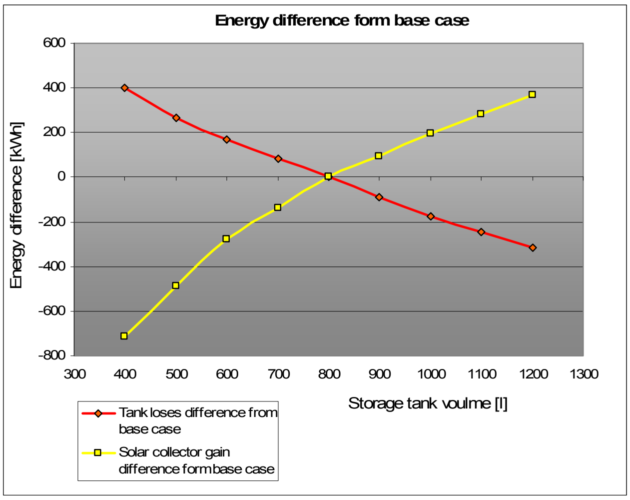

Figure 9-29: Energy difference from the base case as function of the storage tank volume

Table 9-10: Simulation results as function of the storage tank total volume

Storage tank volume															
Parameter [liters]	$Q_{SH,target}$ [kWh/a]	$Q_{SH,eff}$ [kWh/a]	$Q_{solar,tank}$ [kWh/a]	$Q_{solar,loses}$ [kWh/a]	Q_{boiler} [kWh/a]	E_{boiler} [kWh/a]	Q_{DHW} [kWh/a]	V_{DHW40} [l/a]	$Q_{tank,loses}$ [kWh/a]	$Q_{cond,gain}$ [kWh/a]	n_{boiler} [1/a]	t_{boiler} [kWh/a]	$Solar_{\%}$ [%]	η_{boiler} [%]	f_{sav} [%]
400	-8379	-8408	3570	664	9167	8689	-3038	55	-1281	749	7649	1706	28.0%	105.5%	-4.34%
500	-8379	-8356	3797	657	9022	8563	-3038	55	-1413	734	6611	1907	29.5%	105.4%	-2.83%
600	-8379	-8358	4004	648	8917	8444	-3038	0	-1509	735	6056	1859	30.9%	105.6%	-1.40%
700	-8379	-8358	4146	639	8867	8388	-3039	0	-1598	734	5332	1803	31.8%	105.7%	-0.72%
800	-8379	-8358	4283	632	8814	8328	-3038	0	-1680	733	5242	1782	32.6%	105.8%	0.00%
900	-8379	-8343	4379	626	8797	8325	-3038	0	-1771	727	5739	1879	33.1%	105.7%	0.04%
1000	-8379	-8343	4480	622	8781	8299	-3038	0	-1853	730	5666	1863	33.6%	105.8%	0.34%
1100	-8379	-8342	4565	616	8768	8287	-3038	0	-1923	728	4870	1837	34.1%	105.8%	0.49%
1200	-8379	-8342	4654	612	8753	8269	-3038	0	-1995	728	4860	1824	34.6%	105.9%	0.70%

9.3.4. Collector loop

Collector area

The first parameter analysis that concern the collector loop is the variation of the collector area. As expected the solar fraction increases for a bigger collector area, from a 50% bigger collector area there's a solar fraction increase of 5.5 % and a final energy saving of about 7% (Figure 9-30).

The effective final energy saving of the auxiliary heater per year should be compared to the higher investment costs caused by an higher collector area to find a cost-related optimized value.

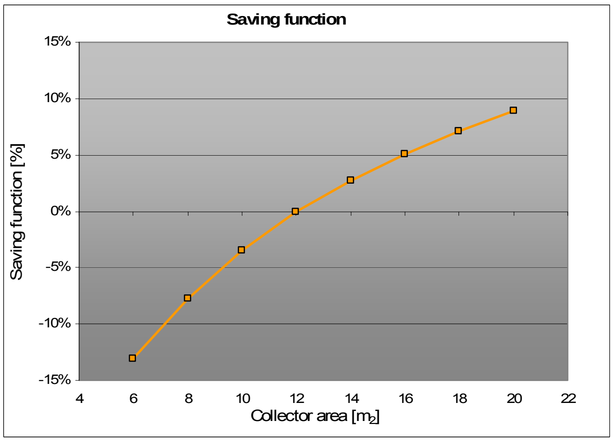

Figure 9-30: Saving function as function of the collector area

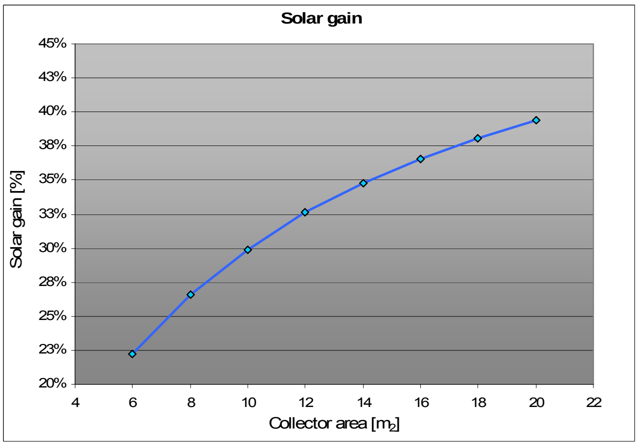

Figure 9-31: Solar fraction as function of the collector area

Table 9-11: Simulation results as function of the collector area

Collector area															
Parameter [m^2]	$Q_{SH,target}$ [kWh/a]	$Q_{SH,eff}$ [kWh/a]	$Q_{solar,tank}$ [kWh/a]	$Q_{solar,loses}$ [kWh/a]	Q_{boiler} [kWh/a]	E_{boiler} [kWh/a]	Q_{DHW} [kWh/a]	V_{DHW40} [l/a]	$Q_{tank,loses}$ [kWh/a]	$Q_{cond,gain}$ [kWh/a]	n_{boiler} [1/a]	t_{boiler} [kWh/a]	$Solar_{\%}$ [%]	η_{boiler} [%]	f_{sav} [%]
6	-8379	-8360	2870	483	9947	9417	-3037	133	-1399	823	6143	2038	22.3%	105.6%	-13.08%
8	-8379	-8359	3461	558	9483	8970	-3038	0	-1527	786	5790	1935	26.6%	105.7%	-7.72%
10	-8379	-8359	3909	601	9116	8617	-3038	0	-1608	757	5351	1844	29.9%	105.8%	-3.47%
12	-8379	-8358	4283	632	8814	8328	-3038	0	-1680	733	5242	1782	32.6%	105.8%	0.00%
14	-8379	-8358	4586	654	8575	8100	-3039	0	-1744	713	4989	1727	34.7%	105.9%	2.73%
16	-8379	-8357	4836	665	8365	7901	-3038	0	-1785	696	4946	1688	36.5%	105.9%	5.12%
18	-8379	-8356	5047	680	8191	7738	-3038	0	-1823	681	4769	1651	38.0%	105.9%	7.08%
20	-8379	-8356	5244	687	8026	7582	-3038	0	-1854	667	4614	1614	39.4%	105.9%	8.96%

Collector a_1 coefficient

Another parameter that is analyzed is the solar collector efficiency parameter a_1. This parameter is varied form the base case value of 3.5 W/m2.K to a optimal value of 1.0 W/m2.K. This study is very theoretical because so low a_1 coefficients are practically not reachable with standard collectors. The result of the saving function and solar fraction are show by the Figure 9-32 and Figure 9-33 respectively.

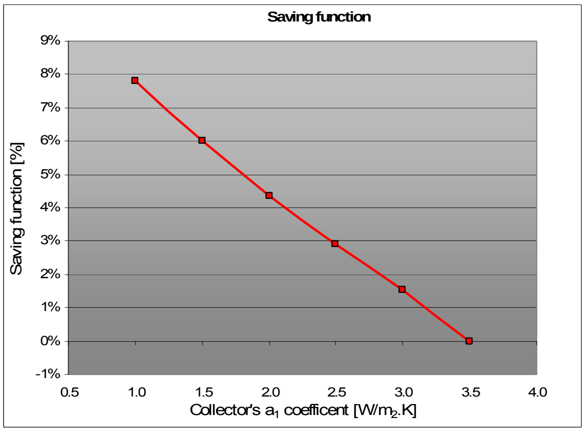

Figure 9-32: Saving function as function of the collector a_1 coefficient

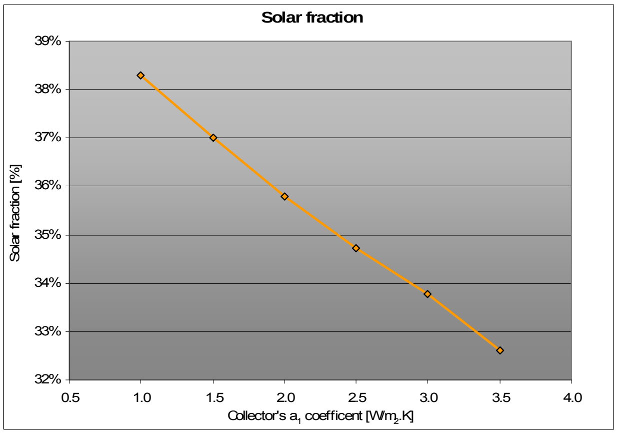

Figure 9-33: Solar fraction as function of the collector a_1 coefficient

Table 9-12: Simulation results as function of the collector a_1 coefficient

Collector a_1 coefficent															
Parameter [$W/m_2.K$]	$Q_{SH,target}$ [kWh/a]	$Q_{SH,eff}$ [kWh/a]	$Q_{solar,tank}$ [kWh/a]	$Q_{solar,loses}$ [kWh/a]	Q_{boiler} [kWh/a]	E_{boiler} [kWh/a]	Q_{DHW} [kWh/a]	V_{DHW40} [l/a]	$Q_{tank,loses}$ [kWh/a]	$Q_{cond,gain}$ [kWh/a]	n_{boiler} [1/a]	t_{boiler} [kWh/a]	$Solar_{\%}$ [%]	η_{boiler} [%]	f_{sav} [%]
3.50	-8379	-8358	4283	632	8814	8328	-3038	0	-1680	733	5242	1782	32.6%	105.8%	0.00%
3.00	-8379	-8358	4445	653	8679	8200	-3039	0	-1708	722	4968	1750	33.8%	105.8%	1.53%
2.50	-8379	-8358	4571	668	8558	8085	-3039	0	-1712	711	4987	1726	34.7%	105.8%	2.92%
2.00	-8379	-8357	4719	691	8429	7964	-3039	0	-1732	700	4824	1697	35.8%	105.8%	4.36%
1.50	-8379	-8356	4884	712	8281	7827	-3038	110	-1751	687	4716	1667	37.0%	105.8%	6.02%
1.00	-8379	-8356	5060	734	8124	7679	-3038	110	-1769	673	4580	1636	38.3%	105.8%	7.79%

Collector loop pump flow rate

The collector loop pump flow rate is varied to check if there are possible optimizations in the solar fraction or in the overall system efficiency. During the analysis the variations of the pump flow rate are maintained small, so that the collector loop can always be considered as a low flow system.

The results are show in Figure 9-34 and Figure 9-35 respectively. The system optimum referred to the saving function is reached for a value of 10 kg/h, it means 2 kg/h lower than the basis case value, however the gain is minimal, in the order of 2 ‰.

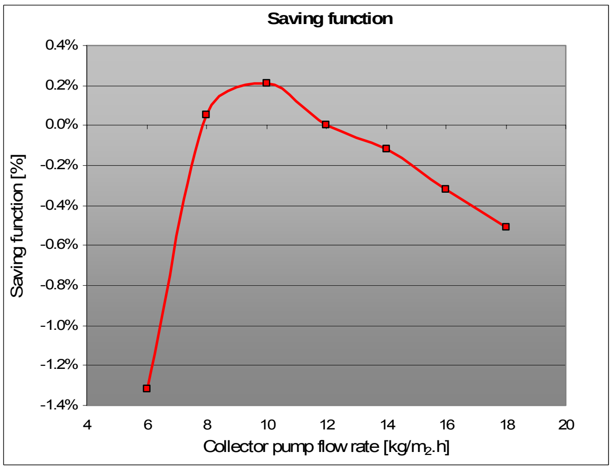

Figure 9-34: Saving function as function of the collector pump flow rate

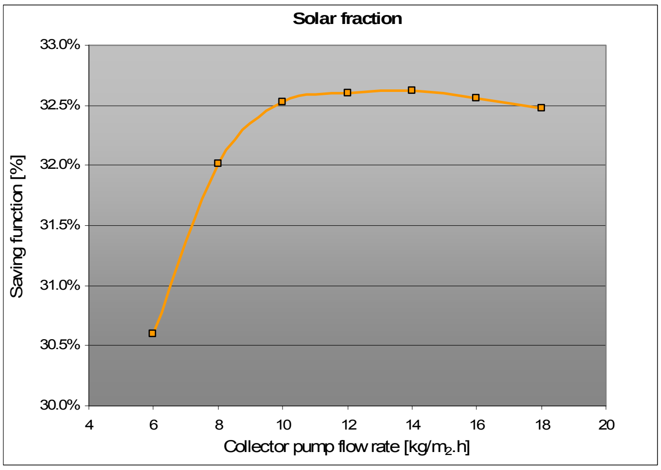

Figure 9-35: Solar fraction as function of the collector pump flow rate

Table 9-13: Simulation results as function of the collector pump flow rate

Collector pump flow rate															
Parameter [kg/h.m^2]	$Q_{SH,target}$ [kWh/a]	$Q_{SH,eff}$ [kWh/a]	$Q_{solar,tank}$ [kWh/a]	$Q_{solar,loses}$ [kWh/a]	Q_{boiler} [kWh/a]	E_{boiler} [kWh/a]	Q_{DHW} [kWh/a]	V_{DHW40} [l/a]	$Q_{tank,loses}$ [kWh/a]	$Q_{cond,gain}$ [kWh/a]	n_{boiler} [1/a]	t_{boiler} [kWh/a]	$Solar_{\%}$ [%]	η_{boiler} [%]	f_{sav} [%]
6	-8379	-8359	3958	554	8931	8438	-3038	0	-1471	744	5021	1807	30.6%	105.8%	-1.32%
8	-8379	-8358	4169	589	8811	8323	-3038	55	-1565	734	5034	1779	32.0%	105.9%	0.05%
10	-8379	-8358	4262	618	8798	8310	-3038	0	-1643	733	5117	1774	32.5%	105.9%	0.21%
12	-8379	-8358	4283	632	8814	8328	-3038	0	-1680	733	5242	1782	32.6%	105.8%	0.00%
14	-8379	-8358	4293	639	8823	8338	-3038	0	-1700	733	5249	1784	32.6%	105.8%	-0.12%
16	-8379	-8358	4289	641	8841	8354	-3039	0	-1712	735	5372	1792	32.6%	105.8%	-0.32%
18	-8379	-8359	4281	640	8857	8370	-3038	0	-1720	736	5405	1796	32.5%	105.8%	-0.51%

Relative height of the storage inlet form the collector loop (without stratified charging mode)

In the following section is analyzed the influence that a fixed storage tank inlet has in comparison with the collector loop stratified charging mode.

In a stratified charged storage system the water coming from the solar collector enters the storage tank at the height where the water temperature inside the tank has the same temperature. During this analysis instead, the water from the collector loop enters the storage tank at a fix relative height that's varied from 0.3 to 0.75.

As Figure 9-36 shows the optimum relative height for a fix solar inlet is about 0.4. Compared to the base case operating with a stratified charger, it's noticeable that there's a repercussion in the saving function of about -1.3%. This result is not so bad considering the lower cost of a storage tank without a stratified charging system.

It should be economically analyzed if the cost of a stratified charging system worth the small increase in the system performance.

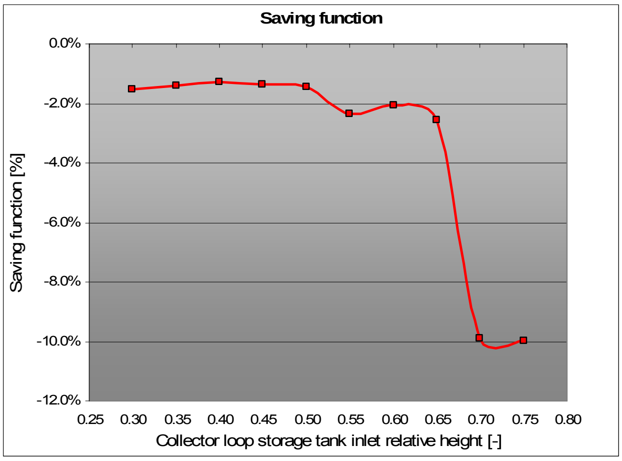

Figure 9-36: Saving function as function of the collector loop storage inlet

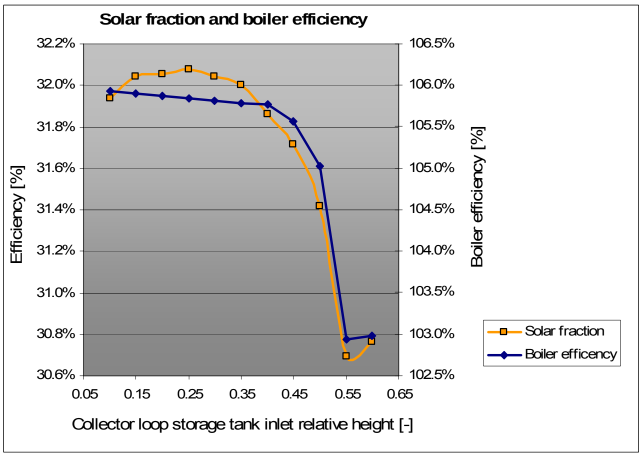

Figure 9-37: Solar fraction and boiler efficiency as function of the collector loop storage inlet

Table 9-14: Simulation results as function of the collector loop storage inlet

Tank inlet form collector loop without stratified charging															
Parameter [-]	$Q_{SH,target}$ [kWh/a]	$Q_{SH,eff}$ [kWh/a]	$Q_{solar,tank}$ [kWh/a]	$Q_{solar,loses}$ [kWh/a]	Q_{boiler} [kWh/a]	E_{boiler} [kWh/a]	Q_{DHW} [kWh/a]	V_{DHW40} [l/a]	$Q_{tank,loses}$ [kWh/a]	$Q_{cond,gain}$ [kWh/a]	n_{boiler} [1/a]	t_{boiler} [kWh/a]	$Solar_{\%}$ [%]	η_{boiler} [%]	f_{sav} [%]
0.30	-8379	-8359	4103	652	8939	8456	-3038	0	-1625	739	5548	1816	31.4%	105.7%	-1.54%
0.35	-8379	-8359	4123	650	8923	8443	-3038	0	-1629	737	5483	1814	31.5%	105.7%	-1.38%
0.40	-8379	-8359	4137	651	8917	8435	-3038	0	-1637	738	5372	1807	31.6%	105.7%	-1.28%
0.45	-8379	-8358	4139	652	8923	8440	-3038	0	-1645	738	5526	1811	31.6%	105.7%	-1.35%
0.50	-8379	-8358	4136	655	8930	8448	-3038	0	-1650	738	5620	1822	31.5%	105.7%	-1.45%
0.55	-8379	-8359	4084	664	8999	8524	-3037	0	-1667	738	9558	1895	31.1%	105.6%	-2.35%
0.60	-8379	-8357	4112	664	8971	8498	-3038	0	-1668	733	4678	1775	31.3%	105.6%	-2.05%
0.65	-8379	-8347	4078	667	9002	8541	-3038	0	-1675	730	4337	1761	31.1%	105.4%	-2.56%
0.70	-8379	-8351	3672	716	9508	9151	-3038	0	-1770	672	4190	1951	27.7%	103.9%	-9.89%
0.75	-8379	-8350	3671	714	9502	9157	-3038	0	-1765	663	4093	1969	27.8%	103.8%	-9.96%

9.3.5. Domestic hot water

<u>DHW reserved volume</u>

In order to see how much must be the minimum water volume in the top of the storage tank reserved to the DHW to assure that a comfort is reached, the position of the sensor 1 has been varied form a relative height of 0.6 to 0.9. This variation represent a volume change from 320 to 80 liters respectively.

To analyze the DHW comfort a special check function is implemented in the simulation. This function gives at the end of the simulation an output that displays how many liters of water are supplied under the set comfort temperature value of 40°C.

As the Figure 9-38 shows, for the given draw profile of 200 liter/day the volume of 240 liters reserved for DHW chosen for the base case, seems not the be necessary. As the parameter analysis illustrates, a volume of only 80 liters allows a final energy saving in the order of 3.5% with only a negative comfort of 55 liters under 40°C over an year (Figure 9-40).

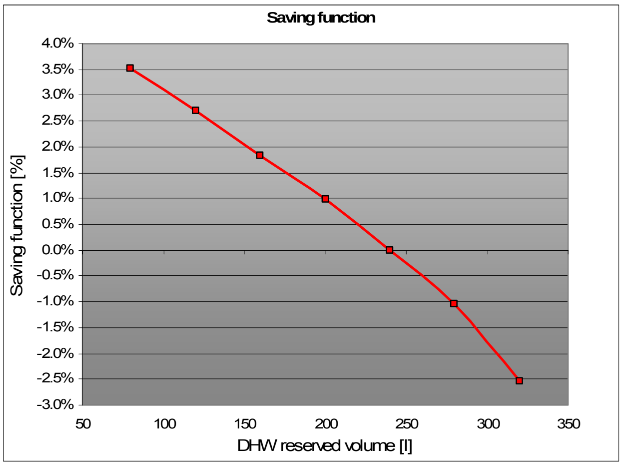

Figure 9-38: Saving function as function of the DHW reserved volume

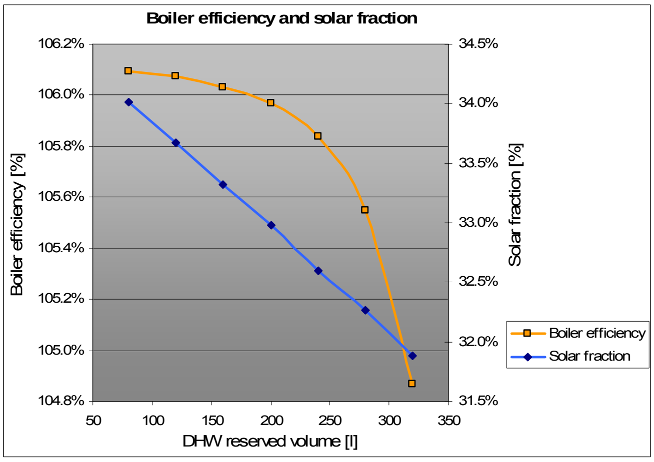

Figure 9-39: Boiler efficiency and solar fraction as function of the DHW reserved volume

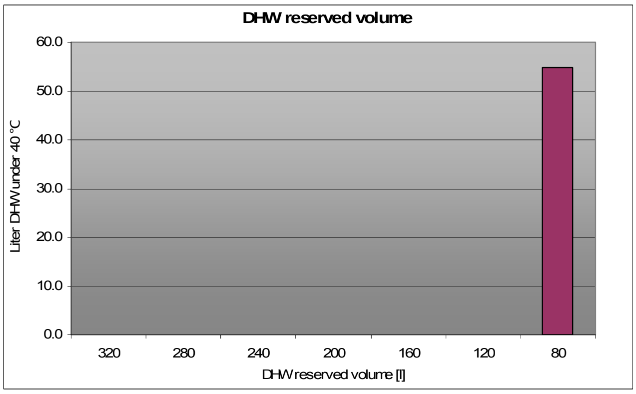

Figure 9-40: Liters of DHW that don't match the comfort temperature of 40 °C over a year as function of the DHW reserved volume

This result depends in large manner on the choice of the DHW heat exchanger. Using an external heat exchanger for DHW preparation as in this case shows that a much lower water volume maintained at an high temperature is needed to guarantee a satisfying DHW comfort.

The results could have been different if an internal DHW heat exchanger were chosen, in such a case the amount of volume maintained at an higher temperature should have been probably higher. This option is not examined further.

Table 9-15: Simulation results as function of the DHW reserved volume

DHW reserved tank volume																
Parameter [kg/h]	$Q_{SH,target}$ [kWh/a]	$Q_{SH,eff}$ [kWh/a]	$Q_{solar,tank}$ [kWh/a]	$Q_{solar,loses}$ [kWh/a]	Q_{boiler} [kWh/a]	E_{boiler} [kWh/a]	Q_{DHW} [kWh/a]	V_{DHW40} [l/a]	$Q_{tank,loses}$ [kWh/a]	$Q_{cond,gain}$ [kWh/a]	n_{boiler} [1/a]	t_{boiler} [kWh/a]	$Solar_{\%}$ [%]	η_{boiler} [%]	f_{sav} [%]
320	-8379	-8350	4214	639	8954	8539	-3039	0	-1755	703	7908	2048	31.9%	104.9%	-2.53%
280	-8379	-8356	4253	636	8882	8415	-3039	0	-1717	727	5720	1862	32.3%	105.5%	-1.05%
240	-8379	-8358	4283	632	8814	8328	-3038	0	-1680	733	5242	1782	32.6%	105.8%	0.00%
200	-8379	-8358	4318	627	8739	8246	-3038	0	-1641	732	5065	1738	33.0%	106.0%	0.98%
160	-8379	-8359	4349	623	8668	8175	-3038	0	-1603	730	5161	1709	33.3%	106.0%	1.83%
120	-8379	-8360	4379	618	8596	8103	-3038	0	-1562	727	5179	1686	33.7%	106.1%	2.69%
80	-8379	-8360	4408	615	8524	8034	-3036	55	-1521	724	5239	1673	34.0%	106.1%	3.52%

DHW set temperature in storage tank

The set value of the water temperature in the storage tank reserved for the domestic hot water is varied from 50 to 64 °C to check how much energy can be saved. Figure 9-42 illustrates the comfort value in liter under 40°C (a 0 liters value is the optimum).

As Figure 9-41 demonstrates it's possible to lower the temperature to 58°C without loosing any comfort and saving about 0.3 % of the final energy. Lowering the set temperature under this value leads to a loose in the DHW comfort. This negative effect is not so high, and can be considered as acceptable. The variation in the saving function is not so marked because the boiler supply set temperature remain 65°C, only the set temperature of the controller is varied.

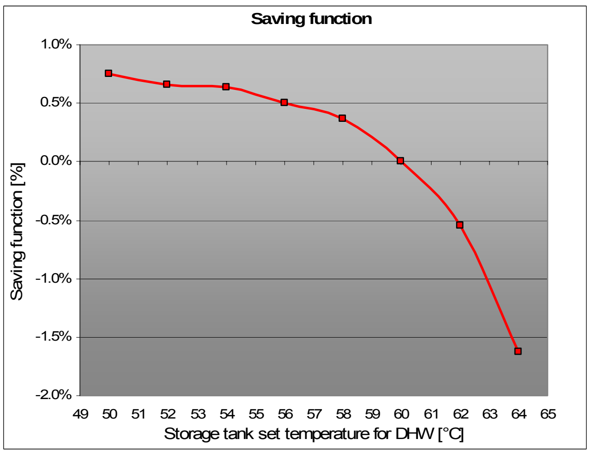

Figure 9-41: Saving function as function of the storage tank set temperature for DHW

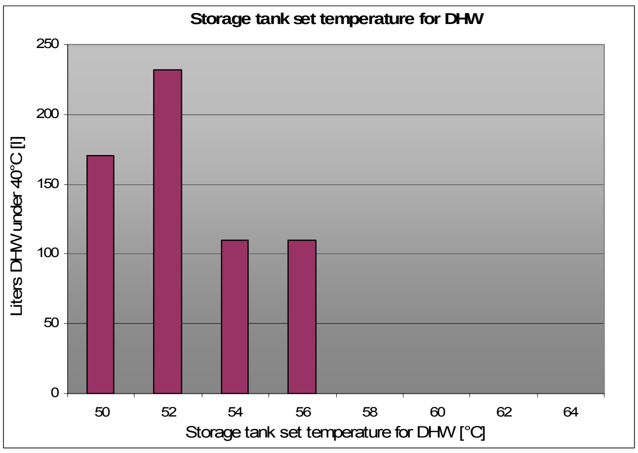

Figure 9-42: Liters of DHW that don't match the comfort temperature of 40 °C over a year as function of the storage tank set temperature for DHW

Table 9-16: Simulation results as function of the storage tank set temperature for DHW

Boiler set temperature for DHW and SH																
Parameter [°C]	$Q_{SH,target}$ [kWh/a]	$Q_{SH,eff}$ [kWh/a]	$Q_{solar,tank}$ [kWh/a]	$Q_{solar,loses}$ [kWh/a]	Q_{boiler} [kWh/a]	E_{boiler} [kWh/a]	Q_{DHW} [kWh/a]	V_{DHW40} [l/a]	$Q_{tank,loses}$ [kWh/a]	$Q_{cond,gain}$ [kWh/a]	n_{boiler} [1/a]	t_{boiler} [kWh/a]	$Solar_{\%}$ [%]	η_{boiler} [%]	f_{sav} [%]
60	-8379	-8361	4243	637	8842	8406	-3036	0	-1659	698	7814	1952	32.3%	105.2%	-0.95%
62	-8379	-8360	4275	632	8806	8329	-3037	0	-1664	724	5455	1854	32.6%	105.7%	-0.01%
65	-8379	-8358	4283	632	8814	8328	-3038	0	-1680	733	5242	1782	32.6%	105.8%	0.00%
67	-8379	-8359	4294	631	8816	8328	-3039	0	-1691	736	5368	1739	32.6%	105.9%	-0.01%
70	-8379	-8359	4289	630	8843	8353	-3039	0	-1712	741	5165	1660	32.6%	105.9%	-0.31%

9.3.6. Space heating loop

Maximum allowed temperature in the space heating pipes

The maximum temperature allowed to flow in the space heating pipes must be in some heating systems technically lowered to reach and acceptable comfort or because of material problems.

In this paragraph the maximum allowed water temperature for the space heating supply is varied to check if there's a change in the overall system efficiency. As Figure 9-43 illustrates, the saving function curve is practically constant. The small difference in the overall efficiency is probably correlated to a the smaller effective energy delivered by the space heating to the building.

As the results demonstrate it's possible to limit the entering water temperature practically without loosing in the overall system efficiency.

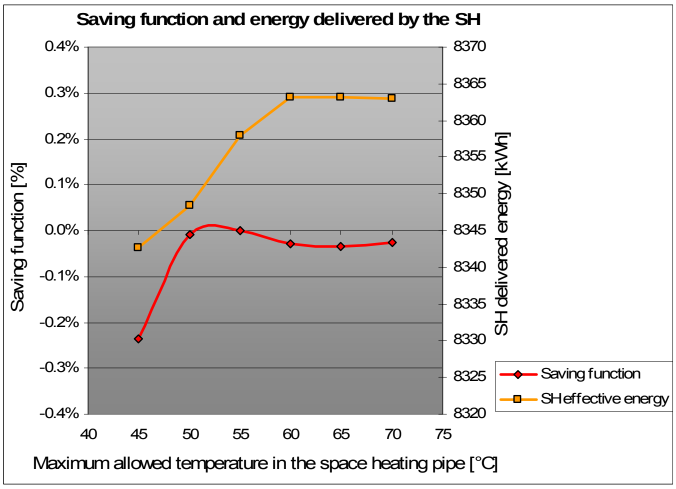

Figure 9-43: Saving function and energy delivered by the space heating as function of the maximum allowed water temperature entering the space heating loop

Table 9-17: Simulation results as function of the maximum allowed mass flow rate of the space heating pump

Maximum allowed temperature entering the SH pipe															
Parameter [°C]	$Q_{SH,target}$ [kWh/a]	$Q_{SH,eff}$ [kWh/a]	$Q_{solar,tank}$ [kWh/a]	$Q_{solar,loses}$ [kWh/a]	Q_{boiler} [kWh/a]	E_{boiler} [kWh/a]	Q_{DHW} [kWh/a]	V_{DHW40} [l/a]	$Q_{tank,loses}$ [kWh/a]	$Q_{cond,gain}$ [kWh/a]	n_{boiler} [1/a]	t_{boiler} [kWh/a]	$Solar_{\%}$ [%]	η_{boiler} [%]	f_{sav} [%]
40	-8379	-8229	4262	634	8708	8272	-3038	0	-1683	692	6502	1165	32.8%	105.3%	0.67%
45	-8379	-8343	4274	633	8811	8347	-3039	0	-1683	714	6111	1462	32.6%	105.6%	-0.24%
50	-8379	-8348	4281	632	8807	8328	-3038	0	-1681	726	5665	1677	32.6%	105.7%	-0.01%
55	-8379	-8358	4283	632	8814	8328	-3038	0	-1680	733	5242	1782	32.6%	105.8%	0.00%
60	-8379	-8363	4285	632	8817	8330	-3038	0	-1680	734	5115	1800	32.6%	105.8%	-0.03%
65	-8379	-8363	4284	632	8818	8331	-3039	0	-1680	734	5111	1799	32.6%	105.8%	-0.03%
70	-8379	-8363	4285	632	8817	8330	-3038	0	-1680	734	5110	1799	32.6%	105.8%	-0.03%

Maximum allowed mass flow of the space heating pump

As Figure 9-44 shows the variation of the maximum mass flow rate of the space heating pump don't have any influence in the overall efficiency. The results demonstrate that is possible to use a very low maximal mass flow rate and match the heat load demand during all the year with only minimal variations. It follows that an higher power pump with greater mass flow rate capability would never be used at the maximum of its capacity.

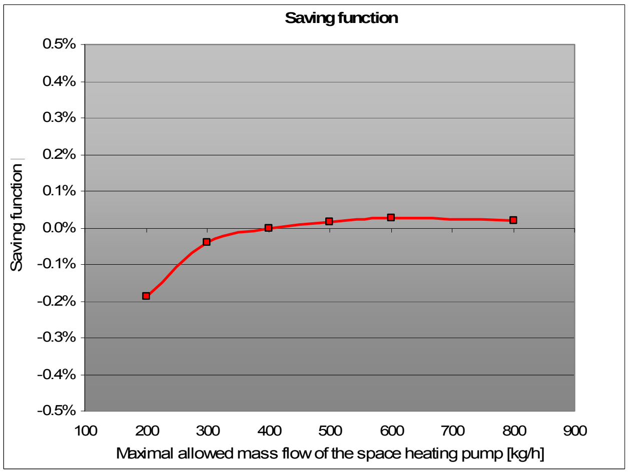

Figure 9-44: Saving function as function of the maximum allowed mass flow entering the space heating pump

Table 9-18: Simulation results as function of the maximum allowed mass flow entering the space heating pump

Maximum mass flow of the SH pump															
Parameter [kg/h]	$Q_{SH,target}$ [kWh/a]	$Q_{SH,eff}$ [kWh/a]	$Q_{solar,tank}$ [kWh/a]	$Q_{solar,loses}$ [kWh/a]	Q_{boiler} [kWh/a]	E_{boiler} [kWh/a]	Q_{DHW} [kWh/a]	V_{DHW40} [l/a]	$Q_{tank,loses}$ [kWh/a]	$Q_{cond,gain}$ [kWh/a]	n_{boiler} [1/a]	t_{boiler} [kWh/a]	$Solar_{\%}$ [%]	η_{boiler} [%]	f_{sav} [%]
200	-8379	-8346	4278	632	8816	8343	-3038	0	-1688	728	5531	1877	32.6%	105.7%	-0.19%
300	-8379	-8353	4282	632	8813	8331	-3038	0	-1682	732	5336	1815	32.6%	105.8%	-0.04%
400	-8379	-8358	4283	632	8814	8328	-3038	0	-1680	733	5242	1782	32.6%	105.8%	0.00%
500	-8379	-8361	4285	631	8814	8326	-3038	0	-1679	733	5127	1762	32.6%	105.9%	0.02%
600	-8379	-8363	4285	631	8815	8326	-3038	0	-1678	733	5131	1749	32.6%	105.9%	0.03%
800	-8379	-8366	4286	631	8816	8326	-3039	0	-1677	734	5110	1734	32.6%	105.9%	0.02%

Dead band space heating charging loop

In this paragraph it's checked which influence has the dead band value of the boiler sensor for the space heating on the overall system efficiency. The dead band value is varied from 2°C to 10°C. The difference caused by the variation of this parameter practically consist in the waited time before the auxiliary heater is started again to heat the storage tank water.

As the Figure 9-45 shows the improvement in the overall efficiency are practically unnoticeable. The base case can so be considered as already optimized.

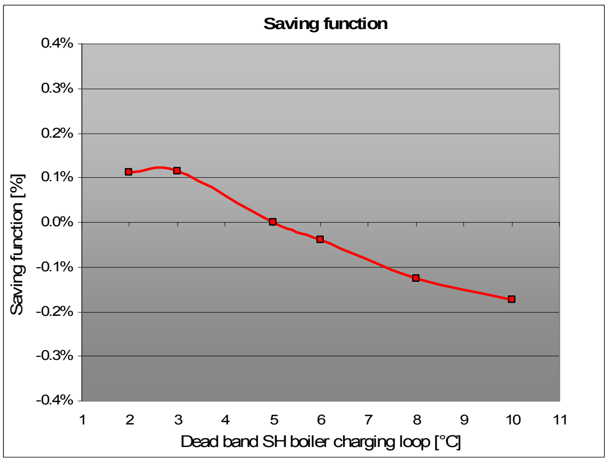

Figure 9-45: Saving function as function of the dead band during the SH charging loop

Table 9-19 Simulation results as function of the dead band during the SH charging loop

Space heating charging loop dead band															
Parameter [°C]	$Q_{SH,target}$ [kWh/a]	$Q_{SH,eff}$ [kWh/a]	$Q_{solar,tank}$ [kWh/a]	$Q_{solar,loses}$ [kWh/a]	Q_{boiler} [kWh/a]	E_{boiler} [kWh/a]	Q_{DHW} [kWh/a]	V_{DHW40} [l/a]	$Q_{tank,loses}$ [kWh/a]	$Q_{cond,gain}$ [kWh/a]	n_{boiler} [1/a]	t_{boiler} [kWh/a]	$Solar_{\%}$ [%]	η_{boiler} [%]	f_{sav} [%]
2	-8379	-8362	4290	631	8807	8318	-3039	0	-1676	733	9614	1728	32.7%	105.9%	0.11%
3	-8379	-8359	4289	631	8806	8318	-3039	0	-1677	733	6963	1747	32.6%	105.9%	0.11%
5	-8379	-8358	4283	632	8814	8328	-3038	0	-1680	733	5242	1782	32.6%	105.8%	0.00%
6	-8379	-8356	4282	632	8815	8331	-3038	0	-1681	732	5098	1802	32.6%	105.8%	-0.04%
8	-8379	-8352	4277	633	8818	8338	-3038	0	-1685	731	4792	1831	32.6%	105.8%	-0.12%
10	-8379	-8348	4276	633	8819	8342	-3038	0	-1688	729	5497	1867	32.5%	105.7%	-0.17%

Space heating storage tank sensor relative position

The position of the space heating storage tank sensor used by the auxiliary heater controller (sensor no. 2 Figure 5-10) is varied from 0.45 to 0.575. As Figure 9-46 shows there isn't any improvement in the overall system efficiency. It seems that the optimum value is already reached in the base case (relative height of 0.55).

Figure 9-47 illustrates that there's a correlation between the overall system efficiency and the numbers of boiler starts during a year.

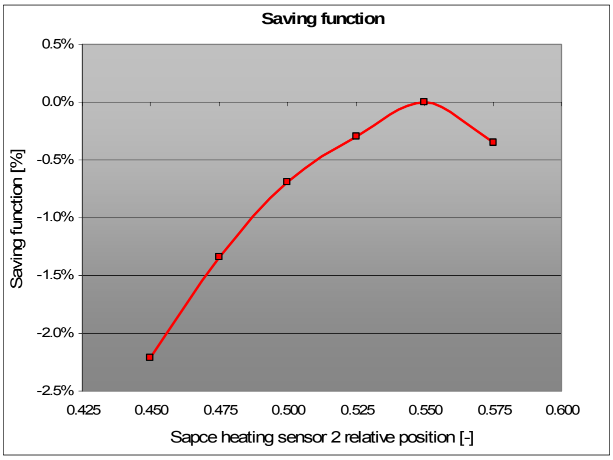

Figure 9-46: Saving function as function of the relative position of the sensor 2 (SH)

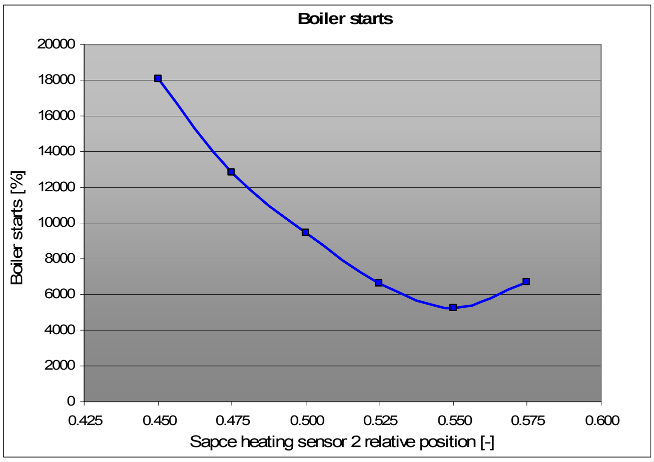

Figure 9-47: Boiler starts as function of the relative position of the sensor 2 (SH)

Table 9-20: Simulation results as function of the relative position of the sensor 2 (SH)

SH sensor position															
Parameter [-]	$Q_{SH,target}$ [kWh/a]	$Q_{SH,eff}$ [kWh/a]	$Q_{solar,tank}$ [kWh/a]	$Q_{solar,loses}$ [kWh/a]	Q_{boiler} [kWh/a]	E_{boiler} [kWh/a]	Q_{DHW} [kWh/a]	V_{DHW40} [l/a]	$Q_{tank,loses}$ [kWh/a]	$Q_{cond,gain}$ [kWh/a]	n_{boiler} [1/a]	t_{boiler} [kWh/a]	$Solar_{\%}$ [%]	η_{boiler} [%]	f_{sav} [%]
0.450	-8379	-8338	4221	640	8914	8512	-3039	0	-1735	692	18079	2262	32.0%	104.7%	-2.21%
0.475	-8379	-8339	4243	637	8875	8439	-3039	0	-1718	709	12816	2127	32.2%	105.2%	-1.34%
0.500	-8379	-8338	4263	635	8839	8386	-3038	0	-1704	719	9472	2026	32.4%	105.4%	-0.70%
0.525	-8379	-8343	4272	633	8822	8352	-3038	0	-1692	728	6642	1919	32.5%	105.6%	-0.30%
0.550	-8379	-8358	4283	632	8814	8328	-3038	0	-1680	733	5242	1782	32.6%	105.8%	0.00%
0.575	-8379	-8418	4293	630	8852	8357	-3039	0	-1668	736	6706	1571	32.6%	105.9%	-0.35%

Storage tank outlet to the space heating loop

During this analysis the storage tank outlet to the space heating loop is varied from the relative height of 0.5 to 0.7. The position of the space heating sensor is maintained in all simulation variants at a relative position of 0.05 lower than the storage tank outlet.

As the Figure 9-48 clearly illustrates there's an optimum at the relative height of 0.65, it is also noticeable that at a relative height of 0.7 there's a fall in the overall system efficiency. This effect is probably due to the fact that in this case the outlet port is at the same height as the storage tank sensor for the DHW, increasing also the number of the boiler starts.

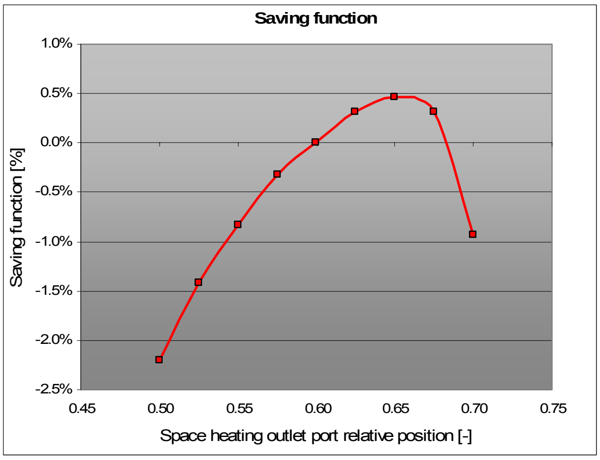

Figure 9-48: Saving function as function of the space heating storage tank outlet

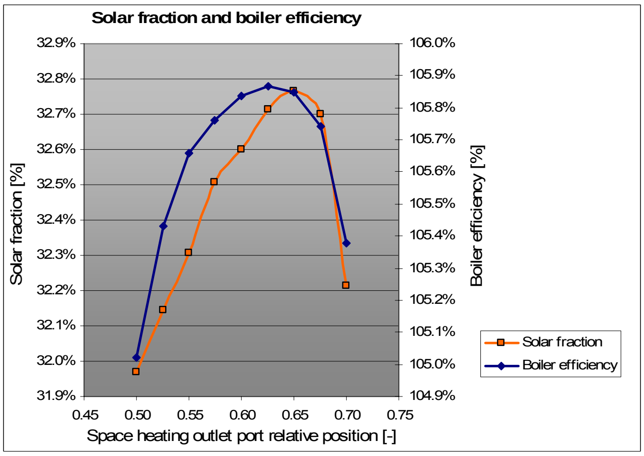

Figure 9-49: Solar fraction and boiler efficiency as function of the space heating storage outlet

Table 9-21: Simulation results as function of the space heating storage tank outlet

SH outlet (sensor postioned always 0.05 lower)															
Parameter [-]	$Q_{SH,target}$ [kWh/a]	$Q_{SH,eff}$ [kWh/a]	$Q_{solar,tank}$ [kWh/a]	$Q_{solar,loses}$ [kWh/a]	Q_{boiler} [kWh/a]	E_{boiler} [kWh/a]	Q_{DHW} [kWh/a]	V_{DHW40} [l/a]	$Q_{tank,loses}$ [kWh/a]	$Q_{cond,gain}$ [kWh/a]	n_{boiler} [1/a]	t_{boiler} [kWh/a]	$Solar_{\%}$ [%]	η_{boiler} [%]	f_{sav} [%]
0.500	-8379	-8352	4223	639	8938	8511	-3038	55	-1748	708	8343	2065	32.0%	105.0%	-2.20%
0.525	-8379	-8355	4241	636	8904	8445	-3038	0	-1729	723	6989	1951	32.1%	105.4%	-1.41%
0.550	-8379	-8357	4256	634	8872	8397	-3038	0	-1711	730	6409	1878	32.3%	105.7%	-0.83%
0.575	-8379	-8357	4277	633	8835	8354	-3038	0	-1695	732	5948	1830	32.5%	105.8%	-0.32%
0.600	-8379	-8358	4283	632	8814	8328	-3038	0	-1680	733	5242	1782	32.6%	105.8%	0.00%
0.625	-8379	-8358	4293	630	8788	8301	-3038	0	-1665	732	4784	1735	32.7%	105.9%	0.32%
0.650	-8379	-8357	4295	630	8774	8289	-3039	0	-1653	730	4271	1663	32.8%	105.8%	0.46%
0.675	-8379	-8357	4283	631	8778	8302	-3039	0	-1648	726	3876	1561	32.7%	105.7%	0.31%
0.700	-8379	-8353	4227	639	8857	8405	-3039	0	-1675	718	4514	1035	32.2%	105.4%	-0.93%

Space heating storage tank inlet (without stratified charging mode)

In the following paragraph is analyzed the influence that a fixed storage tank inlet have in comparison with the stratified charging mode.

For a fixed space heating storage inlet the water from the space heating loop enters the storage tank at a fix relative height that is varied from 0.1 to 0.6. As the Figure 9-50 shows the optimum relative height is about 0.15-0.2.

In this optimized case the overall system efficiency drop is less than 1% compared to the stratified charging mode of the base case and it can be considered a good result.

Also in this case it should be economically analyzed if the cost of a stratified charging system worth the major gain in the system efficiency.

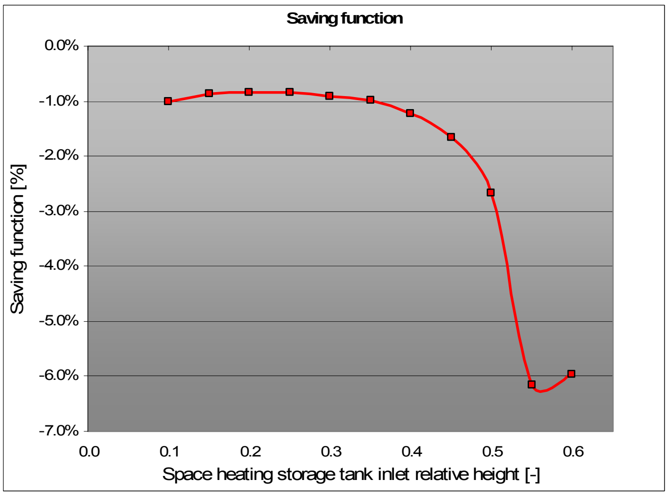

Figure 9-50: Saving function as function of the space heating storage tank inlet

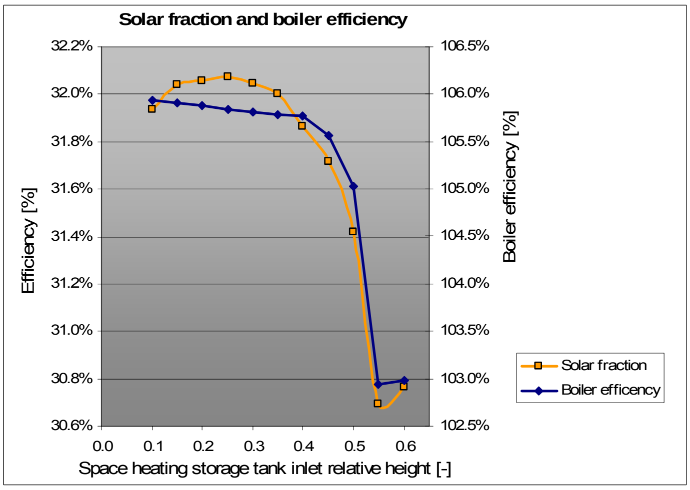

Figure 9-51: Solar fraction and boiler efficiency as function of the space heating storage tank inlet

Table 9-22: Simulation results as function of the space heating storage tank inlet (without stratified charging mode)

SH tank inlet without stratified charging															
Parameter [-]	$Q_{SH,target}$ [kWh/a]	$Q_{SH,eff}$ [kWh/a]	$Q_{solar,tank}$ [kWh/a]	$Q_{solar,loses}$ [kWh/a]	Q_{boiler} [kWh/a]	E_{boiler} [kWh/a]	Q_{DHW} [kWh/a]	V_{DHW40} [l/a]	$Q_{tank,loses}$ [kWh/a]	$Q_{cond,gain}$ [kWh/a]	n_{boiler} [1/a]	t_{boiler} [kWh/a]	$Solar_{\%}$ [%]	η_{boiler} [%]	f_{sav} [%]
0.10	-8379	-8357	4205	641	8911	8411	-3038	0	-1697	745	5450	1792	31.9%	105.9%	-1.00%
0.15	-8379	-8357	4217	639	8895	8399	-3038	0	-1694	742	5107	1787	32.0%	105.9%	-0.85%
0.20	-8379	-8357	4218	639	8892	8398	-3038	0	-1692	741	5172	1791	32.1%	105.9%	-0.85%
0.25	-8379	-8357	4219	638	8888	8398	-3038	0	-1690	739	5149	1797	32.1%	105.8%	-0.84%
0.30	-8379	-8358	4215	639	8892	8403	-3038	0	-1689	739	5275	1804	32.0%	105.8%	-0.91%
0.35	-8379	-8358	4209	639	8897	8411	-3038	0	-1689	739	5256	1809	32.0%	105.8%	-1.00%
0.40	-8379	-8358	4190	640	8916	8430	-3038	0	-1690	740	5306	1819	31.9%	105.8%	-1.23%
0.45	-8379	-8357	4171	642	8937	8466	-3038	0	-1693	733	5830	1875	31.7%	105.6%	-1.66%
0.50	-8379	-8351	4134	646	8979	8549	-3038	0	-1704	712	7460	2030	31.4%	105.0%	-2.66%
0.55	-8379	-8337	4053	656	9100	8840	-3038	0	-1756	602	31200	2562	30.7%	102.9%	-6.16%
0.60	-8379	-8357	4059	655	9088	8825	-3039	0	-1730	590	5525	1954	30.8%	103.0%	-5.98%

Space heating pipe

In this section the influence of the space heating pipe parameters (loss coefficient and length) is analyzed to find which variation on the system performance they have. The first parameter study is performed on the pipe loss coefficient. Figure 9-52 illustrates that if the pipe heat exchange coefficient is increased a better system efficiency is reached. Other side if the coefficient is lowered the saving function goes to the negative side.

This effect is easily explained considering Figure 9-53, as it's illustrated for an higher value of the pipe heat loss coefficient both the solar fraction and the boiler efficiency get higher. This effect is a consequence of the return temperature of the space heating loop that for an higher loss coefficient is much lower, because the water loses its heat faster and enter the storage tank with a lower temperature.

This facts lead to a better solar and boiler efficiency. This correlation between space heating return temperature and both solar and boiler efficiency is explained in greater detail in section 10.2.

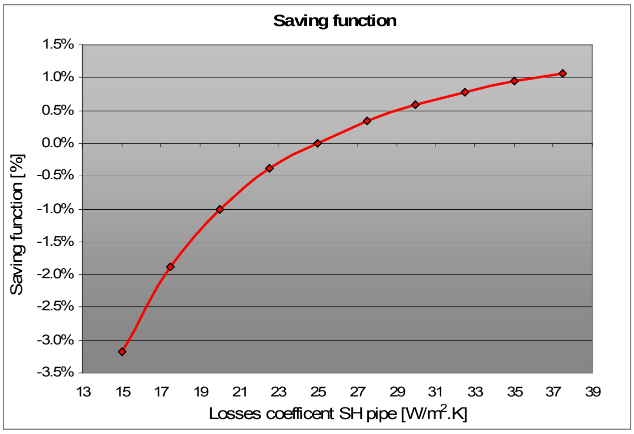

Figure 9-52: Saving function as function of the space heating pipe loss coefficient

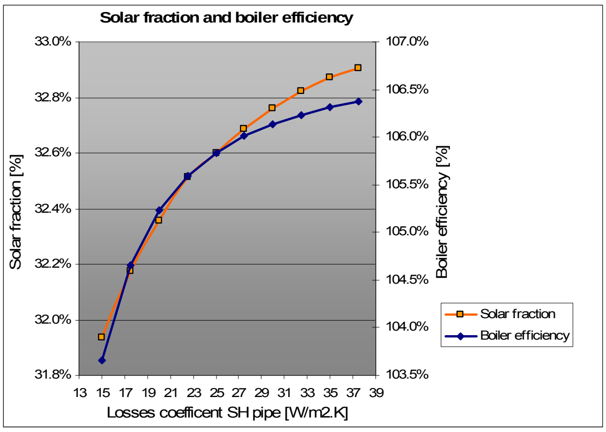

Figure 9-53: Boiler efficiency and solar fraction as function of the space heating pipe loss coefficient

Table 9-23: Simulation results as function of the space heating pipe loss coefficient

SH pipe loses coefficent															
Parameter [W/m²K]	$Q_{SH,target}$ [kWh/a]	$Q_{SH,eff}$ [kWh/a]	$Q_{solar,tank}$ [kWh/a]	$Q_{solar,loses}$ [kWh/a]	Q_{boiler} [kWh/a]	E_{boiler} [kWh/a]	Q_{DHW} [kWh/a]	V_{DHW40} [l/a]	$Q_{tank,loses}$ [kWh/a]	$Q_{cond,gain}$ [kWh/a]	n_{boiler} [1/a]	t_{boiler} [kWh/a]	$Solar_{\%}$ [%]	η_{boiler} [%]	f_{sav} [%]
15.0	-8379	-8325	4203	643	8907	8593	-3038	0	-1723	620	7064	1909	31.9%	103.7%	-3.18%
17.5	-8379	-8348	4234	638	8880	8485	-3038	0	-1706	677	6257	1881	32.2%	104.7%	-1.88%
20.0	-8379	-8353	4255	635	8852	8412	-3038	0	-1695	706	5793	1851	32.4%	105.2%	-1.01%
22.5	-8379	-8355	4273	633	8827	8360	-3038	0	-1686	722	5382	1814	32.5%	105.6%	-0.38%
25.0	-8379	-8358	4283	632	8814	8328	-3038	0	-1680	733	5242	1782	32.6%	105.8%	0.00%
27.5	-8379	-8359	4293	630	8799	8300	-3038	0	-1675	739	5007	1751	32.7%	106.0%	0.33%
30.0	-8379	-8358	4301	629	8787	8279	-3038	0	-1671	744	4972	1727	32.8%	106.1%	0.59%
32.5	-8379	-8360	4308	628	8778	8262	-3038	0	-1668	747	4943	1704	32.8%	106.2%	0.78%
35.0	-8379	-8360	4314	628	8769	8248	-3038	0	-1665	750	4926	1686	32.9%	106.3%	0.95%
37.5	-8379	-8360	4317	627	8764	8239	-3038	0	-1663	752	4933	1669	32.9%	106.4%	1.07%

A second parameter that's varied to check its influence on the overall system efficiency is the space heating pipe length.

As for the loss coefficient also in this case an higher efficiency is noticeable for a longer space heating pipe (Figure 9-54), the effect is also due to a lower return temperature from the space heating loop, leading to a better solar and boiler efficiency (Figure 9-55).

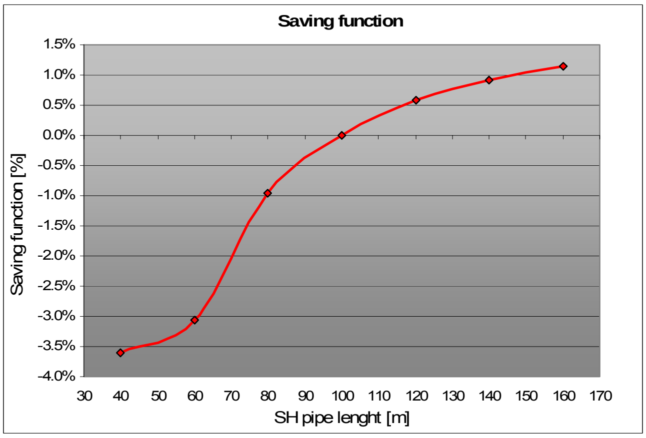

Figure 9-54: Saving function as function of the space heating pipe length

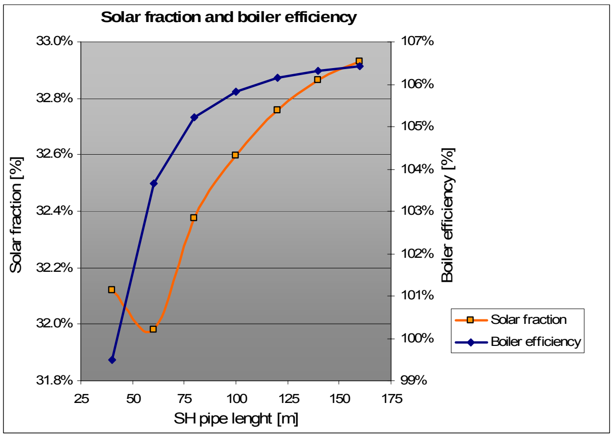

Figure 9-55: Boiler efficiency and solar fraction as function of the space heating pipe length

Table 9-24: Simulation results as function of the space heating pipe length

SH pipe lenght															
Parameter [m]	$Q_{SH,target}$ [kWh/a]	$Q_{SH,eff}$ [kWh/a]	$Q_{solar,tank}$ [kWh/a]	$Q_{solar,loses}$ [kWh/a]	Q_{boiler} [kWh/a]	E_{boiler} [kWh/a]	Q_{DHW} [kWh/a]	V_{DHW40} [l/a]	$Q_{tank,loses}$ [kWh/a]	$Q_{cond,gain}$ [kWh/a]	n_{boiler} [1/a]	t_{boiler} [kWh/a]	$Solar_{\%}$ [%]	η_{boiler} [%]	f_{sav} [%]
40.0	-8379	-7814	4091	656	8584	8627	-3038	0	-1794	354	14958	2132	32.1%	99.5%	-3.59%
60.0	-8379	-8317	4205	642	8896	8583	-3038	0	-1723	619	7096	1909	32.0%	103.6%	-3.07%
80.0	-8379	-8349	4257	635	8847	8407	-3038	0	-1695	705	5791	1850	32.4%	105.2%	-0.96%
100.0	-8379	-8358	4283	632	8814	8328	-3038	0	-1680	733	5242	1782	32.6%	105.8%	0.00%
120.0	-8379	-8360	4301	629	8788	8280	-3038	0	-1671	744	4987	1727	32.8%	106.1%	0.58%
140.0	-8379	-8362	4314	628	8771	8251	-3038	0	-1665	750	4923	1687	32.9%	106.3%	0.92%
160.0	-8379	-8362	4320	627	8761	8232	-3038	0	-1661	754	4954	1654	32.9%	106.4%	1.15%

Space heating load

To check how the model behaves under different space heating load conditions the input from the load file that represent the building is multiplied by a constant so to make the $Q_{SH,target}$ value at the end of the year change. The base case load file represent a building which has an energy requirement of 60 kWh/m^{2}a as described in section 5.3.6.

The base case is compared with other two variant, which represent a 30 kWh/m^{2}a and 100 kWh/m^{2}a building respectively. The heating power input of the load file is multiplied by 0.5 to replicate the 30 kWh/m^{2}a variant and by 1.66 to simulate a 100 kWh/m^{2}a house.

The results are resumed in table Table 9-25. As the η_{solar} colon shows the boiler has a its best efficiency for the base case variant.

Table 9-25: Simulation results as function of the space heating load

Space heating load															
Parameter [kWh/m²a]	$Q_{SH,target}$ [kWh/a]	$Q_{SH,eff}$ [kWh/a]	$Q_{solar,tank}$ [kWh/a]	$Q_{solar,loses}$ [kWh/a]	Q_{boiler} [kWh/a]	E_{boiler} [kWh/a]	Q_{DHW} [kWh/a]	V_{DHW40} [l/a]	$Q_{tank,loses}$ [kWh/a]	$Q_{cond,gain}$ [kWh/a]	n_{boiler} [1/a]	t_{boiler} [kWh/a]	$Solar_{\%}$ [%]	η_{boiler} [%]	f_{sav} [%]
30	-4190	-4148	4164	643	4737	4514	-3038	0	-1697	402	7296	1105	46.7%	104.9%	45.79%
60	-8379	-8358	4283	632	8814	8328	-3038	0	-1680	733	5242	1782	32.6%	105.8%	0.00%
100	-13966	-13842	4319	629	14289	13704	-3039	0	-1703	981	5661	2315	23.1%	104.3%	-64.56%

9.3.7. Conclusions

The detailed parameter analysis performed from section 9.3.1 to 9.3.6 on the Direct Feed Flow Controlled system concept shows that the system has a solid behavior. The choice of the base case parameters could be considered as practically optimized.

For some parameter as the collector area, the space heating length, and the storage tank stratified charging system a cost based analysis is necessary to find the cost related optimal values taking into account the higher or lower investment costs.

9.4. Reference model parameter analysis

9.4.1. Introduction

In this section are presented the parameter analysis results of the reference model described in chapter 6. The goal is also here to find possibilities of optimization and to check the solidity of the simulation model. The parameters analyzed for the reference system are restricted to the sensor and port positions into the storage tank, the variation of the mass flow or the temperature of the auxiliary heater and the space heating loop parameters. The collector loop and the domestic hot water loop is no more investigated in detail.

The value of the saving function is always referred to the base case of the reference system described in section 6. A positive value of the saving function means a better system efficiency referred to the auxiliary final energy needed (see section 7.2)

9.4.2. Auxiliary heater

<u>**Storage tank outlet to the boiler**</u>

In this parameter study the height of the storage tank outlet to the boiler loop is changed from a relative height of 0.1 to a value of 0.5. The temperature sensor 1 used by the auxiliary heater controller in the storage tank it's always placed at the same height as the outlet.

As it's showed by the Figure 9-56 at a relative height of about 0.45 the maximal overall system efficiency is reached. A small change in the effective energy delivered to the building is noticeable so to make impossible to confirm the small saving function increase of only about 0.2%.

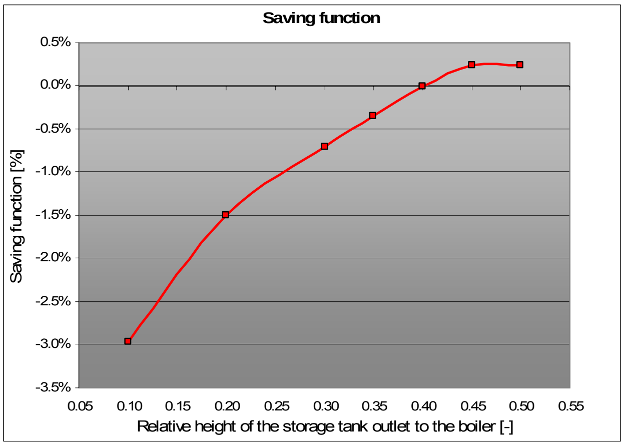

Figure 9-56: Saving function as function of the relative height of the storage tank outlet to the boiler

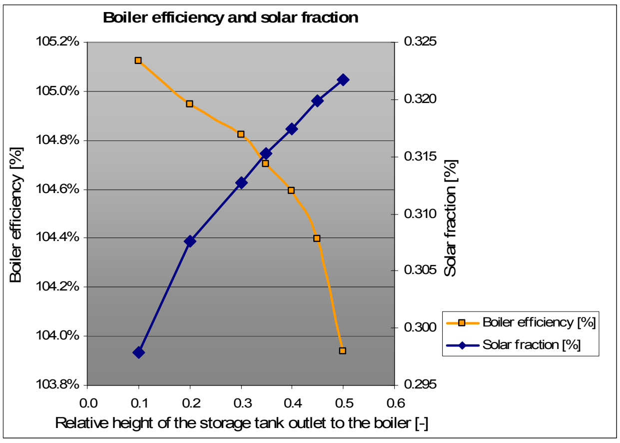

Figure 9-57: Boiler efficiency and solar fraction as function of the relative height of the storage tank outlet to the boiler

Table 9-26: Simulation results as function of the relative height of the storage tank outlet to the boiler

Realtive position of the tank outlet to the boiler															
Parameter [-]	$Q_{SH,target}$ [kWh/a]	$Q_{SH,eff}$ [kWh/a]	$Q_{solar,tank}$ [kWh/a]	$Q_{solar,loses}$ [kWh/a]	Q_{boiler} [kWh/a]	E_{boiler} [kWh/a]	Q_{DHW} [kWh/a]	V_{DHW40} [l/a]	$Q_{tank,loses}$ [kWh/a]	$Q_{cond,gain}$ [kWh/a]	n_{boiler} [1/a]	t_{boiler} [kWh/a]	$Solar_{\%}$ [%]	η_{boiler} [%]	f_{sav} [%]
0.10	-8379	-8351	3940	669	9225	8775	-3037	0	-1750	699	932	1995	29.8%	105.1%	-2.96%
0.20	-8379	-8350	4058	658	9078	8650	-3038	0	-1725	681	1097	1991	30.8%	104.9%	-1.50%
0.30	-8379	-8349	4115	651	8997	8583	-3037	0	-1704	670	1358	1992	31.3%	104.8%	-0.71%
0.35	-8379	-8348	4145	648	8955	8553	-3037	110	-1694	662	1550	1998	31.5%	104.7%	-0.36%
0.40	-8379	-8354	4171	646	8924	8533	-3038	0	-1684	655	1800	2005	31.7%	104.6%	0.00%
0.45	-8379	-8339	4193	643	8876	8503	-3038	0	-1673	645	2240	2021	32.0%	104.4%	0.23%
0.50	-8379	-8326	4209	641	8837	8502	-3038	0	-1665	630	9611	2135	32.2%	103.9%	0.24%

Auxiliary heater mass flow rate for the space heating charging loop

In the base case of the reference model the mass flow rate of the boiler during the space heating charging loop is set to 400 kg/h. Figure 9-58 illustrates how the overall system efficiency varies by changing this parameter. The optimum is found at about 300 kg/h with am auxiliary final energy saving in the order of about 0.4%. Table 9-27 shows that also here the effective energy delivered to the building has some small variation so to make impossible a fair comparison most of all due to a so small gain in the saving function.

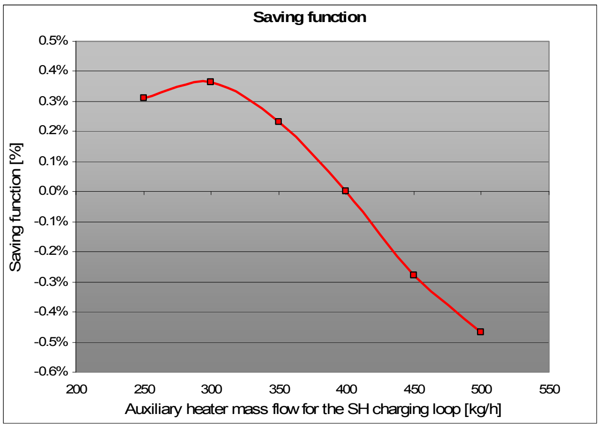

Figure 9-58: Saving function as function of the boiler mass flow rate during the SH charging loop.

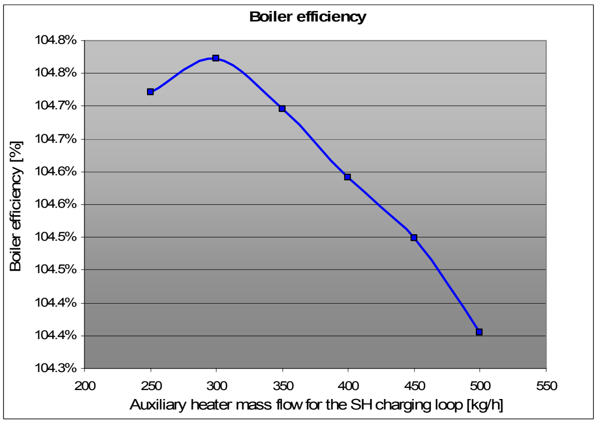

Figure 9-59:Boiler efficiency as function of the boiler mass flow rate during the SH charging loop.

Table 9-27: Simulation results as function of the boiler mass flow rate during the SH charging loop.

Boiler mass flow for the SH charging loop															
Parameter [kg/h]	$Q_{SH,target}$ [kWh/a]	$Q_{SH,eff}$ [kWh/a]	$Q_{solar,tank}$ [kWh/a]	$Q_{solar,loses}$ [kWh/a]	Q_{boiler} [kWh/a]	E_{boiler} [kWh/a]	Q_{DHW} [kWh/a]	V_{DHW40} [l/a]	$Q_{tank,loses}$ [kWh/a]	$Q_{cond,gain}$ [kWh/a]	n_{boiler} [1/a]	t_{boiler} [kWh/a]	$Solar_{\%}$ [%]	η_{boiler} [%]	f_{sav} [%]
250	-8379	-8326	4168	646	8897	8496	-3037	0	-1683	658	64237	2422	31.8%	104.7%	0.31%
300	-8379	-8331	4173	646	8897	8491	-3037	110	-1682	660	2628	2006	31.8%	104.8%	0.36%
350	-8379	-8337	4174	645	8902	8503	-3038	0	-1681	657	1965	2003	31.8%	104.7%	0.23%
400	-8379	-8354	4171	646	8924	8533	-3038	0	-1684	655	1800	2005	31.7%	104.6%	0.00%
450	-8379	-8353	4167	646	8931	8546	-3038	0	-1686	652	1757	1990	31.7%	104.5%	-0.28%
500	-8379	-8356	4166	646	8935	8562	-3038	0	-1687	647	1769	1952	31.7%	104.4%	-0.47%

9.4.3. Space heating loop

<u>Relative position of the storage tank space heating temperature sensor</u>

As the Figure 9-60 shows there are no possibilities of overall system efficiency improvement changing the relative position of the storage tank sensor 2 used by the auxiliary heater controller. The base case value of 0.6 can be considered as already optimized. If the sensor height is raised, is no more possible to match the space heat demand of the building as the $Q_{SH,eff}$ colon in

Table 9-28 illustrates.

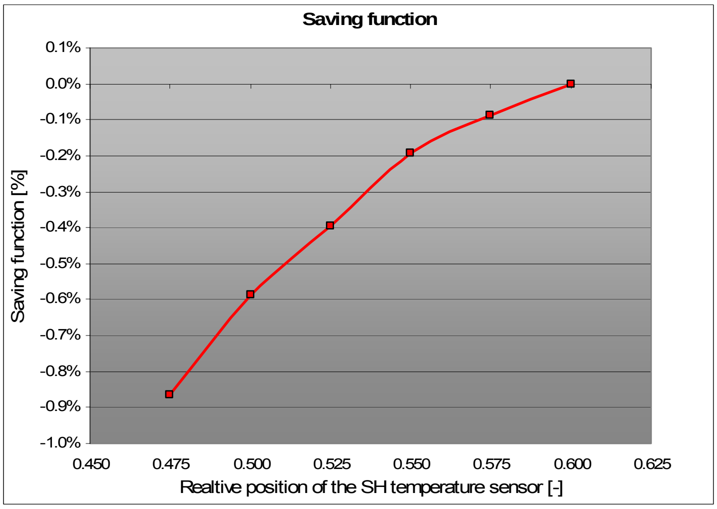

Figure 9-60: Saving function as function of the position of the sensor 2 used by the SH controller

Table 9-28: Simulation results as function of the position of the sensor 2 used by the SH controller

Realtive position of the space heating temperature sensor 2															
Parameter [-]	$Q_{SH,target}$ [kWh/a]	$Q_{SH,eff}$ [kWh/a]	$Q_{solar,tank}$ [kWh/a]	$Q_{solar,loses}$ [kWh/a]	Q_{boiler} [kWh/a]	E_{boiler} [kWh/a]	Q_{DHW} [kWh/a]	V_{DHW40} [l/a]	$Q_{tank,loses}$ [kWh/a]	$Q_{cond,gain}$ [kWh/a]	n_{boiler} [1/a]	t_{boiler} [kWh/a]	$Solar_{\%}$ [%]	η_{boiler} [%]	f_{sav} [%]
0.650	-8379	-3472	4258	634	3898	3709	-3038	0	-1630	328	595	436	52.1%	105.1%	56.41%
0.625	-8379	-4842	4238	637	5301	5058	-3038	0	-1642	419	644	802	44.3%	104.8%	40.60%
0.600	-8379	-8354	4171	646	8924	8533	-3038	0	-1684	655	1800	2005	31.7%	104.6%	0.00%
0.575	-8379	-8346	4169	646	8920	8530	-3037	110	-1684	654	1978	2013	31.7%	104.6%	-0.09%
0.550	-8379	-8347	4166	646	8926	8539	-3038	0	-1687	652	2237	2019	31.7%	104.5%	-0.19%
0.525	-8379	-8346	4163	646	8930	8556	-3038	0	-1689	648	2321	2033	31.7%	104.4%	-0.40%
0.500	-8379	-8346	4159	647	8937	8572	-3037	0	-1692	642	2826	2056	31.7%	104.2%	-0.59%
0.475	-8379	-8347	4152	648	8949	8596	-3037	0	-1696	634	7128	2111	31.6%	104.1%	-0.86%

Space heating outlet

The position of the storage tank outlet to the space heating loop is varied from the relative height position of 0.5 to 0.7. The space heating sensor used by the boiler controller is always placed at the same height as the storage outlet.

As Figure 9-61 illustrates there are no interesting possibility of optimization concerning this parameter.

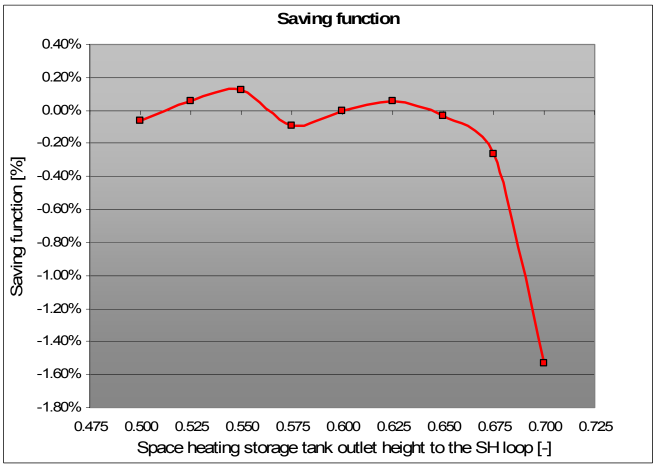

Figure 9-61: Saving function as functions of the relative height of the storage tank outlet to the space heating

Table 9-29: Simulation results as function of the relative height of the storage tank outlet to the space heating

Space heating tank outlet															
Parameter [°C]	$Q_{SH,target}$ [kWh/a]	$Q_{SH,eff}$ [kWh/a]	$Q_{solar,tank}$ [kWh/a]	$Q_{solar,loses}$ [kWh/a]	Q_{boiler} [kWh/a]	E_{boiler} [kWh/a]	Q_{DHW} [kWh/a]	V_{DHW40} [l/a]	$Q_{tank,loses}$ [kWh/a]	$Q_{cond,gain}$ [kWh/a]	n_{boiler} [1/a]	t_{boiler} [kWh/a]	$Solar_{\%}$ [%]	η_{boiler} [%]	f_{sav} [%]
0.500	-8379	-8310	4165	646	8903	8527	-3037	0	-1700	647	4114	2085	31.8%	104.4%	-0.06%
0.525	-8379	-8313	4163	646	8903	8517	-3037	110	-1697	651	3342	2071	31.8%	104.5%	0.06%
0.550	-8379	-8326	4173	646	8903	8512	-3037	110	-1693	653	2771	2060	31.8%	104.6%	0.12%
0.575	-8379	-8341	4163	647	8925	8530	-3037	0	-1690	656	2155	2034	31.7%	104.6%	-0.09%
0.600	-8379	-8354	4171	646	8924	8533	-3038	0	-1684	655	1800	2005	31.7%	104.6%	0.00%
0.625	-8379	-8346	4173	645	8909	8518	-3038	0	-1678	655	1623	1963	31.8%	104.6%	0.06%
0.650	-8379	-8347	4168	646	8911	8525	-3038	0	-1676	655	1590	1908	31.8%	104.5%	-0.03%
0.675	-8379	-8346	4160	647	8918	8545	-3039	0	-1675	656	1692	1764	31.7%	104.4%	-0.26%
0.700	-8379	-8360	4121	652	9004	8653	-3039	0	-1707	656	5239	1225	31.3%	104.1%	-1.53%

Space heating pump flow rate

Varying the space heating pump mass flow rate of the reference system don't show any possibility of optimization. Figure 9-63 shows that strongly reducing the flow rate of the pump implies a lower efficiency of the auxiliary heater. The solar fraction is instead maintained more or less constant.

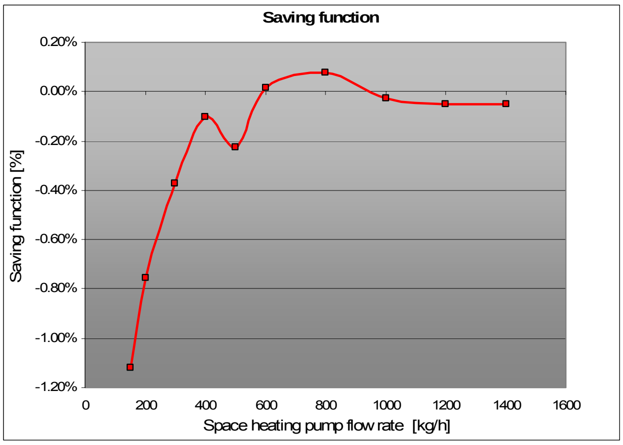

Figure 9-62 Saving function as function of the space heating pump flow rate

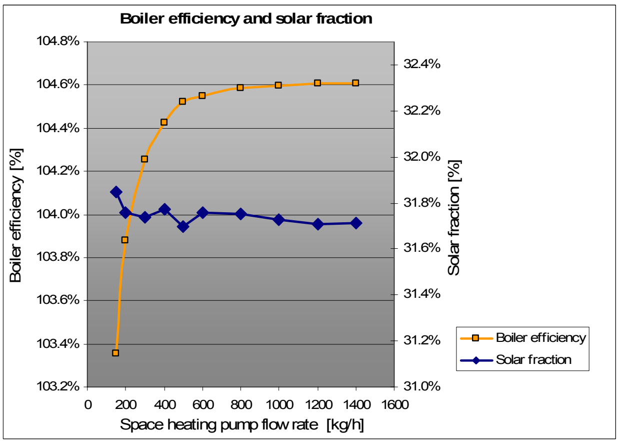

Figure 9-63: Boiler efficiency and solar fraction as function of the space heating pump flow rate

Table 9-30: Simulations results as function of the space heating pump flow rate

Space heating pump flow rate															
Parameter [kg/h]	$Q_{SH,target}$ [kWh/a]	$Q_{SH,eff}$ [kWh/a]	$Q_{solar,tank}$ [kWh/a]	$Q_{solar,loses}$ [kWh/a]	Q_{boiler} [kWh/a]	E_{boiler} [kWh/a]	Q_{DHW} [kWh/a]	V_{DHW40} [l/a]	$Q_{tank,loses}$ [kWh/a]	$Q_{cond,gain}$ [kWh/a]	n_{boiler} [1/a]	t_{boiler} [kWh/a]	$Solar_{\%}$ [%]	η_{boiler} [%]	f_{sav} [%]
1400	-8379	-8356	4168	646	8930	8537	-3038	0	-1683	655	1953	2012	31.7%	104.6%	-0.05%
1200	-8379	-8356	4167	646	8931	8537	-3038	0	-1684	655	1877	2009	31.7%	104.6%	-0.05%
1000	-8379	-8354	4169	646	8927	8535	-3038	0	-1684	655	1833	2004	31.7%	104.6%	-0.03%
800	-8379	-8342	4169	646	8917	8526	-3038	0	-1685	654	1778	1992	31.8%	104.6%	0.08%
600	-8379	-8346	4171	646	8919	8531	-3038	0	-1686	653	1715	1965	31.8%	104.5%	0.01%
500	-8379	-8363	4169	646	8938	8552	-3038	0	-1686	653	1709	1944	31.7%	104.5%	-0.22%
400	-8379	-8349	4175	645	8919	8542	-3038	0	-1687	648	1657	1906	31.8%	104.4%	-0.10%
300	-8379	-8354	4173	645	8929	8564	-3038	0	-1689	643	1572	1849	31.7%	104.3%	-0.37%
200	-8379	-8358	4178	645	8931	8597	-3037	110	-1692	626	1454	1761	31.8%	103.9%	-0.76%
150	-8379	-8354	4189	644	8918	8628	-3038	0	-1693	596	1340	1715	31.8%	103.4%	-1.12%

Boiler charging loop same as DFFC system but traditional SH management

The purpose of this section is to analyze which effect has the space heat management alone on the overall system efficiency. To check this, the boiler loading loop of the reference system has been modified to match that of the Direct Feed Flow Controlled system. It means that in this analysis there's only one storage tank inlet for the supply water coming from the boiler and it's placed at the top of the tank (relative height 1.0). The set supply temperature of the auxiliary heater is fixed at 65°C. The only thing that differs from the boiler loop of the Direct

Feed Flow Controlled concept is the mass flow rate of the boiler pump when working controlled by the space heating sensor (Sensor 2). In this case the mass flow is set to a fix value of 300 kg/h. When the boiler operates to heat the water reserved for the DHW the auxiliary heater mass flow is 200 kg/h, same as for the Direct Feed Flow Controlled system.

As Figure 9-64 shows the efficiency of this system variant compared to the base case of the reference system might improve the overall efficiency. Reducing the space heating pump flow rate it's possible to gain in the boiler efficiency. The solar fraction remain instead more or less constant as Figure 9-65 illustrates. As consequence of the lower mass flow rate, the water exits the space heating pipe at a lower temperature, it follows that the water enters the auxiliary heater at a minor temperature, increasing so its efficiency.

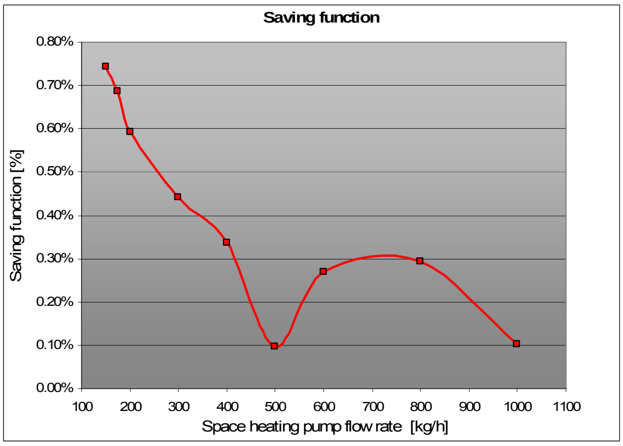

Figure 9-64: Saving function as function of the SH pump flow rate

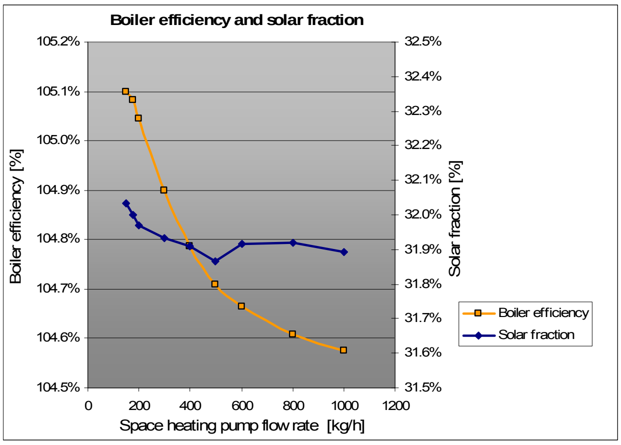

Figure 9-65: Boiler efficiency and solar fraction as function of the SH pump flow rate

Table 9-31: Simulation result as function of the SH pump flow rate

Space heating pump flow rate															
Parameter [kg/h]	$Q_{SH,target}$ [kWh/a]	$Q_{SH,eff}$ [kWh/a]	$Q_{solar,tank}$ [kWh/a]	$Q_{solar,loses}$ [kWh/a]	Q_{boiler} [kWh/a]	E_{boiler} [kWh/a]	Q_{DHW} [kWh/a]	V_{DHW40} [l/a]	$Q_{tank,loses}$ [kWh/a]	$Q_{cond,gain}$ [kWh/a]	n_{boiler} [1/a]	t_{boiler} [kWh/a]	$Solar_{\%}$ [%]	η_{boiler} [%]	f_{sav} [%]
1000	-8379	-8347	4194	643	8914	8524	-3039	0	-1701	672	4746	1504	31.9%	104.6%	0.10%
800	-8379	-8332	4193	643	8900	8508	-3039	0	-1701	673	4793	1494	31.9%	104.6%	0.29%
600	-8379	-8342	4196	643	8907	8510	-3039	0	-1701	678	4881	1484	31.9%	104.7%	0.27%
500	-8379	-8360	4195	642	8926	8524	-3039	0	-1701	682	4925	1479	31.9%	104.7%	0.10%
400	-8379	-8346	4197	642	8911	8504	-3039	0	-1702	685	4990	1462	31.9%	104.8%	0.34%
300	-8379	-8351	4202	642	8911	8495	-3039	0	-1702	691	5025	1443	31.9%	104.9%	0.44%
200	-8379	-8355	4209	641	8910	8482	-3039	0	-1703	699	4957	1418	32.0%	105.0%	0.59%
175	-8379	-8352	4212	641	8905	8474	-3039	0	-1704	701	4858	1411	32.0%	105.1%	0.69%
150	-8379	-8352	4218	640	8901	8469	-3039	0	-1705	701	4718	1409	32.0%	105.1%	0.74%

Space heating pipe

In this section the influence of the space heating pipe parameters is analyzed to find if their variation makes the system performance change. The first parameter study presented is the variation in the pipes loss coefficient.

Figure 9-66 illustrates that also for the reference system there's a strong correlation between the pipe heat exchange coefficient and the system efficiency. Also here the effect is easily explained considering Figure 9-67, which illustrates that for an higher value of the pipe heat loss coefficient both the solar fraction and the boiler efficiency are higher.

As said before this effect is a consequence of the return temperature from the space heating loop that for an higher loss coefficient is much lower due to the faster cool process of the water. This lead to a better solar and boiler efficiency. This correlation between space heating return temperature and solar and boiler efficiency is explained in grater detail in section 10.2.

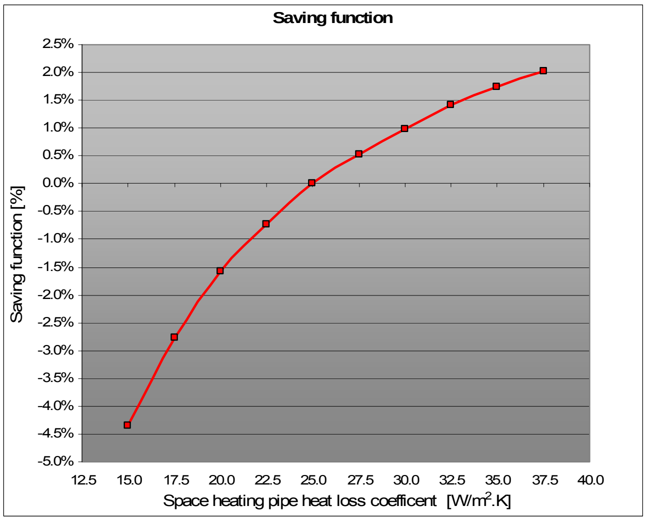

Figure 9-66: Saving function as function of the space heating pipe loss coefficient

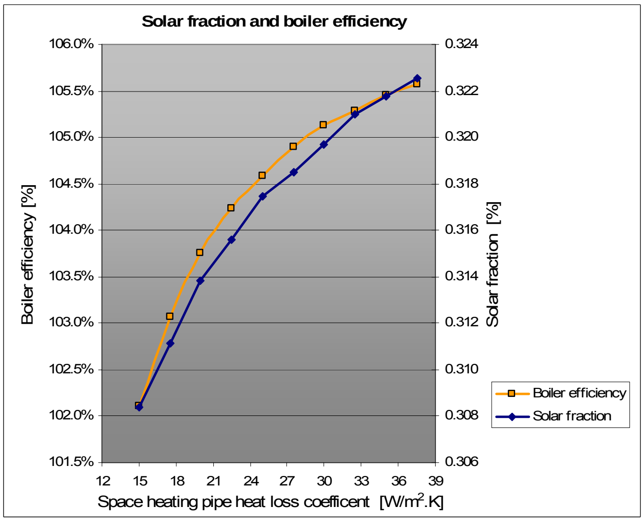

Figure 9-67: Solar fraction and boiler efficiency as function of the space heating pipe loss coefficient

Table 9-32: Simulation results as function of the space heating pipe loss coefficient

Space heating pipe heat loss coefficent															
Parameter [W/m^2.k]	$Q_{SH,target}$ [kWh/a]	$Q_{SH,eff}$ [kWh/a]	$Q_{solar,tank}$ [kWh/a]	$Q_{solar,loses}$ [kWh/a]	Q_{boiler} [kWh/a]	E_{boiler} [kWh/a]	Q_{DHW} [kWh/a]	V_{DHW40} [l/a]	$Q_{tank,loses}$ [kWh/a]	$Q_{cond,gain}$ [kWh/a]	n_{boiler} [1/a]	t_{boiler} [kWh/a]	$Solar_{\%}$ [%]	η_{boiler} [%]	f_{sav} [%]
15.0	-8379	-8384	4076	657	9092	8904	-3038	0	-1724	522	1727	2207	30.8%	102.1%	-4.35%
17.5	-8379	-8374	4105	654	9039	8770	-3038	0	-1711	579	1793	2136	31.1%	103.1%	-2.78%
20.0	-8379	-8368	4134	650	8992	8667	-3038	0	-1699	614	1800	2080	31.4%	103.8%	-1.57%
22.5	-8379	-8362	4152	648	8959	8595	-3037	110	-1691	638	1823	2040	31.6%	104.2%	-0.73%
25.0	-8379	-8354	4171	646	8924	8533	-3038	0	-1684	655	1800	2005	31.7%	104.6%	0.00%
27.5	-8379	-8347	4181	645	8903	8488	-3038	0	-1679	669	1805	1973	31.8%	104.9%	0.52%
30.0	-8379	-8343	4193	643	8881	8448	-3038	0	-1674	679	1780	1944	32.0%	105.1%	0.99%
32.5	-8379	-8337	4206	641	8857	8412	-3038	0	-1669	686	1771	1926	32.1%	105.3%	1.42%
35.0	-8379	-8332	4214	640	8841	8384	-3037	110	-1666	692	1761	1904	32.2%	105.5%	1.75%
37.5	-8379	-8328	4222	639	8827	8361	-3038	0	-1663	697	1748	1888	32.3%	105.6%	2.01%

Figure 9-68 illustrates the effect of the space heating pipe length on the overall system efficiency. Also here the correlation between pipe length and auxiliary final energy saved is explained by the fact that the return temperature is much lower for a longer space heating pipe, leading to a higher solar and boiler efficiency (Figure 9-69)

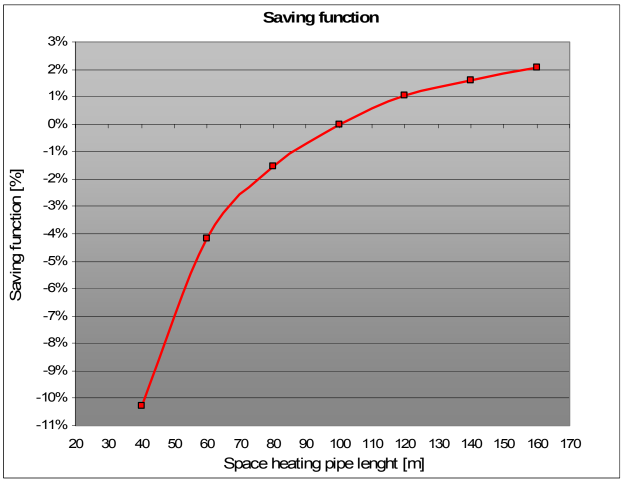

Figure 9-68: Saving function as function of the space heating pipe length

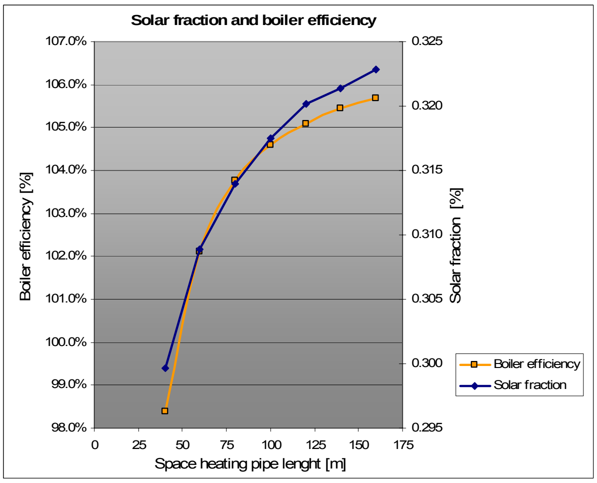

Figure 9-69: Boiler efficiency and solar fraction as function of the space heating pipe length

Table 9-33: Simulation results as function of the space heating pipe length

Space heating pipe length															
Parameter [m]	$Q_{SH,target}$ [kWh/a]	$Q_{SH,eff}$ [kWh/a]	$Q_{solar,tank}$ [kWh/a]	$Q_{solar,loses}$ [kWh/a]	Q_{boiler} [kWh/a]	E_{boiler} [kWh/a]	Q_{DHW} [kWh/a]	V_{DHW40} [l/a]	$Q_{tank,loses}$ [kWh/a]	$Q_{cond,gain}$ [kWh/a]	n_{boiler} [1/a]	t_{boiler} [kWh/a]	$Solar_{\%}$ [%]	η_{boiler} [%]	f_{sav} [%]
40.0	-8379	-8397	3987	666	9256	9409	-3037	110	-1782	276	1431	2427	30.0%	98.4%	-10.27%
60.0	-8379	-8370	4079	657	9076	8889	-3037	110	-1725	521	1737	2201	30.9%	102.1%	-4.17%
80.0	-8379	-8365	4135	650	8989	8663	-3038	0	-1699	614	1810	2079	31.4%	103.8%	-1.53%
100.0	-8379	-8354	4171	646	8924	8533	-3038	0	-1684	655	1800	2005	31.7%	104.6%	0.00%
120.0	-8379	-8343	4199	642	8873	8443	-3037	110	-1672	677	1787	1949	32.0%	105.1%	1.06%
140.0	-8379	-8345	4213	640	8854	8396	-3038	0	-1666	693	1760	1909	32.1%	105.5%	1.60%
160.0	-8379	-8346	4231	638	8833	8358	-3037	110	-1661	703	1731	1876	32.3%	105.7%	2.05%

Space heating load

Also for the reference model it’s checked how the model behaves under different space heating loads. As described before the input from the load file that represent the building is multiplied by a constant so to make the $Q_{SH,target}$ value at the end of the year change. The base case load file represent a building with an energy requirement of 60 kWh/m^{2}a as described in section 5.3.6.

The base case is compared with other two variant, which represent a 30 kWh/m^{2}a and 100 kWh/m^{2}a building respectively. The heating power input of the load file is multiplied by 0.5 to replicate the 30 kWh/m^{2}a variant and by 1.66 to simulate a 100 kWh/m^{2}a house.

The results are resumed in Table 9-34. In this case, as the η_{solar} colon shows, the boiler has the best efficiency for the 30 kWh/m^{2}a variant but is very near to that of the 60 kWh/m^{2}a simulation. For a 100 kWh/m^{2}a heat load the reference system cover only the 97.5% of the heat needed.

Table 9-34: Simulation results as function of the space heating load

Space heating load															
Parameter [kWh/m^{2}a]	$Q_{SH,target}$ [kWh/a]	$Q_{SH,eff}$ [kWh/a]	$Q_{solar,tank}$ [kWh/a]	$Q_{solar,loses}$ [kWh/a]	Q_{boiler} [kWh/a]	E_{boiler} [kWh/a]	Q_{DHW} [kWh/a]	V_{DHW40} [l/a]	$Q_{tank,loses}$ [kWh/a]	$Q_{cond,gain}$ [kWh/a]	n_{boiler} [1/a]	t_{boiler} [kWh/a]	Solar$_{\%}$ [%]	η_{boiler} [%]	f_{sav} [%]
30	-4190	-4105	4072	652	4796	4582	-3038	0	-1706	379	1385	890	45.8%	104.7%	46.30%
60	-8379	-8354	4171	646	8924	8533	-3038	0	-1684	655	1800	2005	31.7%	104.6%	0.00%
100	-13966	-13619	4181	645	14188	13718	-3038	0	-1691	885	1026	3082	22.7%	103.4%	-60.77%

9.4.4. Conclusions

The detailed parameter analysis performed for the reference system concept shows that also this model has a solid behavior. Also here there aren't big possibility of optimization concerning the parameter analyzed. The choice of the base case parameters seems to be already practically optimized.

10. *Comparison between the two concepts*

10.1. Introduction

The two system concepts analyzed in detail in section 9.3 and 9.4 are now compared directly to found what are the major differences and which are the strength of the Direct Feed Flow Controlled model over a traditional combisystem represented by the reference system.

For this comparison no parameters change is made over the base case of both concepts due to the fact that the optimization analysis performed in the previous sections didn't brought to any significant improvements.

10.2. Space heating control management

A big difference between the two system concepts consists in the space heating control management. One side it's present a mass flow controlled space heating loop other side a temperature controlled space heating system. A key point cleared by the simulations performed concern the difference in the space heating return temperature between the two concepts. In the Direct Feed Flow Controlled system it's possible to reach very low return temperature of the water coming from the space heating loop due to the fact that the mass flow of the space heating pump is much lower.

In Figure 10-1 is plotted the return temperature of the space heating loop as function of the heating power for different supply temperature of the Direct Feed Flow Controlled combisystem and as comparison it's also plotted the power dependant curve of the reference system. As it's shown there is a large difference in the return temperature between the two concepts that can reach 10 °C

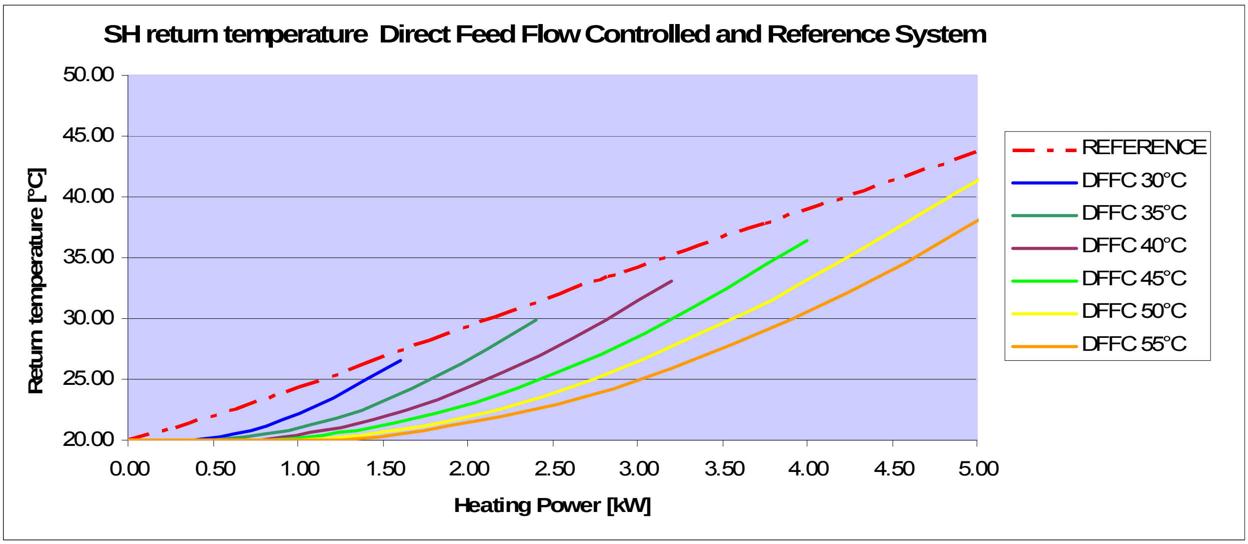

Figure 10-1: Space heating return temperature as function of the heating power and the supply temperature.

To better understand the behavior of the two space heating control systems their heating curves are presented in the following paragraphs.

As said before the reference system controls the heating power varying the supply temperature that goes into the space heating loop by mean of a tempering valve (see section 6.4.3). Figure 10-2 illustrates how the heating power varies as function of the supply temperature.

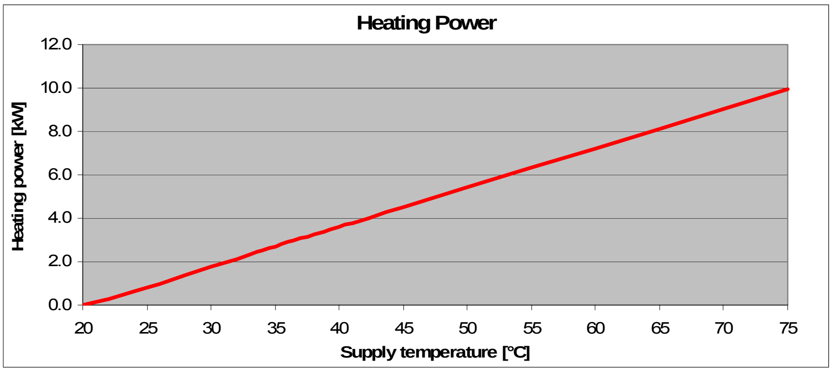

Figure 10-2: Heating power as function of the supply temperature of the reference system

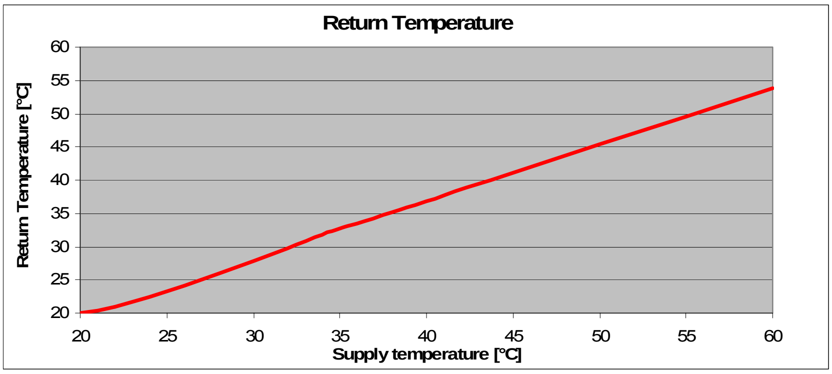

Figure 10-3: Return temperature as function of the supply temperature of the reference system

The heat management of the Direct Feed Flow Controlled system is instead controlled by the mass flow rate of the space heating pump as described in section 5.4.3. Figure 10-4 shows how the heating power and the return temperature vary as function of the pump mass flow rate and the supply temperature. Each color represents a different supply temperature. In this case the supply temperature is not directly controlled but it depends on the chosen value of the maximal temperature allowed to flow into the space heating pipes (for the base case a value of 55°C is chosen). If the water temperature at the storage tank outlet is lower than the set temperature of the temperature limiting valve the supply temperature is simply the storage tank outlet temperature.

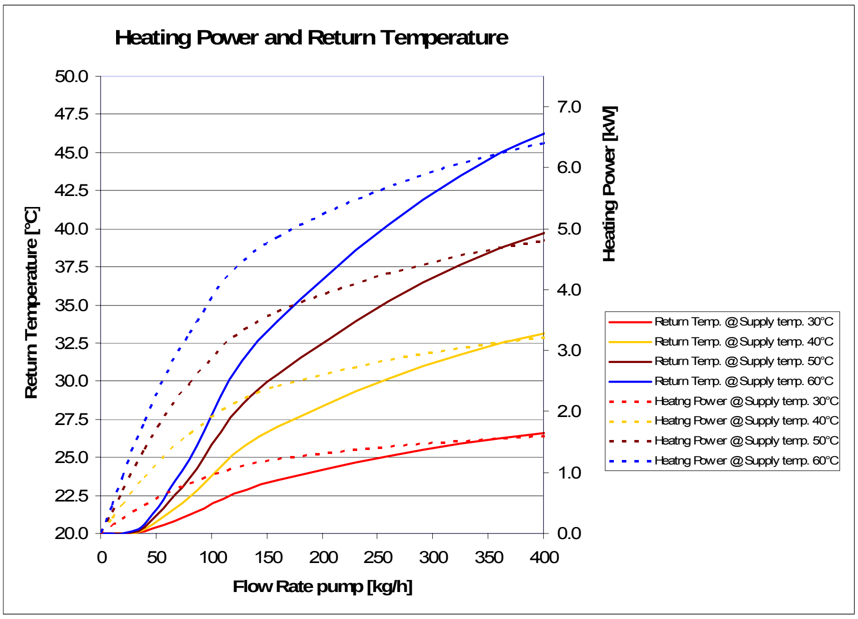

Figure 10-4: Heating power and return temperature as function of the supply temperature and the mass flow rate of the space heating pump

Another interesting point concerning the Direct Feed Flow Controlled model is given by the fact that for an higher supply temperature to the space heating loop it's possible to get an even lower return temperature as Figure 10-4 demonstrates. This is a consequence of the equation 10-1 which describes the heating power delivered by a pipe for a given supply temperature and a flow rate. See Appendix A for more detail about how the equation is derived.

$$\dot{Q}(l_{Pipe}) = \left(T_{Supply} - T_{Room} - \left(T_{Supply} - T_{Room}\right) \cdot \exp\left(-\frac{d_{pipe} \cdot \pi \cdot l_{Pipe}}{\dot{m} \cdot c_p} \cdot K_{pipe} \right) \right) \cdot c_p \cdot \dot{m} \qquad \textbf{\textit{Equation 10-1}}$$

With: T_{supply} : Temperature of the water supply entering the space heating loop [°C]

T_{room} = 20°C : Room temperature at which heat is exchanged

l_{pipe} = 100 m : Pipe length

d_{pipe} = 0.025 m : Pipe diameter

K_{pipe} = 25 [W/m^2.K] : Heat losses coefficient of the pipe

c_p = 4.190 [J/kg.K] : Specific heat of the water

$\dot{m}$: Mass flow rate of the space heating pump [kg/h]

The consequences of this variation in the return temperature leads to a difference in the boiler and solar efficiency. Bringing lower return temperature into the lower part of the storage tank come out in an higher system efficiency. This is due to the fact that the feed water entering the boiler loop has consequently a lower temperature leading to an higher condensation gain and increasing so the auxiliary heater efficiency. Other side also the middle temperature of the solar collectors drops, increasing the solar gain.

10.3. Overall system efficiency

In this section the overall system efficiency of the two concepts is compared. The saving function is referred to the base case of the reference system ($f_{sav,ref}$). The parameters chosen are for both systems are them of the base case models described in section 5 and 6. Because of the minimal optimization possibility non changes are made.

In

Table 10-1 are contained the simulation output results for both concepts. Last colon shows the saving function and demonstrates that the Direct Feed Flow Controlled concept has an overall system efficiency in the order of 2.4% higher compared to the reference system. It follows that with a Direct Feed Flow Controlled combisystem it's possible to save about 305 kWh per year of auxiliary final energy (in this case gas).

Table 10-1: Overall system efficiency comparison of the DFFC concept referred to the reference system.

	$Q_{SH,target}$ [kWh/a]	$Q_{SH,eff}$ [kWh/a]	$Q_{solar,tank}$ [kWh/a]	$Q_{solar,loses}$ [kWh/a]	Q_{boiler} [kWh/a]	E_{boiler} [kWh/a]	Q_{DHW} [kWh/a]	V_{DHW40} [l/a]	$Q_{tank,loses}$ [kWh/a]	$Q_{cond,gain}$ [kWh/a]	n_{boiler} [1/a]	t_{boiler} [kWh/a]	$Solar_{\%}$ [%]	η_{boiler} [%]	f_{sav} [%]
DFFC basis case	-8379	-8335	4283	632	8814	8328	-3038	0	-1680	733	5242	1782	0.326	1.058	2.40%
Reference basis case	-8379	-8334	4171	646	8924	8533	-3038	0	-1684	655	1800	2005	0.317	1.046	0.00%

It's now interesting to check how the two solar combisystem concepts behaves varying the parameters of the simulated floor space heating pipe. This study is most of all worthy the note to check if the better efficiency of the Direct Feed Flow Controlled combisystem is only reached in the base case variant or if the possibility of an auxiliary energy saving includes a larger range of possible space heating element variants.

The space heating pipe loss coefficient is varied to simulate a different insulation condition between the heating element and the place at which heat is exchanged. The results are shown in the following figures. Figure 10-5 shows that the overall system efficiency of the Direct Feed Flow Controlled combisystem remains for all the simulated range always at least 1.2% higher than that of the reference system. The boiler efficiency and the solar fraction follow a similar curve as Figure 10-6 and Figure 10-7 respectively show.

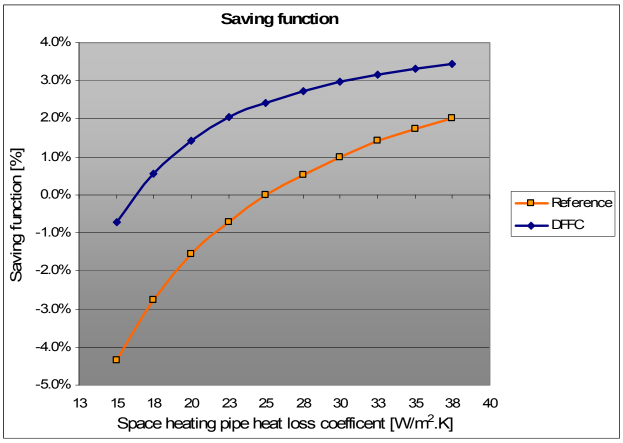

Figure 10-5: Saving function comparison between the DFFC and reference system as function of the space heating pipe heat loss coefficient

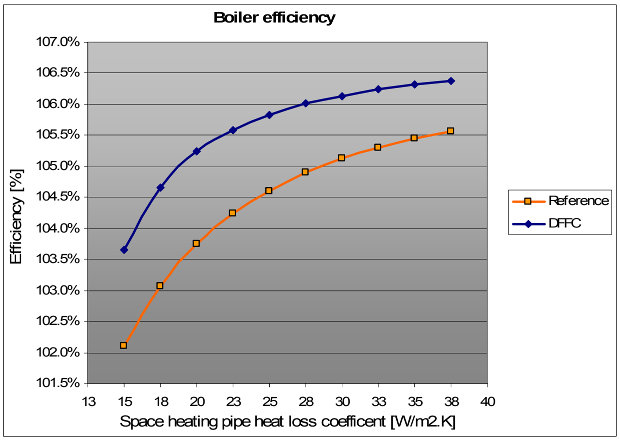

Figure 10-6: Boiler efficiency comparison between the DFFC and reference system as function of the space heating pipe heat loss coefficient

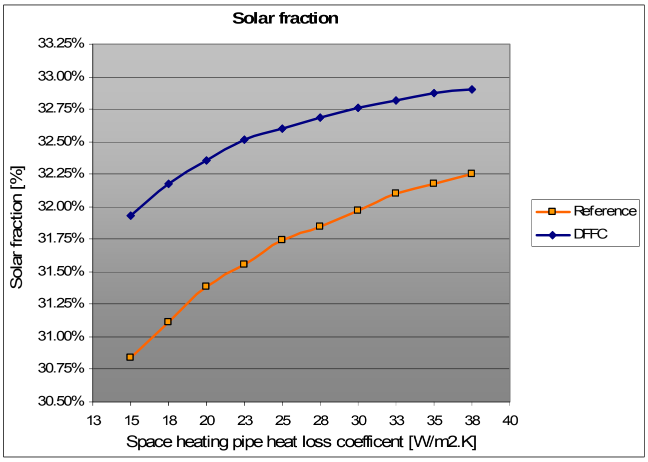

Figure 10-7: Solar fraction comparison between the DFFC and reference system as function of the space heating pipe heat loss coefficient

From Figure 10-8 to Figure 10-10 are plotted the saving function, the boiler efficiency and the solar fraction as function of the heating pipe length for both concepts. Also here the Direct Feed Flow Controlled combisystem shows always an higher efficiency compared to the traditional system.

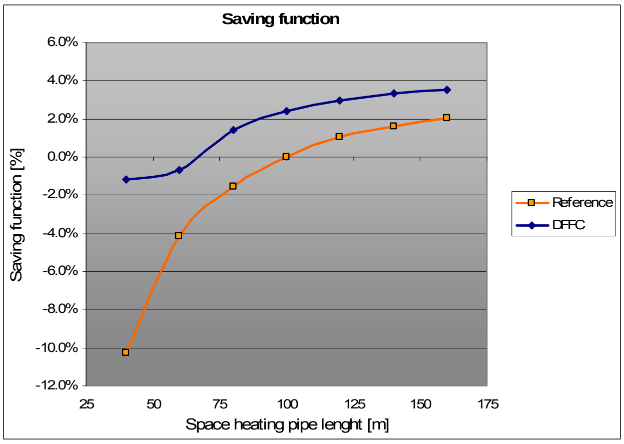

Figure 10-8: Saving function comparison between the DFFC and reference system as function of the space heating pipe length

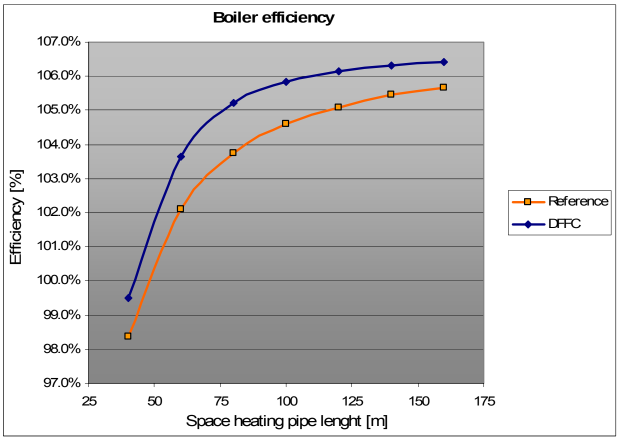

Figure 10-9: Boiler efficiency comparison between the DFFC and reference system as function of the space heating pipe length

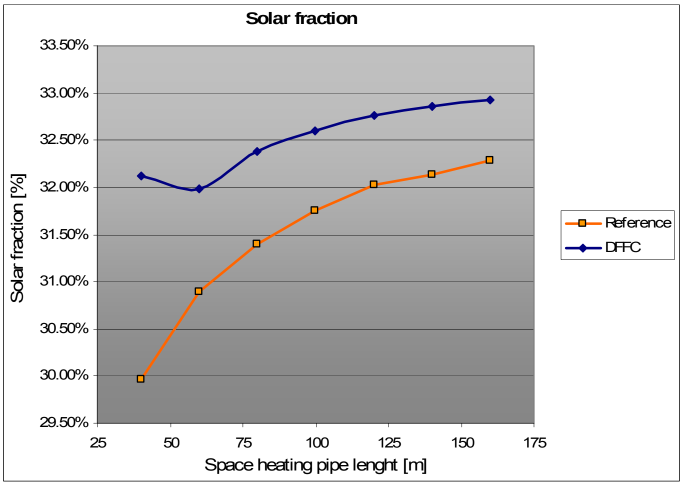

Figure 10-10: Solar fraction comparison between the DFFC and reference system as function of the space heating pipe length

11. *Direct Feed versus Heat Exchangers*

11.1. Introduction

The purpose of this section is to show the difference in the boiler, solar and overall system efficiency that the introduction of one or more heat exchanger in the storage tank instead of the direct feed concept cause. This analysis is performed and then compared to the Direct Feed Flow Controlled basis case of section 5.

The effect that the introduction of an heat exchanger has is tested on the solar loop and the space heating loop. A closed solar loop is a common variant in a solar combisystem. Other side the heat exchanger for the space heating loop would allow to avoid all the problems concerned in the assembly of a non-pressurized system that could be a problem for non skilled technicians.

The heat exchanger is simulated using the model integrated in TRNSYS Type 140. Equation 11-1 represents how the capacity rate of the heat exchanger is calculated in the simulation model. The heat exchanger parameters are fitted to match the data measured in a test done at the SPF (the documentation is maintained reserved).

$$UA_0 = UA_{EX} \cdot \dot{m}_{EX}^{\,b_1} \cdot \left(T_{HX,in} - T_{s,i}\right)^{b_2} \cdot \left(\frac{T_{HX,in} + T_{s,i}}{2}\right)^{b_3}$$ ***Equation 11-1***

With:
UA_{EX} = Capacity rate from the TRNSYS – Deck [kJ/hK]
$\dot{m}_{EX}$ = Mass flow rate through the heat exchanger [kg/s]
$T_{HX,in}$ = Inlet temperature of the heat exchanger [°C]
$T_{s,i}$ = Temperature of corresponding store tank node i [°C]
b_1 = exponent parameter 1 [-]
b_2 = exponent parameter 2 [-]
b_3 = exponent parameter 3 [-]

In this case the exponents b_1 and b_2 are set to zero. It follows that the heat exchanger coefficient UA_0 is only dependent on the water temperature entering the heat exchanger and the storage temperature at the node j of the heat exchanger.

Two different heat exchangers are modeled, one for the solar loop and another one for the space heating loop.

Table 11-1 shows the parameters used in TRNSYS Type 140 for the solar loop heat exchanger.

Table 11-1: Solar loop heat exchanger parameters [1)]Relative height: Storage bottom = 0, Storage top = 1

Solar Loop Heat Exchanger	Relative inlet position[1)]	0.3..0.8 [-]
	Relative outlet position[1)]	0.0 [-]
	Heat exchanger volume	5.73 [l]
	Specific heat capacity of the fluid	3.7 [kJ/kg.K]
	Nominal heat transfer rate	120 kJ/h.K
	Heat exchanger area	2 [m^2]
	Exponent b1	0 [-]
	Exponent b2	0 [-]
	Exponent b3	0.5 [-]

To simulate a variation in the heat exchanger area during the parameter study the value of UA_0 is modified as Table 11-2 shows.

Table 11-2: UA_0 coefficient as function of the solar loop heat exchanger area

Heat Exchanger Area [m^2]	UA_0 [kJ/hK]
0.5	60
1	120
1.5	180
2	240
2.5	300
3	360
4	480
5	600

Figure 11-1 illustrates how the capacity rate of the solar loop heat exchanger varies as a function of the mean temperature calculated between the inlet temperature and the storage temperature at the concerned node.

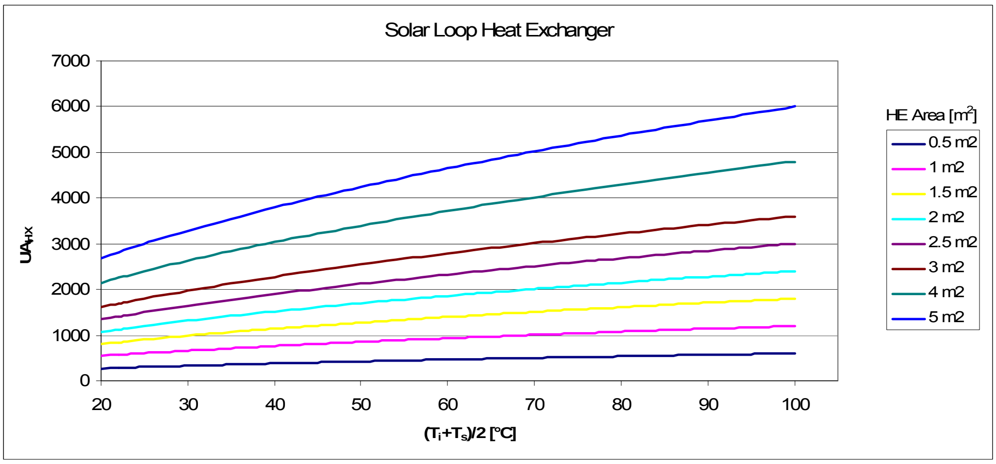

Figure 11-1: Solar loop heat exchanger capacity rate curves

In Table 11-3 are given the parameter used to simulate the space heating loop heat exchanger. Table 11-4 shows how the capacity rate is varied to simulate a variation in the heat exchanger area.

Table 11-3: Space heating loop heat exchanger parameters 1)Relative height: Storage bottom = 0, Storage top = 1

Space Heating Loop Heat Exchanger	Relative outlet position 1)	0.65 [-]
	Relative inlet position 1)	0.3..0.55 [-]
	Heat exchanger volume	5.73 [l]
	Specific heat capacity of the fluid	4.181 [kJ/kg.K]
	Nominal heat transfer rate	760 kJ/h.K
	Heat exchanger area	2 [m^2]
	Exponent b1	0 [-]
	Exponent b2	0 [-]
	Exponent b3	0.29 [-]

Table 11-4: UA_0 coefficient as function of the space heating loop heat exchanger area

Heat Exchanger Area [m^2]	UA_0 [kJ/hK]
0.5	190
1	380
1.5	570
2	760
2.5	950
3	1140
4	1520
5	1900

In Figure 11-2 are plotted the heat exchanger capacity rate curves for different mean temperatures and area values.

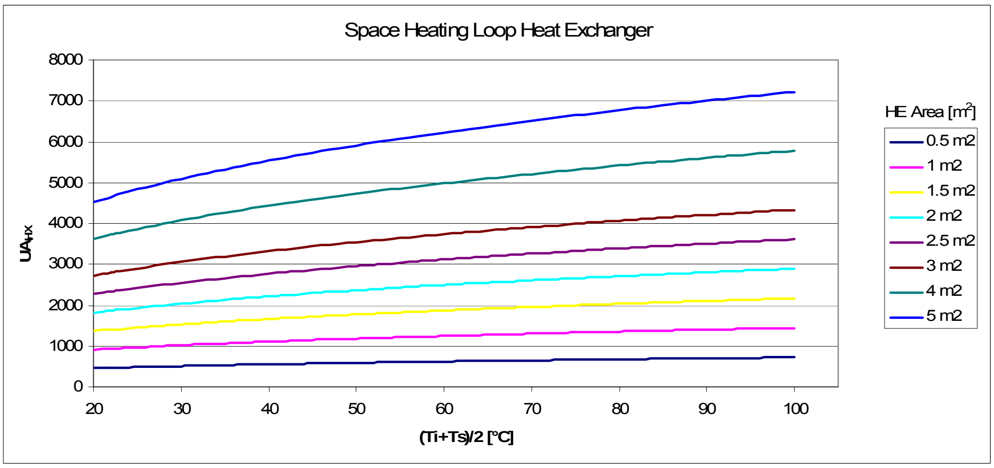

Figure 11-2: Space heating loop heat exchanger capacity rate curves

11.2. Solar loop heat exchanger

The first analysis performed consists in introducing into the storage tank an heat exchanger only for solar loop. All others parameter of the storage are maintained unchanged as Figure 11-3 shows.

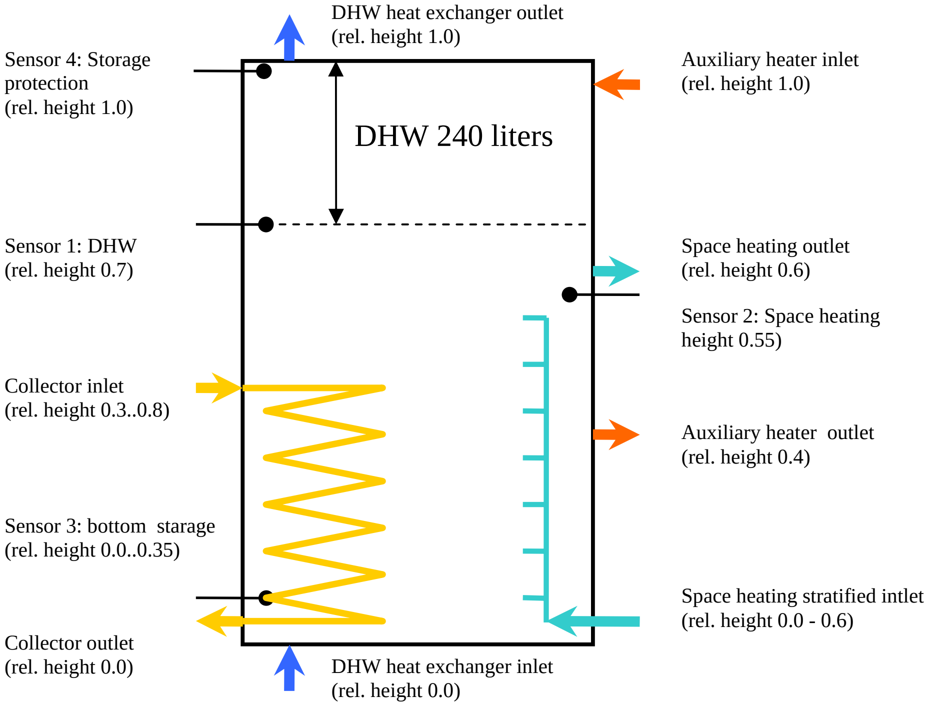

Figure 11-3: Storage tank detail

A short parameter study was necessary to optimize the heat exchanger inlet and outlet position and the relative height of the sensor 3 of the storage tank used to control the collector pump operation.

Heat exchanger inlet

Figure 11-4 illustrates how the saving function varies according to the relative height of the heat exchanger inlet. During the simulation the position of sensor 3 is always placed at 2/3 of the heat exchanger inlet relative height. The heat exchanger outlet position is fixed at 0.0 (the bottom of the storage) and its area is 2 m^2.

The maximum of this curve is found at about an inlet relative height of 0.4. This optimized inlet height will be used as basis for further parameter analysis on the solar loop.

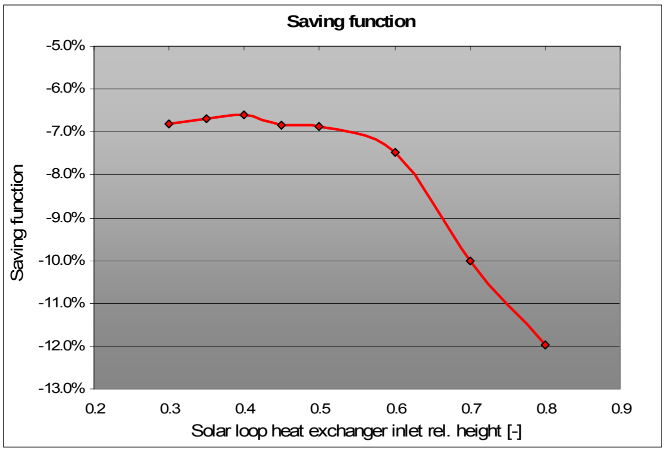

Figure 11-4: Saving function as function of the heat exchanger inlet relative height

Table 11-5: Simulation results as function of the heat exchanger inlet relative height

Solar loop heat exchanger inlet and sensor 3 position																	
Heat exchanger area [m^2]	Heat exchanger inlet rel. height [-]	Sensor 3 rel. Height [-]	$Q_{SH,target}$ [kWh/a]	$Q_{SH,eff}$ [kWh/a]	$Q_{solar,tank}$ [kWh/a]	$Q_{solar,loses}$ [kWh/a]	Q_{boiler} [kWh/a]	E_{boiler} [kWh/a]	Q_{DHW} [kWh/a]	V_{DHW40} [l/a]	$Q_{tank,loses}$ [kWh/a]	$Q_{cond,gain}$ [kWh/a]	n_{boiler} [1/a]	t_{boiler} [kWh/a]	$Solar_{\%}$ [%]	η_{boiler} [%]	f_{sav} [%]
2.0	0.80	0.53	-8379	-8358	3019	581	9867	9326	-3038	0	-1469	819	5600	1947	23.3%	105.8%	-11.98%
2.0	0.70	0.47	-8379	-8358	3227	587	9683	9160	-3038	0	-1492	801	5614	1908	24.9%	105.7%	-10.00%
2.0	0.60	0.40	-8379	-8359	3439	576	9466	8950	-3038	0	-1487	786	5898	1920	26.5%	105.8%	-7.47%
2.0	0.50	0.33	-8379	-8360	3514	586	9408	8900	-3038	0	-1504	780	5943	1917	27.1%	105.7%	-6.87%
2.0	0.45	0.30	-8379	-8361	3520	591	9403	8897	-3038	0	-1504	778	6013	1914	27.1%	105.7%	-6.84%
2.0	0.40	0.27	-8379	-8360	3543	601	9383	8879	-3038	0	-1508	776	6078	1911	27.3%	105.7%	-6.61%
2.0	0.35	0.23	-8379	-8360	3541	610	9388	8884	-3038	0	-1511	776	6080	1911	27.3%	105.7%	-6.68%
2.0	0.30	0.20	-8379	-8361	3529	613	9399	8894	-3038	0	-1508	777	6138	1914	27.2%	105.7%	-6.80%

Sensor position

Given the fixed optimized inlet and outlet positions of the heat exchanger found above, the position of the sensor 3 is varied to check which is its influence. Figure 11-5 shows that there's an evident optimum position of the sensor at a relative height of about 0.05 - 0.1.

The sensor position of 0.1 will be used as optimized value for the last parameter study concerning the heat exchanger area.

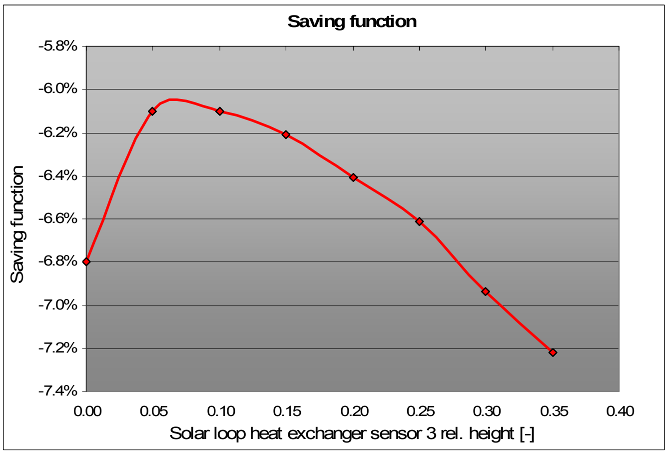

Figure 11-5: Saving function as function of the sensor 3 relative height

Table 11-6 Simulation results as function of the sensor 3 relative height

Solar loop heat exchanger sensor 3 position																	
Heat exchanger area [m^2]	Heat exchanger inlet rel. height [-]	Sensor 3 rel. Height [-]	$Q_{SH,target}$ [kWh/a]	$Q_{SH,eff}$ [kWh/a]	$Q_{solar,tank}$ [kWh/a]	$Q_{solar,loses}$ [kWh/a]	Q_{boiler} [kWh/a]	E_{boiler} [kWh/a]	Q_{DHW} [kWh/a]	V_{DHW40} [l/a]	$Q_{tank,loses}$ [kWh/a]	$Q_{cond,gain}$ [kWh/a]	n_{boiler} [1/a]	t_{boiler} [kWh/a]	$Solar_{\%}$ [%]	η_{boiler} [%]	f_{sav} [%]
2.0	0.40	0.00	-8379	-8360	3555	725	9393	8894	-3037	0	-1530	774	6006	1911	27.3%	105.6%	-6.80%
2.0	0.40	0.05	-8379	-8361	3619	678	9333	8836	-3038	0	-1533	770	5873	1899	27.8%	105.6%	-6.10%
2.0	0.40	0.10	-8379	-8360	3612	649	9335	8836	-3038	0	-1528	771	6056	1903	27.8%	105.7%	-6.10%
2.0	0.40	0.15	-8379	-8361	3597	630	9346	8845	-3038	0	-1524	772	6116	1906	27.7%	105.7%	-6.21%
2.0	0.40	0.20	-8379	-8360	3571	614	9365	8861	-3038	0	-1517	775	5989	1903	27.5%	105.7%	-6.41%
2.0	0.40	0.25	-8379	-8360	3543	601	9383	8879	-3038	0	-1508	776	6078	1911	27.3%	105.7%	-6.61%
2.0	0.40	0.30	-8379	-8361	3509	591	9412	8905	-3038	0	-1502	779	6083	1917	27.0%	105.7%	-6.94%
2.0	0.40	0.35	-8379	-8360	3470	582	9437	8929	-3038	0	-1488	782	6237	1922	26.8%	105.7%	-7.22%

Heat exchanger area

Using the parameter found performing the optimization study of the previous paragraphs, the heat exchanger area is varied to see which consequence this change has on the overall system efficiency.

The saving function is plotted in Figure 11-6 and demonstrates that the increase in system efficiency for an area above 1.5 m^2 is very limited.

The overall system efficiency fall compared to the Direct Feed Flow Controlled combisystem base case of chapter 5 is considerable.

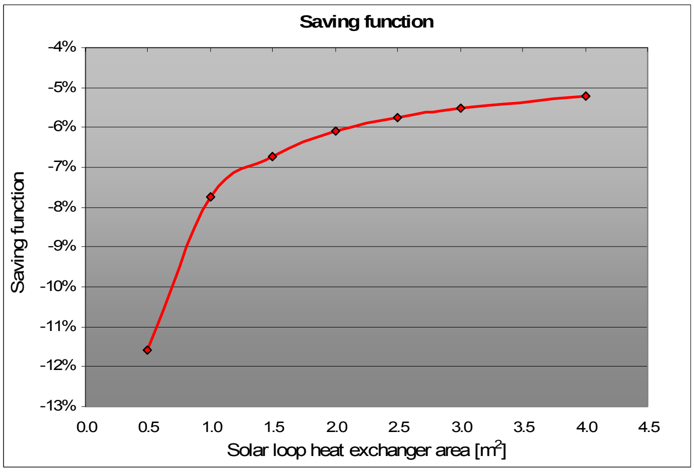

Figure 11-6: Saving function as function of the heat exchanger area

Table 11-7: Simulation results as function of the heat exchanger area

Solar loop heat exchanger area																	
Heat exchanger area [m^2]	Heat exchanger inlet rel. height [-]	Sensor 3 rel. Height [-]	$Q_{SH,target}$ [kWh/a]	$Q_{SH,eff}$ [kWh/a]	$Q_{solar,tank}$ [kWh/a]	$Q_{solar,loses}$ [kWh/a]	Q_{boiler} [kWh/a]	E_{boiler} [kWh/a]	Q_{DHW} [kWh/a]	V_{DHW40} [l/a]	$Q_{tank,loses}$ [kWh/a]	$Q_{cond,gain}$ [kWh/a]	n_{boiler} [1/a]	t_{boiler} [kWh/a]	$Solar_{\%}$ [%]	η_{boiler} [%]	f_{sav} [%]
0.5	0.40	0.10	-8379	-8361	2999	721	9800	9292	-3037	0	-1380	804	6478	2017	23.3%	105.5%	-11.58%
1.0	0.40	0.10	-8379	-8361	3417	684	9480	8973	-3037	0	-1478	783	6163	1935	26.4%	105.7%	-7.75%
1.5	0.40	0.10	-8379	-8361	3542	663	9389	8887	-3038	0	-1512	775	6110	1914	27.3%	105.6%	-6.71%
2.0	0.40	0.10	-8379	-8360	3612	649	9335	8836	-3038	0	-1528	771	6056	1903	27.8%	105.7%	-6.10%
2.5	0.40	0.10	-8379	-8360	3653	640	9303	8806	-3038	0	-1537	768	6022	1896	28.1%	105.6%	-5.74%
3.0	0.40	0.10	-8379	-8360	3680	633	9282	8786	-3038	0	-1544	766	5822	1888	28.3%	105.6%	-5.50%
4.0	0.40	0.10	-8379	-8360	3717	624	9257	8761	-3038	0	-1555	765	5879	1886	28.5%	105.7%	-5.21%

11.3. Space heating loop heat exchanger

In this section are shown the results caused by the introduction of an heat exchanger in the space heating loop and the influence it has on the overall system efficiency. In the performed study the solar loop remains direct feed charged and all other parameters concerning the storage tank are maintained unchanged as Figure 11-7 shows.

As for section 11.2 also here a short parameter study is performed to optimize the heat exchanger inlet position and the relative height of the sensor 2 used to control the auxiliary heater operation. The heat exchanger outlet position is maintained at fixed relative height of 0.65.

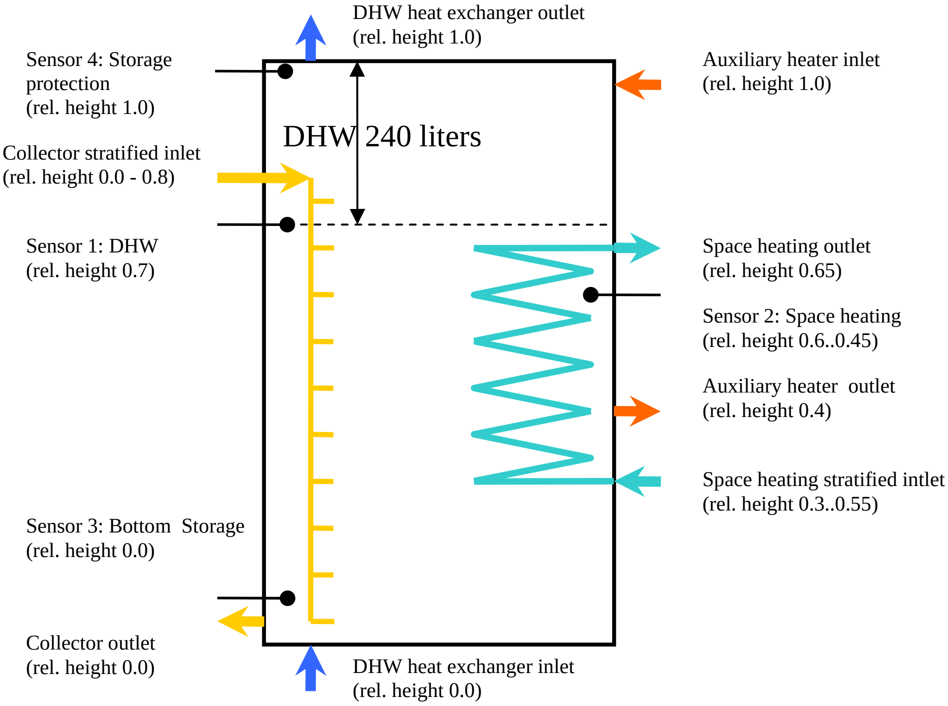

Figure 11-7: Storage tank detail

Heat exchanger inlet

Maintaining the relative position of the heat exchanger outlet and the sensor 2 fixed at 0.65 and 0.55 respectively, the heat exchanger inlet position is varied from 0.3 to 0.55. Its area is set to 2 m^2.

The effects over the overall system efficiency are shown by the saving function in Figure 11-8. As the figure illustrates for an inlet relative height of less than 0.4 the effective energy delivered to the building falls down below 8300 kWh/a. As consequence an optimized value of this parameter can be considered between 0.4 and 0.45.

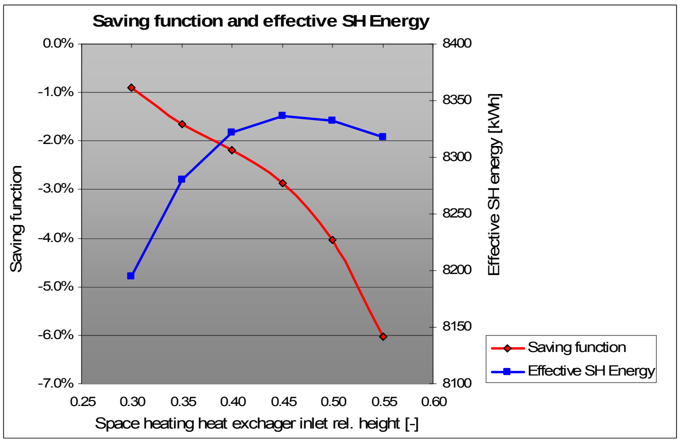

Figure 11-8: Saving function as function of the space heating heat exchanger inlet height

Table 11-8: Simulation results as function of the space heating heat exchanger tank inlet relative height

Space heating loop heat exchanger tank inlet rel. Height																	
Heat exchanger area [m²]	Heat exchanger inlet rel. height [-]	Sensor 3 rel. Height [-]	$Q_{SH,target}$ [kWh/a]	$Q_{SH,eff}$ [kWh/a]	$Q_{solar,tank}$ [kWh/a]	$Q_{solar,loses}$ [kWh/a]	Q_{boiler} [kWh/a]	E_{boiler} [kWh/a]	Q_{DHW} [kWh/a]	V_{DHW40} [l/a]	$Q_{tank,loses}$ [kWh/a]	$Q_{cond,gain}$ [kWh/a]	n_{boiler} [1/a]	t_{boiler} [kWh/a]	$Solar_{\%}$ [%]	η_{boiler} [%]	f_{sav} [%]
2.0	0.30	0.55	-8379	-8194	4151	645	8793	8402	-3036	0	-1691	671	4169	1412	32.0%	104.7%	-0.89%
2.0	0.35	0.55	-8379	-8280	4152	644	8878	8466	-3037	0	-1692	690	4065	1570	31.8%	104.9%	-1.66%
2.0	0.40	0.55	-8379	-8321	4139	646	8937	8509	-3038	0	-1696	704	4278	1700	31.5%	105.0%	-2.18%
2.0	0.45	0.55	-8379	-8336	4119	648	8978	8567	-3038	0	-1701	698	5325	1891	31.3%	104.8%	-2.87%
2.0	0.50	0.55	-8379	-8332	4083	652	9024	8665	-3038	0	-1716	671	9287	2174	31.0%	104.1%	-4.05%
2.0	0.55	0.55	-8379	-8317	4039	658	9085	8830	-3038	0	-1747	599	30028	2510	30.7%	102.9%	-6.03%

Sensor Position

Given a fix optimized value of 0.4 for the heat exchanger inlet position, the height of the sensor 2 is varied. As the Figure 11-9 shows, the limit value for the sensor height is about at 0.55, if the sensor is placed above this point the heat demand is not matched anymore. Below the relative height of 0.55 the overall system efficiency falls down. So this value will be considered as an optimum and will be used for the last analysis performed on the heat exchanger area.

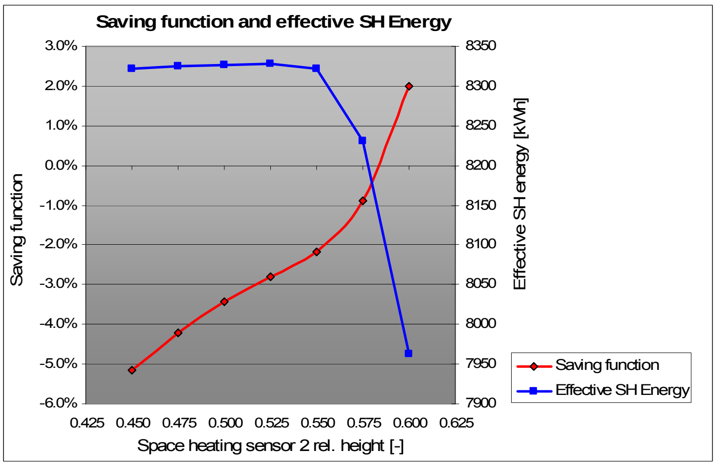

Figure 11-9: Saving function as function of the sensor 2 relative position in storage

Table 11-9: Simulation results as function of the sensor 2 relative position in storage

Space heating sensor 2 rel. Height																	
Heat exchanger area [m^2]	Heat exchanger inlet rel. height [-]	Sensor 2 rel. Height [-]	$Q_{SH,target}$ [kWh/a]	$Q_{SH,eff}$ [kWh/a]	$Q_{solar,tank}$ [kWh/a]	$Q_{solar,loses}$ [kWh/a]	Q_{boiler} [kWh/a]	E_{boiler} [kWh/a]	Q_{DHW} [kWh/a]	V_{DHW40} [l/a]	$Q_{tank,loses}$ [kWh/a]	$Q_{cond,gain}$ [kWh/a]	n_{boiler} [1/a]	t_{boiler} [kWh/a]	Solar$_{\%}$ [%]	η_{boiler} [%]	f_{sav} [%]
2.0	0.40	0.600	-8379	-7963	4128	647	8555	8162	-3037	62	-1666	658	5472	925	32.5%	104.8%	1.99%
2.0	0.40	0.575	-8379	-8231	4146	645	8823	8401	-3036	0	-1681	690	4467	1346	31.9%	105.0%	-0.88%
2.0	0.40	0.550	-8379	-8321	4139	646	8937	8509	-3038	0	-1696	704	4278	1700	31.5%	105.0%	-2.18%
2.0	0.40	0.525	-8379	-8329	4123	648	8974	8562	-3038	0	-1709	702	5643	1940	31.4%	104.8%	-2.81%
2.0	0.40	0.500	-8379	-8327	4103	650	9008	8614	-3038	0	-1724	693	9461	2139	31.2%	104.6%	-3.44%
2.0	0.40	0.475	-8379	-8325	4075	653	9051	8679	-3038	0	-1741	679	14391	2293	30.9%	104.3%	-4.21%
2.0	0.40	0.450	-8379	-8322	4049	657	9094	8758	-3038	0	-1760	658	21507	2454	30.7%	103.8%	-5.16%

Heat exchanger area

The influence of the heat exchanger area on the overall system efficiency is illustrated by the Figure 11-10. A minimum heat exchanger area of 2 m^2 is necessary to met the energy demand for space heating. For higher value of the heat exchanger area there isn't an high improvement on the final auxiliary energy saved.

The overall system efficiency compared to the base case of the Direct Feed Flow Controlled combisystem described in chapter 5 is about 2% less.

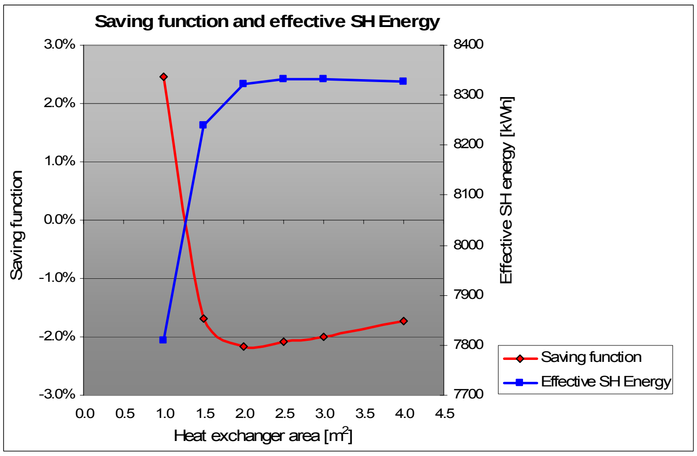

Figure 11-10: Saving function as function of the space heating heat exchanger area

Table 11-10: Simulation results function of the space heating heat exchanger area

Space heating heat exchanger area																	
Heat exchanger area [m^2]	Heat exchanger inlet rel. height [-]	Sensor 2 rel. Height [-]	$Q_{SH,target}$ [kWh/a]	$Q_{SH,eff}$ [kWh/a]	$Q_{solar,tank}$ [kWh/a]	$Q_{solar,loses}$ [kWh/a]	Q_{boiler} [kWh/a]	E_{boiler} [kWh/a]	Q_{DHW} [kWh/a]	V_{DHW40} [l/a]	$Q_{tank,loses}$ [kWh/a]	$Q_{cond,gain}$ [kWh/a]	n_{boiler} [1/a]	t_{boiler} [kWh/a]	$Solar_{\%}$ [%]	η_{boiler} [%]	f_{sav} [%]
0.5	0.40	0.550	-8379	-6223	4048	656	6925	6672	-3036	123	-1695	506	3141	733	36.8%	103.8%	19.89%
1.0	0.40	0.550	-8379	-7809	4083	651	8468	8123	-3036	123	-1688	625	4196	990	32.4%	104.3%	2.46%
1.5	0.40	0.550	-8379	-8241	4126	648	8868	8468	-3037	0	-1696	681	4412	1477	31.6%	104.7%	-1.68%
2.0	0.40	0.550	-8379	-8321	4139	646	8937	8509	-3038	0	-1696	704	4278	1700	31.5%	105.0%	-2.18%
2.5	0.40	0.550	-8379	-8331	4144	645	8941	8502	-3038	0	-1695	713	4454	1790	31.6%	105.2%	-2.09%
3.0	0.40	0.550	-8379	-8331	4146	645	8937	8494	-3038	0	-1694	717	4633	1834	31.6%	105.2%	-1.99%
4.0	0.40	0.550	-8379	-8327	4156	644	8921	8472	-3038	0	-1692	721	4878	1867	31.7%	105.3%	-1.74%

11.4. Solar and space heating loop heat exchangers

The final test is performed on a system working with two separate heat exchangers, one for the solar loop and one for the space heating loop. The parameters chosen for the heat exchangers inlet and outlet relative height as for the position of the sensors are the optimized value described on the previous sections. These are resumed in Figure 11-11. For both heat exchangers an area of 2 m^2 is chosen.

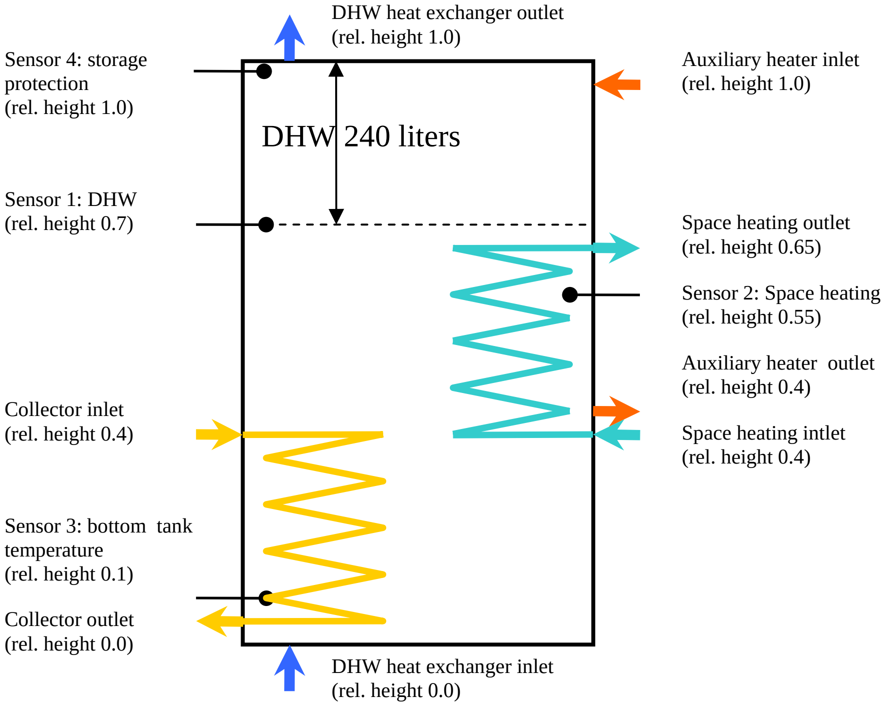

Figure 11-11: Storage tank detail

As Table 11-11 shows the effect that the introduction of the two heat exchanger cause in the overall system efficiency is relevant. The fall of about -8.2% compared to a direct feed system is considerable. The conclusion is that a direct feed system has a much higher efficiency, most of all due to a better solar fraction.

Table 11-11: Simulation results of the system represented by the Figure 11-11

Solar and space heating loop both with heat exchangers														
$Q_{SH,target}$ [kWh/a]	$Q_{SH,eff}$ [kWh/a]	$Q_{solar,tank}$ [kWh/a]	$Q_{solar,loses}$ [kWh/a]	Q_{boiler} [kWh/a]	E_{boiler} [kWh/a]	Q_{DHW} [kWh/a]	V_{DHW40} [l/a]	$Q_{tank,loses}$ [kWh/a]	$Q_{cond,gain}$ [kWh/a]	n_{boiler} [1/a]	t_{boiler} [kWh/a]	$Solar_{\%}$ [%]	η_{boiler} [%]	f_{sav} [%]
-8379	-8323	3482	662	9446	9009	-3038	0	-1547	739	4956	1826	26.8%	104.9%	-8.18%

12. *Conclusions*

The conclusions of this concentrated simulation effort show that the Direct Feed Flow Controlled concept has good potential for efficiency improvement compared to a standard solar combisystem. This is most of all due to the uncommon space heating management, controlled by varying the mass flow rate and not as in traditional systems by changing the supply temperature. As a result the return temperature coming from the space heating loop can be significantly lowered. In some cases it reaches a value near room temperature. This effect, described in great detail in section 10.2, brings higher boiler efficiency and a better solar gain, thus lowering the need for non renewable final energy.

Another point in favor of the Direct Feed Flow Controlled concept is the likely lower investment cost of the whole system. This point must still be confirmed by a detailed economic analysis that goes beyond the goals of this work, but would probably merit further investigation.

The results produced by the comparison of a direct feed concept and a “closed loop” concept presented in section 11 are also interesting. The simulations show that a storage tank system charged directly by the solar collector and uncharged by the space heating loop without use of any heat exchangers allows for significantly higher system efficiency. The investment cost is also reduced because any additional costs for the heat exchangers are added.

The main problem of the Direct Feed Flow Controlled concept is the lack of practical experience concerning the assemblage of this kind of system. The montage and planning difficulties that a non-pressurized storage tank implies need to be practically analyzed and resolved.

13. *Acknowledgments*

This thesis was written in cooperation with the Institute of Solar technology (SPF). During this period I have benefited from contact with many people, whom I would like to thank.

- First of all I would like to thank my supervisor, Peter Vogelsanger for his support and his advice throughout the process.
- Many thanks to Michel Haller and Sebastian Laipple for their support during the preparation of the TRNSYS simulation model.
- The author also wishes to thank Prof. A. Steinfeld of the ETHZ for encouraging the project.

14. *References*

14.1. Literature

[1] TRNSYS 16, User guide. University of Wisconsin Solar Energy Laboratory.

[2] Der Heizungsbauer Planung und Berechnung von Warmwasserheizungsanlagen, Ulrich Soller, Hartmut Munkel, 1990

[3] Handbuch haustechnische Planung / Fritz Steimle ; Hrsg.: Ruhrgas AG Esse, 2000

[4] Industry Newsletter IEA Tasks 26 Nr. 3, “Solar Combisystem” , January 2003

[5] MULTIPORT Store – Model for TRNSYS Type 140 v. 1.99, Harald Drück, November 2000

[6] TRNSYS Type 170 (gas/oil/biomass-boiler module), USER MANUAL v. 3.03 June 2003

[7] Type 269 Boiler Model Version 1.13, Michael Haller.

[8] Wärmeerzeuger für die Raumheizung und Warmwasserbereitung, Verbundprojekt ISOTEG, FfE, Oktober 2002

[9] Hoval TopGas® (12,16,22), Hoval (Schweiz)

[10] Handbuch der Gebäudetechnik. Planungsgrundlagen und Beispiele. Heizung/Lüftung/Energiesparen Band 1, Wolfram Pistohl

[11] Handbuch der Gebäudetechnik. Planungsgrundlagen und Beispiele. Heizung/Lüftung/Energiesparen Band 2, Wolfram Pistohl

[12] Realistic Domestic Hot-Water Profiles in Different Time Scales, Ulrike Jordan, Klaus Vajen, FB. Physik, FG. Solar, version 2.0

14.2. Internet Links

[L-1] http://www.baseconsultants.com/IEA32/

[L-2] http://www.iea-shc.org/

[L-3] http://www.transsolar.de

[L-4] http://www.spf.ch

[L-5] http://www.vaillant.com

[L-6] http://www.buderus.com

[L-7] http://sel.me.wisc.edu/trnsys/

[L-8] http://www.hoval.ch

[L-9] http://www.vaillant.com

Appendix A - Controller Type 290

Introduction

The Non-standard Type 290 space heating pump controller was written to allow the special space heating management of the Direct Feed Flow Controlled model described in chapter 5. The duty of this controller is to vary the mass flow rate of the space heating pump to match a set power given by an external file (the building load file). In this file is contained the heating power needed (P_{need}) by the building to maintain the a set temperature inside the building (T_{room}), temperature that is also contained in the load file.

This controller, using the two input from the load file (P_{need} and T_{room}) combined with the input of the water supply temperature at entrance of space heating pipe (T_{supply}) and all the parameters that characterize the heating pipe (l_{pipe}, d_{pipe}, K_{pipe}), chooses the adequate mass flow of the space heating pump.

Theory

Given the inlet temperature T_{supply} of a fluid flowing into a pipe, a given heat losses coefficient to the environment K_{pipe}, the mass flow $\dot{m}$, the pipe diameter d_{pipe} and the room temperature T_{room} it's possible to find the temperature of the fluid at the end of the pipe as shows equation A-3. Known the inlet and outlet temperature of the pipe is derived the heat power delivered by the pipe to the environment (equation A-4 and A-5).

Solving equation A-5 in reverence to $\dot{m}$ allow to find the needed mass flow to match the needed heating power. Unfortunately this equation don't have any analytic solution and must be solved numerically. This task is performed by non-standard TRNSYS type 290.

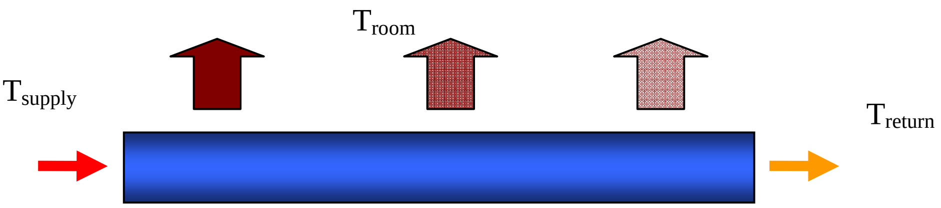

Figure A-1: Heating pipe detail

$$\frac{dT_{return}}{dx} = \frac{d_{pipe} \cdot \pi}{\dot{m} \cdot c_p} \cdot K_{pipe} \cdot \left(T_{Room} - T_{return}\right) \qquad \textit{Equation A-1}$$

$$\frac{T_{Room} - T_{return}(x)}{T_{Room} - T_{Supply}} = \exp\left(-\frac{d_{pipe} \cdot \pi \cdot x}{\dot{m} \cdot c_p} \cdot K_{pipe}\right)$$ ***Equation A-2***

$$T_{return}(l_{pipe}) = T_{Room} + \left(T_{Supply} - T_{Room}\right) \cdot \exp\left(-\frac{d_{pipe} \cdot \pi \cdot l_{pipe}}{\dot{m} \cdot c_p} \cdot K_{pipe}\right)$$ ***Equation A-3***

$$\dot{Q} = \left(T_{Supply} - T_{return}(l_{Pipe})\right) \cdot c_p \cdot \dot{m}$$ ***Equation A-4***

$$\dot{Q}(l_{Pipe}) = \left(T_{Supply} - T_{Room} - \left(T_{Supply} - T_{Room}\right) \cdot \exp\left(-\frac{d_{pipe} \cdot \pi \cdot l_{Pipe}}{\dot{m} \cdot c_p} \cdot K_{pipe}\right)\right) \cdot c_p \cdot \dot{m}$$ ***Equation A-5***

Type description

Description of the parameters, input and output of the pump controller for space heating Type 290.

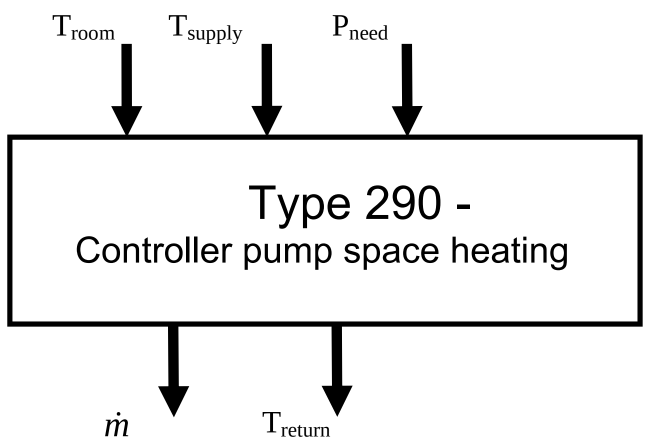

Figure A-2: Type 290 black box illustration

PARAMETER 7

1	Length of the space heating pipe (l_{pipe})	m
2	Diameter of the space heating pipe (d_{pipe})	m
3	Loses coefficient of the space heating pipe (K_{pipe})	$W/m^2.K$
4	Specific heat capacity of the heating fluid (c_p)	J/kg.K
5	Maximum flow rate of the space heating pump	Kg/h
6	Accuracy in the calculation of the heat power	kW
7	Increment in the iterative calculation of the heat power	kg/h

INPUTS 3

1	$\mathbf{T_{room}}$	Temperature inside the building	°C
2	$\mathbf{T_{supply}}$	Temperature of the hot water entering the heating pipe	°C
3	$\mathbf{P_{need}}$	Needed heating power for space heating	kW

OUTPUTS 2

1	$\dot{m}$	Flow rate of the space heating pump to match the needed heat	kg/h
2	$\mathbf{T_{return}}$	Temperature of the hot water exiting the heating pipe	°C

Appendix B - Controller Type 291

Introduction

The Non-standard Type 291 space heating tempering valve controller was written to allow the space heating power control of the Reference System model described in chapter 6. The duty of this controller is to vary the set supply temperature of the space heating tempering valve so to match a set power given by an external file (the building load file). In this file is contained the heating power needed (P_{need}) by the building to maintain the a set temperature inside the building (T_{room}), temperature that is also contained in the load file.

This controller, using the two input from the load file (P_{need} and T_{room}), combined with the input of the water supply temperature at entrance of space heating pipe (T_{supply}) and all the parameters that characterize the floor heating pipe (l_{pipe} , d_{pipe} , K_{pipe}), chooses the adequate set temperature of the tempering valve.

Theory

Given the inlet temperature T_{supply} of fluid flowing into a pipe, the pipe heat losses coefficient K_{pipe}, the mass flow $\dot{m}$ of the fluid, the pipe diameter d_{pipe}, the room temperature T_{room} it's possible to find the temperature of the fluid at the end of the pipe as shows equation B-1. With the known inlet and outlet temperature of the pipe, through equation B-1 and B-2 it's possible to find the heat power delivered by the pipe to the environment.

Solving the equation B-3 in function of T_{supply} it's found the set value of the tempering valve needed to match the space heating load.

$$T_{return}(l_{pipe}) = T_{Room} + \left(T_{Supply} - T_{Room}\right) \cdot \exp\left(-\frac{d_{pipe} \cdot \pi \cdot l_{pipe}}{\dot{m} \cdot c_p} \cdot K_{pipe}\right) \qquad \textbf{Equation B-1}$$

$$\dot{Q} = \left(T_{Supply} - T_m(l_{Pipe})\right) \cdot c_p \cdot \dot{m} \qquad \textbf{Equation B-2}$$

$$\dot{Q}(l_{Pipe}) = \left(T_{Supply} - T_{Room} - \left(T_{Supply} - T_{Room}\right) \cdot \exp\left(-\frac{d_{pipe} \cdot \pi \cdot l_{Pipe}}{\dot{m} \cdot c_p} \cdot K_{pipe}\right)\right) \cdot c_p \cdot \dot{m} \qquad \textbf{Equation B-3}$$

$$T_{Supply} = \frac{\dot{Q}(l_{Pipe})}{\dot{m} \cdot c_p \cdot \left(1 - \exp\left(-\frac{d_{pipe} \cdot \pi \cdot l_{Pipe}}{\dot{m} \cdot c_p} \cdot K_{pipe}\right)\right)} + T_{Room} \qquad \textbf{Equation B-4}$$

Type description

Description of the parameters, input and output of the Type 291 controller for space heating.

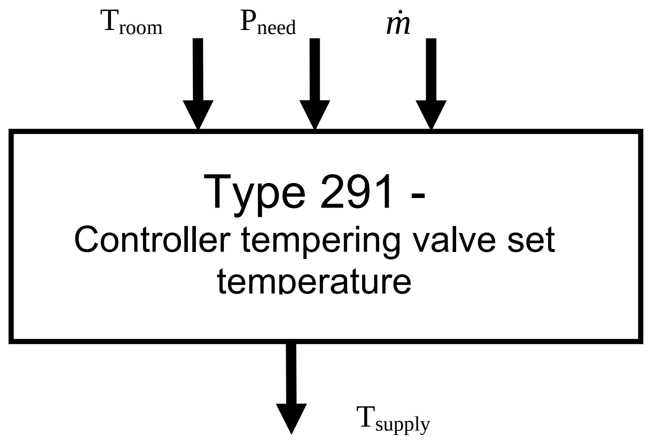

Figure B-1: Type 291 black box illustration

PARAMETER 4

1	Length of the space heating pipe	m
2	Diameter of the space heating pipe	m
3	Loses coefficient of the space heating pipe	$W/m^2.K$
4	Specific heat capacity of the heating fluid (water)	J/kg.K

INPUTS 3

1	$\mathbf{T_{room}}$	Temperature inside the building	°C
2	$\mathbf{P_{need}}$	Needed heating power for space heating	kW
3	$\dot{m}$	Flow rate of the space heating pump	kg/h

OUTPUTS 1

1	$\mathbf{T_{supply}}$	Set temperature of the tempering valve: water temperature entering the space heating pipe	°C

Appendix C – CD files description

The files used to simulate the combisystem variants contained in the CD are here briefly described.

The "Report" folder contains this report in .doc and .pdf format.

The "Simulation" folder is subdivided in 3 sub-folders:

"**Projects**" contains all the necessary files to run the simulation included the TRNSYS deck files.

"**UserLib**" contains all the .dlls of the non-standard TRNSYS Types used in the simulation.

"**NON-Standard Types 290-291**" contains the fortran source code used to compile the Non-standard TRNSYS Type 290 and 291.

TRNSYS deck file description:

NewCon.trd:	Base case of the Direct Feed Flow Controlled combisystem described in section 5.
REFERENCE.trd:	Base case of the reference system described in section 6.
_REFERENCEasNEW.trd:	Reference system model but with same boiler charging loop as the Direct Feed Flow Controlled concept (p. 83-84)
_NewConHEc.trd:	Direct Feed Flow Controlled System with an heat exchanger inside the storage for the collector loop a described in section 11.2
_NewConHEsh.trd:	Direct Feed Flow Controlled System with an heat exchanger inside the storage for the space heating loop a described in section 11.3
_NewConHE2shc.trd:	Direct Feed Flow Controlled System with an heat exchanger inside the storage for the collector loop and an heat exchanger for the space heating loop a described in section 11.4